IDENTIFICATION AND STRUCTURAL CHARACTERIZATION OF A *LEGIONELLA* PHOSPHOINOSITIDE PHOSPHATASE

A Dissertation

Presented to the Faculty of the Graduate School

Of Cornell University

In Partial Fulfillment of the Requirements for the Degree of

Doctor of Philosophy

by

Leila Bahadori Toulabi

January 2014

IDENTIFICATION AND STRUCTURAL CHARACTERIZATION OF A *LEGIONELLA* PHOSPHOINOSITIDE PHOSPHATASE

Leila Bahadori Toulabi, Ph. D.

Cornell University 2014

The bacterial pathogen *Legionella pneumophila* is the causative agent of Legionnaires' disease, which is associated with intracellular replication of the bacteria in macrophages of the human innate immune system. *L. pneumophila* enters host cells through phagocytosis. Once inside the host cells *L. pneumophila* manipulates vesicular trafficking pathways and establishes *Legionella*-containing vacuoles (LCV) that serve two purposes: to provide a safe niche for intracellular bacterial replication and to prevent bacterial degradation by the host's bactericidal lysosomal compartments. *L. pneumophila* uses a type IV secretion system called "Intracellular multiplication/Defective for organelle trafficking" (Icm/Dot), a key virulence factor, to inject almost 300 secreted effector proteins into its host cells. The secreted effector proteins are believed to play important roles in LCV biogenesis and intracellular multiplication of *L. pneumophila*. Several of these effector proteins are capable of interacting with host phosphoinositides (PIs). However, there has been no report to date of a *L. pneumophila*-coded PI- metabolizing enzyme. Given the indispensable role of PIs in vesicle trafficking, the main goal of my research was to identify, characterize, and study the role of *L. pneumophila* PI phosphatases in exploiting host PIs and subverting host cell vesicular trafficking during infection.

I was able to show that *L. pneumophila* encodes an effector protein that we named SidP, which functions as a PI-3-phosphatase specifically hydrolyzing PI(3)P and

$PI(3,5)P_2$ *in vitro*. The enzymatic activity of SidP rescues the growth phenotype of a yeast strain defective in PI(3)P phosphatase activity. My crystal structure of a SidP ortholog from *Legionella longbeachae* reveals that this unique PI-3-phosphatase is comprised of three distinct domains: a large catalytic domain, an appendage domain inserted into the N-terminal portion of the catalytic domain, and a C-terminal α-helical domain. SidP has a small catalytic pocket that likely provides substrate specificity by limiting the accessibility of bulky PIs with multiple phosphate groups. A unique conformation of the conserved arginine residue in the catalytic motif of SidP and the presence of a hydrophobic loop that covers the catalytic motif may participate in regulating the activity of SidP. Together, my identification of a unique family of *Legionella* PI phosphatases highlights a common scheme of exploiting host PI lipids in intracellular bacterial pathogen infections.

BIOGRAPHICAL SKETCH

Leila Toulabi was born and raised in Iran. She completed her undergraduate education at Tehran University in Tehran, Iran, where she received a Bachelor of Science in Biology with a major in Cell and Molecular biology. Having a long-term interest in mathematics and physics as her major in high school, Leila enrolled in the Biophysics program at Tarbiat Modares University, also located in Tehran. She graduated from Tarbiat Modares Univesity with a Master of Science in Biophysics studying the effects of drug carrier (Liposome & Dendrosome) on the stability of lysozyme as a protein cargo supervised by Dr. Beijan Ranjbar. Leila continued her scientific career by joining the lab of Dr. Jeremy Nathans as a research specialist in the department of Molecular Biology and Genetics at Johns Hopkins University in Baltimore, Maryland, USA. In his lab, Leila studied the impact of light damage and retinal detachment in activation or deactivation of genes in the retinal pigment **epithelium**. Leila decided to continue her education and enrolled in the field of Biochemistry, Molecular and Cell Biology at Cornell University in Ithaca, New York, USA. Leila pursued her Ph.D under the supervision of Dr. Yuxin Mao identifying and studying a *Legionella* phosphoinositide phosphatase. Leila plans to Join Dr. Peng Loh's team and begin her postdoctoral work at the National Institute of Health in Bethesda, Maryland, USA. Leila will study carboxypeptidase E (CPE) and explore further CPE functions and interactions that are independent of its enzymatic role.

ACKNOWLEDGEMENTS

I am very grateful to Dr. Yuxin Mao for allowing me to be a part of his lab and for his support and advice. In addition to teaching me how to think about science, to interpret, and organize my work, Dr. Mao allowed me independence and let me explore different scientific approaches. I would like to thank Dr. Mao especially for listening and understanding my feedback as one of his first students.

I would like to thank my committee members, Dr. Chris Fromme, Dr. Holger Sondermann, and Dr. Volker Vogt, for their support and guidance throughout my graduate career.

I would like to thank Dr. Fenghua Hu, who has been always available and happy to help me with any questions.

I would like to thank Dr. Jerry Feigenson and Jim Blankenship whom I have had the privilege of working with as a teaching assistant. It was a great learning experience for me.

I would like to thank Dr. Di Luo Bush for reading my thesis and giving suggestions in various aspects.

I was also fortunate to have great lab mates and friends, FoSheng Hsu, Adam Brady, Xiaochun Wu, Amelia Cheng, and the rest of Mao and Hu labs. Thank you my dear Cornelian friends, Behfar Ardehali, Ella Chang, Lindsey Boroughs, Maxim Kostylev, Mohanram Gudipati, Patrice Ohouo, and Pi-Chiang Hsu. These years in Cornell would not have been the same without you.

Last, but most of all, I would like to thank my family and my best and closest friend Tudor for their love and support. You are there for me to motivate me, comfort me, and make my life more meaningful and colorful. I could not have done any of this without you. A special thank you to my mother; your presence has been a symbol of love, care, understanding, and patience.

TABLE OF CONTENTS

Contents

LIST OF ABBREVIATIONS

3D: three-dimensional

ANTH: AP180 N-terminal homology

AYE: N-(2-acetamido)-2-aminoethanesulfonic acid yeast extract

COPII: coat protein complex II

CR: complement receptor

DAG: Diacylglycerol

Dali: **d**istance-matrix **ali**gnment

EEA1: early endosome antigen 1

ENTH: Epsin N-terminal homology domain

ER: Endoplasmic reticulum

FBS: fetal bovine serum

FERM: 4.1 Ezrin Radixin Moesin

FYVE: Fab 1 (yeast orthologue of PIKfyve)

GAP: GTPase activating protein

GDF: GDI displacement factor

GDI: Guanine nucleotide dissociation inhibitor

GDP: guanine diphosphate

GEF: guanine nucleotide exchange factor

GLUE: GRAM Like Ubiquitin-binding in EAP45

G-proteins: guanine nucleotide-binding proteins

GRAM: glucosyltransferases, Rab-like GTPase activators and myotubularins

GTP: guanine triphosphate

ICDH: anti-isocitrate dehydrogenase

Icm/Dot: Intracellular multiplication/Defective for organelle trafficking

kDa: kilodalton

LadC: *L. pneumophila*-specific adenylate cyclase

LAMP-1: lysosomal-associated membrane protein 1

Lcl: *L. pneumophila* collagen-like protein

LCV: *Legionella*-containing vacuole

LVA: *Legionella* vacuole association

MAD: Multi-wavelength Anomalous Diffraction

MIR: Multiple Isomorphous Replacement

MOMP: major outer membrane protein

MVB: Multivesicular body

PBS: phosphate-buffered saline

PCV: pathogen-containing vacuole

PDB: protein data bank

PH: Pleckstrin homology

PI: phosphoinositide

PI3-kinase: phosphatidylinositide 3-kinase

PLCδ1: phospholipase Cδ1

polyUb: polyubiquitinated

PTEN: phosphatase and tensin homolog deleted on chromosome ten

PX: phox

SAD: Single-wavelength Anomalous Dispersion

SAXS: small angle X-ray scattering

SDS-PAGE: sodium dodecyl sulfate-polyacrylamide gel electrophoresis

SNARE: soluble NSF attachment protein receptor

S-tag: or S15, Lys-Glu-Thr-Ala-Ala-Ala-Lys-Phe-Glu-Arg-Gln-His-Met-Asp-Ser) peptide

T4BSS: type IVB secretion system

TBS: Tris-buffered saline

CHAPTER 1

Introduction

In this chapter, I will first discuss the role of phosphoinositides (PIs) in regulating vesicular trafficking. Then I will specifically talk about the roles of PIs in phagocytosis. I will then discuss how intracellular pathogens utilize and modulate their host PI metabolism during infection. Finally, I will describe the life cycle of *Legionella pneumophila* at the cellular level and the importance of exploiting host PI metabolism for subversion of vesicular trafficking in the host for the pathogenicity of *L. pneumophila*.

1.1 PIs and cellular signaling

Despite being a minor fraction of total cell phospholipids, PIs play major roles in a variety of cellular processes such as cell signaling and survival, membrane trafficking, cytoskeleton rearrangement, and organelle identity (Behnia and Munro, 2005; Di Paolo and De Camilli, 2006; Lemmon, 2008; Takenawa and Itoh, 2006). PIs are inter-convertible phosphorylated derivatives of phosphatidylinositol. The reversible phosphorylations of phosphatidylinositol on the 3,4, and/or 5 hydroxyl groups of the inositol ring by specific kinases yield seven (four in yeast) species of PIs that can be rapidly converted to one another by specific PI kinases and phosphatases (Di Paolo and De Camilli, 2006). The tightly regulated action of specific kinases and phosphatases in each cellular organelle creates different temporal and spatial enrichment of PIs. This differential PI enrichment provides markers for organelle identity. For example, the Golgi complex is predominantly enriched in PI(4)P. The plasma membrane is enriched in

$PI(4,5)P_2$ and PI(4)P, but $PI(3,4,5)P_3$ accumulates transiently in the plasma membrane during signal transduction. Early endosomes are identified with PI(3)P and late endosomes are enriched in $PI(3,5)P_2$ (Behnia and Munro, 2005; Di Paolo and De Camilli, 2006; Lemmon, 2008; Takenawa and Itoh, 2006).

PIs are localized in the cytoplasmic leaflet of organelle membranes and can be recognized by their cognate effector proteins in a very specific manner. The recognition and binding of PIs to their effector proteins is mainly mediated by short protein motifs such as PX, ENTH, FYVE, PH-GRAM, FERM, GLUE, and PH domain families (Balla, 2005; Behnia and Munro, 2005; Di Paolo and De Camilli, 2006; Lemmon, 2008; Takenawa and Itoh, 2006). PIs and GTPases cooperatively interact to recruit specific downstream effector proteins to the membranes in which they reside and mediate an extensive network of signaling events (Botelho et al., 2008). PI metabolizing enzymes can control multiple cellular functions simultaneously through regulation of a single PI species. Therefore tight control of PI levels by PI kinases and phosphatase is necessary in order for cells to orchestrate multiple signaling pathways (Duex et al., 2006).

1.2 PIs and phagocytosis

PIs interconvert during phagocytosis and later stages of phagosomal maturation into the phagolysosome. The dynamic conversion of PIs has an essential role in phagosomal membrane remodeling and phagolysosome biogenesis. Phagocytosis can be divided to two steps: 1) phagosome formation, and 2) phagosomal maturation into a phagolysosome (Deretic V, 2007). Phagosome formation and pathogen uptake are parts of a complicated process that starts with phagocytic cup formation, followed by phagosome extension and phagosome closure.

Membrane and cytoskeleton remodeling processes governed by temporal and spatially regulated phospholipid interconversions are essential for phagosome formation and pathogen uptake. In a newly made phagocytic cup, PI(4)P is converted transiently to PI(4,5)P_2 by PI(4)P kinase. Then, PI(4,5)P_2 is quickly cleaved to diacylglycerol and inositol phosphates by phospholipase C (Scott et al., 2005). These PI changes control actin polymerization and pseudopod extension. Finally, formation of PI(3,4,5)P_3, recruitment of Rho GTPases, and activation of their effectors lead to controlled myosin contraction and phagosomal completion and closure (Dewitt et al., 2006).

The second step of phagocytosis is the maturation of the phagosome into the phagolysosome. Phagosome maturation starts immediately after phagosome closure. A nascent phagosome undergoes serial fusion events with early endosomes, late endosomes, and lysosomes (Desjardins et al., 1994). These steps are governed by the formation of PI(3)P by type III PI3K on the early phagosomal membrane (Ellson et al., 2001; Fratti et al., 2001; Vergne et al., 2003b; Vieira et al., 2001). PI(3)P recruits effector proteins to the cytosolic face of the phagosome through various binding domains such as PX (phox homology), FYVE, Hrs and EEA1 (early endosomal antigen 1). Remodeling of the phagosome membrane along with changing of the lumen to an acidic, oxidative, and degradative environment results in the biogenesis of the phagolysosome (Birkeland and Stenmark, 2004; Vieira et al., 2004). Intracellular pathogens such as *M. tuberculosis* and *L. pneumophila* arrest the trafficking events required for phagolysosome biogenesis in the phagocytosis pathway in order to survive in the host cell (Horwitz, 1983a; Russell et al., 2002).

1.3 Modulation of host PI metabolism by intracellular pathogens

After uptake by their host cells, intracellular pathogens use various strategies to manipulate the host cellular pathways and escape lysosomal degradation(Hilbi, 2006a). Adaptation to the acidic environment of the host lysosome is a survival strategy that has only been evolved by *Coxiella burnetii* (Voth and Heinzen, 2007). Lysing the phagosomal membrane in order to escape to the host cytoplasm and multiply is the method chosen by *Shigella* spp. and *Listeria monocytogenes* (Cossart and Sansonetti, 2004). Some intracellular pathogens form a specialized pathogen-containing vacuole that can avoid fusion with the host lysosomes and provide a safe niche for bacterial replication. These pathogen-containing compartments are derived from a variety of endocytic compartments. For example, *Mycobacterium tuberculosis* amplifies and survives in early endosome-like organelles (Vergne et al., 2004). *Salmonella enterica* resides in a compartment that has characteristics of late endosome (Steele-Mortimer, 2008). *L. pneumophila* forms a *Legionella*-containing vacuole (LCV) that resembles the rough ER membrane (Roy, 2002; Roy and Tilney, 2002).

Regardless of the strategy that a pathogen uses, bacterial pathogens employ their virulent factors to subvert the host cellular machinery in targeted ways that support their survival and replication in host cells. Intracellular gram-negative bacteria use type II, III, or IV secretion systems to directly inject and translocate virulence effector proteins into host cells. These effector proteins play significant roles in targeting key molecules in host cellular processes including immune response, cell proliferation and cell death, cytoskeleton and membrane rearrangement, and vesicular trafficking. Ultimately, these effector proteins serve to subvert the host cellular machinery during infection for the

benefit of the infecting bacteria (Amer and Swanson, 2002; Backert and Meyer, 2006; Coburn et al., 2007; Cossart and Sansonetti, 2004; Rosenberger and Finlay, 2003).

Recently, lipid signaling, and in particular, PI signaling, as well as metabolism have been shown to be important targets for bacterial virulence factors (DeVinney R, 2000; Hilbi, 2006b; Pizarro-Cerdà J, 2004). Considering the pivotal roles of PIs in almost every cellular signaling and vesicular trafficking event, it is not surprising that many intracellular pathogens exploit host PI metabolism as a common strategy to infect their host cells (DeVinney R, 2000; Hilbi, 2006b; Pizarro-Cerdà J, 2004).

Intracellular pathogens can exploit the host PI signaling using different strategies. They can encode PI metabolizing enzymes that directly affect host cell PIs levels. They can make proteins or lipids that affect host PI metabolizing enzymes and by extension, host cells PI levels. They can generate PI-binding effector proteins that attach to PIs on the surface of pathogen-containing vacuole (PCV). Using these strategies, intracellular pathogens modulate PI levels on various compartments in the endocytic/phagocytic pathway, which ultimately results in their transformation into PCV and prevents their fusion with host lysosomes (Pizarro-Cerda and Cossart, 2004).

1.3.1 *Salmonella enterica* infection and PI metabolism

Salmonella enterica is a facultative intracellular pathogen that can infect a variety of eukaryotic cells and causes foodborne gastroenteritis and typhoid fever in humans. *Salmonella* is an invasive bacterium that can induce phagocytosis in non-phagocytic host cells and promote its own internalization through inducing cytoskeleton and

membrane rearrangements. These changes can be observed as membrane ruffles on the host cell surface.

Once inside the host, *Salmonella* resides and replicates in *Salmonella*-containing vacuoles (SCVs), which are late endosome-like vesicles that avoid fusion with lysosomes by exploiting host vesicular trafficking and the endocytic pathway (Cossart and Sansonetti, 2004). The SCV is a dynamic structure that first acquires markers of early endosomes such as Rab5 and EEA1, followed by acquisition of late endosomes molecules such as Rab7 and LAMP1. It excludes the mannose 6-phosphate receptor (M6PR) and cathepsin that are normally found in a mature phagosome (Knodler and Steele-Mortimer, 2003). *Salmonella* pathogenicity, SCV formation, and regulation of SCV trafficking are dependent on an array of bacterial effector proteins that are translocated to the host cell cytosol. Two different type III secretion systems are used to inject about 30 effector proteins into the host cells in order to secure *S. enterica*'s internalization and replication in the host cells (Steele-Mortimer, 2008).

Among other effector proteins, *S. enterica* translocates a PI phosphatase to the host cells. SopB, also called SigD, has 4-phosphatase motifs and a synaptojanin-like 5-phosphatase domain (Marcus et al., 2001). SopB hydrolyzes $PI(4,5)P_2$ to generate PI(5)P at the plasma membrane of host cells (Marcus et al., 2001; Niebuhr et al., 2002; Norris et al., 1998). SopB uses its PI phosphatase activity to enhance pathogenicity at several stages in the bacterial life cycle. SopB is involved in *S. enterica* uptake, biogenesis and maturation of the SCV, and *S. enterica* intracellular survival in host cells. SopB contributes to bacterial uptake and host cell invasion by activating Rho GTPases such as RhoG, leading to actin rearrangements (Patel and Galan, 2006). It also

activates the Rho/Rho kinase/myosin II pathway that promotes actomyosin-mediated contractility (Hanisch et al., 2011). Overall, SopB modulates host plasma membrane PI composition to promote the formation of SCVs (Hernandez et al., 2004; Mallo et al., 2008; Mason et al., 2007; Terebiznik et al., 2002).

SopB promotes SCV maturation through several potential pathways. First SopB recruits Rab5 and its effector Vps34 PI3kinase to nascent SCVs (Mallo et al., 2008). Second it recruits sorting nexins-1 and sorting nexins-3 to nascent SCVs (Braun et al., 2010; Bujny et al., 2008). Finally, SopB may inhibit SCV fusion with lysosomes (Bakowski et al., 2010).

SopB can also activate the PI 3-kinase/Akt survival pathway to avoid host cell death through apoptosis by increasing of PI(5)P levels generated from $PI(4,5)P_2$ dephosphorylation. Although the molecular mechanism of how cell survival signals can be triggered by PI5P is not completely understood yet, it seems that the action of PI5P is connected to growth factor receptor signaling in the host cells. Epidermal growth factor receptor (EGFR) is activated during infection through an unknown mechanism. And, it has been proposed that PI5P can modify EGFR signaling and trafficking by preventing activated EGFR degradation. Accumulation of EGFR and its downstream effectors in endosomes then triggers “endosome-specific” signaling of activated EGFR. This specific EGFR signaling has been suggested to promote the PI3K and Akt pathway and sustain cell survival (Ramel et al., 2009; Ramel et al., 2011; Steele-Mortimer et al., 2000).In addition, SopB may play a role in fluid loss during *Salmonella* infection by hydrolyzing $PI(4,5)P_2$, which disrupts the host cell’s tight junctions and inhibition of the Na^+/H^+ exchange activity, as well as rearrange the actin cytoskeleton and plasma

membrane (Mason et al., 2007). Thus, SopB contributes in various ways to *Salmonella* infection from the early stages of invasion to the intracellular phase of *Salmonella* survival.

1.3.2 *Shigella flexneri* infection and PI metabolism

The facultative intracellular gram-negative enterobacterium *Shigella* is the causative agent of shigellosis or bacillary dysentery, an invasive infection in the human colonic epithelium. Shigellosis manifests as a spectrum of clinical symptoms from a short lasting diarrhea to acute inflammatory bowel disease (Schroeder and Hilbi, 2008).

Among other effector proteins, *Shigella flexneri* encodes a PI phosphatase effector, IpgD, which is a homolog of SopB (Marcus et al., 2001). IpgD can hydrolyze a wide range of PIs *in vitro*, but it functions as a PI-4 phosphatase during infection and hydrolyzes PI(4,5)P_2 at the plasma membrane of host cells to generate PI(5)P (Niebuhr et al., 2002).

The PI phosphatase activity of IpgD contributes to *Shigella flexneri* uptake and its intracellular survival in the host cells. Hydrolysis of PI(4,5)P_2 at the host plasma membrane by IpgD disrupts the interaction between PI(4,5)P_2-binding cytoskeleton proteins and the plasma membrane, resulting in reorganization of the actin cytoskeleton and destabilization of the membrane/cytoskeleton interaction. This weakened interaction facilitates membrane ruffles and filopodia formation, which are required for bacterial uptake (Niebuhr et al., 2002). Furthermore, the IpgD-dependent increase in PI(5)P at the bacterial entry foci at the host plasma membrane activates the host class IA PI 3-kinase (PI3KIA), which results in over production of PI(3,4)P_2 and PI (3,4,5)P_3.

Elevated levels of these PIs activate the serine/threonine kinase Akt/PKBa survival pathway. In the meantime, PI(5)P induces PP2A phosphatase inhibition and prevents Akt from dephosphorylation, therefore keeping the Akt activated and preventing host cell death through apoptosis (Ramel et al., 2009).

1.3.3 *Mycobacterium tuberculosis* infection and PI metabolism

Mycobacterium tuberculosis is the causative agent of the chronic pulmonary disease tuberculosis. *M. tuberculosis* resides and replicates in *Mycobacterium*-containing vacuoles (MCVs). Similar to other intracellular pathogens, MCVs avoid fusion with lysosomes. MCVs are early endosome-like compartments and contain the small GTPase Rab5, a marker for early endosomes. MCVs do not contain late endosomal markers (Rab7) and lysosomal proteins like the vacuolar proton pump, V-ATPase, and hydrolases (Russell et al., 2002).

M. tuberculosis blocks phagosome maturation partly by modulating the host PI metabolism. *M. tuberculosis* encodes two translocated PI phosphatases, SapM and MptpB, which can both hydrolyze PI(3)P on the MCV to prevent the endocytic pathway from progressing by keeping levels of PI(3)P on the MCV low (Beresford et al., 2007; Vergne et al., 2005). SapM is an acid phosphatase present in mycobacterium phagosomes and shows PI-phosphatase activity specifically for PI(3)P *in vitro*. Its enzymatic activity is required for inhibition of phagosome maturation (Vergne et al., 2005). MptpB is a dual-specificity protein phosphatase and PI phosphatase that preferentially hydrolyzes PI(3)P and PI(3,5)P_2 *in vitro* (Beresford et al., 2007). MptpB is an essential secreted virulence factor for maintaining mycobacterial infection (Singh et

al., 2003). Thus, two *M. tuberculosis* PI(3)P phosphatases, SapM and MptpB, most likely work synergistically to deplete PI(3)P from MCVs.

Another strategy used by *M. tuberculosis* to exploit the host PI metabolism is to encode molecules that mimic the PIs. *M. tuberculosis* secretes glycosylated phosphoinositide analogue lipoarabinomannan (LAM), a toxin that also contributes to PI(3)P depletion on the MCV and phagosome maturation arrest (Fratti et al., 2001). This PI analog inhibits activation of the Ca^{2+}/calmodulin PI-3 kinase hVPS34 cascade, which is necessary for PI(3)P production on phagosomes (Vergne et al., 2003b). *M. tuberculosis* also produces another PI analog: phosphatidylinositol mannoside (PIM). PIM is the precursor of LAM and promotes fusion between early endosomes and phagosomes in a PI3K-independent fashion. Therefore, PIM supports the communication between MCVs and endosomes and ensures *M. tuberculosis* access to nutrients despite the inhibition in trafficking resulting from PI(3)P depletion (Vergne et al., 2004). *M. tuberculosis* has evolved two different strategies to keep the MCV low in PI(3)P during its tenancy in the infected macrophages, by blocking PI(3)P synthesis using LAM, and by hydrolyzing PI(3)P using PI-3-phosphatases (SapM and MptpB).

1.4 *Legionella pneumophila is* the causative agent of Legionnaires' disease

The causative agent of Legionnaires' disease, *L. pneumophila*, is a Gram-negative bacterium found in freshwater reservoirs. The primary natural host of *L. pneumophila* are freshwater amoebae (Rowbotham, 1980). When humans aspirate bacteria-containing water or accidentally inhale water aerosols containing *L.*

pneumophila, the bacterium can infect alveolar macrophages and cause respiratory disease (Fraser et al., 1977; Horwitz, 1983b; McDade et al., 1977).

L. pneumophila enters host cells through phagocytosis. Once inside the cell, it resides in a modified phagosome that does not follow nor complete the phagocytosis pathway, thereby avoiding lysosomal fusion. This transformed phagosome is called a *Legionella*-containing vacuole (LCV), which morphologically resembles the host cell's rough endoplasmic reticulum (ER) (Roy, 2002; Roy and Tilney, 2002) and provides a safe niche for bacterial replication. *L. pneumophila* establishes the LCV by hijacking host vesicles and manipulating host intracellular trafficking. Several small GTPases that are involved in endosomal or late secretory pathways are anchored on the LCV during infection and assist in *L. pneumophila*'s pathogenesis. LCVs go through maturation through their interactions with the ER-derived vesicles, mitochondria, and with the ER (Isberg et al., 2009; Kagan and Roy, 2002).

Establishment and maturation of the LCV is dependent on a type IV bacterial secretion system (T4BSS) called Intracellular multiplication/Defective for organelle trafficking (Icm/Dot). Using this secretion system, *L. pneumophila* injects almost 300 secreted effector proteins into its host cells to facilitate LCV formation and maturation (Berger and Isberg, 1993; Horwitz, 1987; Hubber and Roy, 2010; Zhu et al., 2011). Although the Icm/Dot T4BSS is an important virulence factor, the function and host cell targets of the majority of the Icm/Dot–translocated effectors are unclear. Only very small fractions of these effector proteins have known molecular functions, but as a whole, they are believed to play important roles in the LCV biogenesis and intracellular multiplication of *L. pneumophila*.

L. pneumophila can infect a broad range of hosts, including many amoeba species, ciliate protozoa and various macrophage-like mammalian cells, as well as epithelial cells (Fields, 1996; Lau and Ashbolt, 2009). In the 1980s, Horwitz *et al.* defined the life cycle of *L. pneumophila* in human phagocytic cells (Horwitz, 1983a)(Figure 1.1). Rowbotham was the first to show that *L. pneumophila* infects amoebae and also was the first to characterize the life cycle of the bacterium in amoebae (Rowbotham, 1980, 1986) (Figure 2.1). Besides a few observable differences, the *L. pneumophila* infection cycle is highly similar between amoeba and macrophages at the cellular and microscopic levels (Fields et al., 2002). *L. pneumophil*a enters both hosts through phagocytosis and resides in the LCV to avoid lysosomal fusion. During infection in both hosts, the establishment of the LCV involves recruiting ER vesicles, ribosomes and mitochondria (Escoll et al., 2013; Isberg et al., 2009).

The common strategies used by *L. pneumophila* to infect both amoeba and macrophages suggest that the ability of *L. pneumophila* to infect macrophages may have evolved during co-evolution of *L. pneumophila* and amoeba. The mutual interactions between *L. pneumophila* and amoeba may have provided the bacteria with the necessary molecular strategies to infect and survive in mammalian macrophages (Al-Quadan et al., 2012; Cianciotto and Fields, 1992; Franco et al., 2009; Newsome et al., 1985).

1.5 *L. pneumophila* uses the Icm/Dot T4BSS to inject effector proteins into its host

The Icm/Dot T4BSS is essential for LCV formation and *L. pneumophila* replication in both amoeba and macrophages (Segal and Shuman, 1999). This

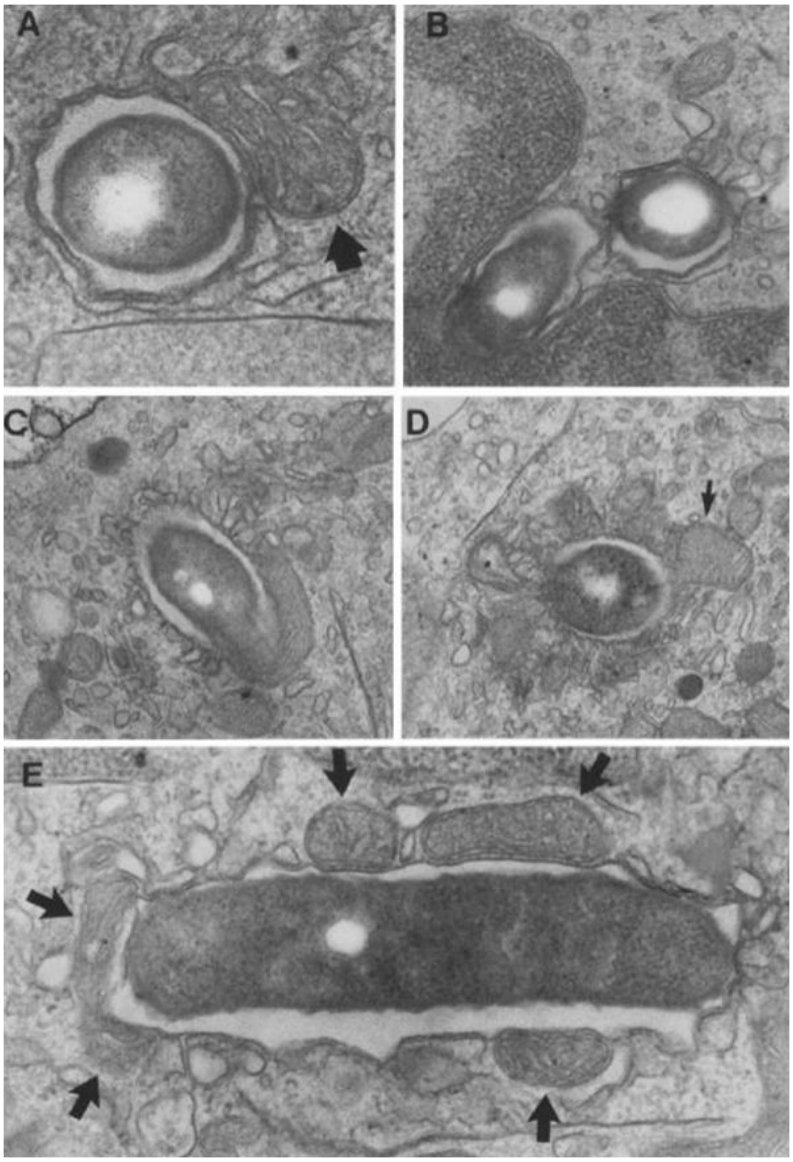

Figure 1.1 Morphology of *L. pneumophila*-containing vacuoles in monocytes 1 hour after infection. Monocytes in monolayer culture were infected with *L. pneumophila*. After 15 minutes incubation with the bacteria, the monocyte monolayer were washed to remove non-monocyte-associated bacteria, incubated for an additional 45 minutes, and fixed for electron microscopy. (A) *L. pneumophila* vacuole with a single mitochondria (arrow) closely apposed to the vacuolar membrane. A few smooth vesicles also surrounded the vacuole. ×78000. (B) Two *L. pneumophila* vacuoles, one of which is located within an invagination of the nuclear envelope. ×41700 (C) *L. pneumophila* vacuoles surrounded by smooth vesicles and a mitochondria ×33000. (D) *L. pneumophila* vacuoles surrounded by a very large number smooth vesicles and at least one mitochondria (arrow). ×32400. (E) *L. pneumophila* vacuole surrounded by 5 mitochondria (arrows) and a few vesicles. × 54000 . Figure and the figure legend are taken from (Horwitz, 1983a).

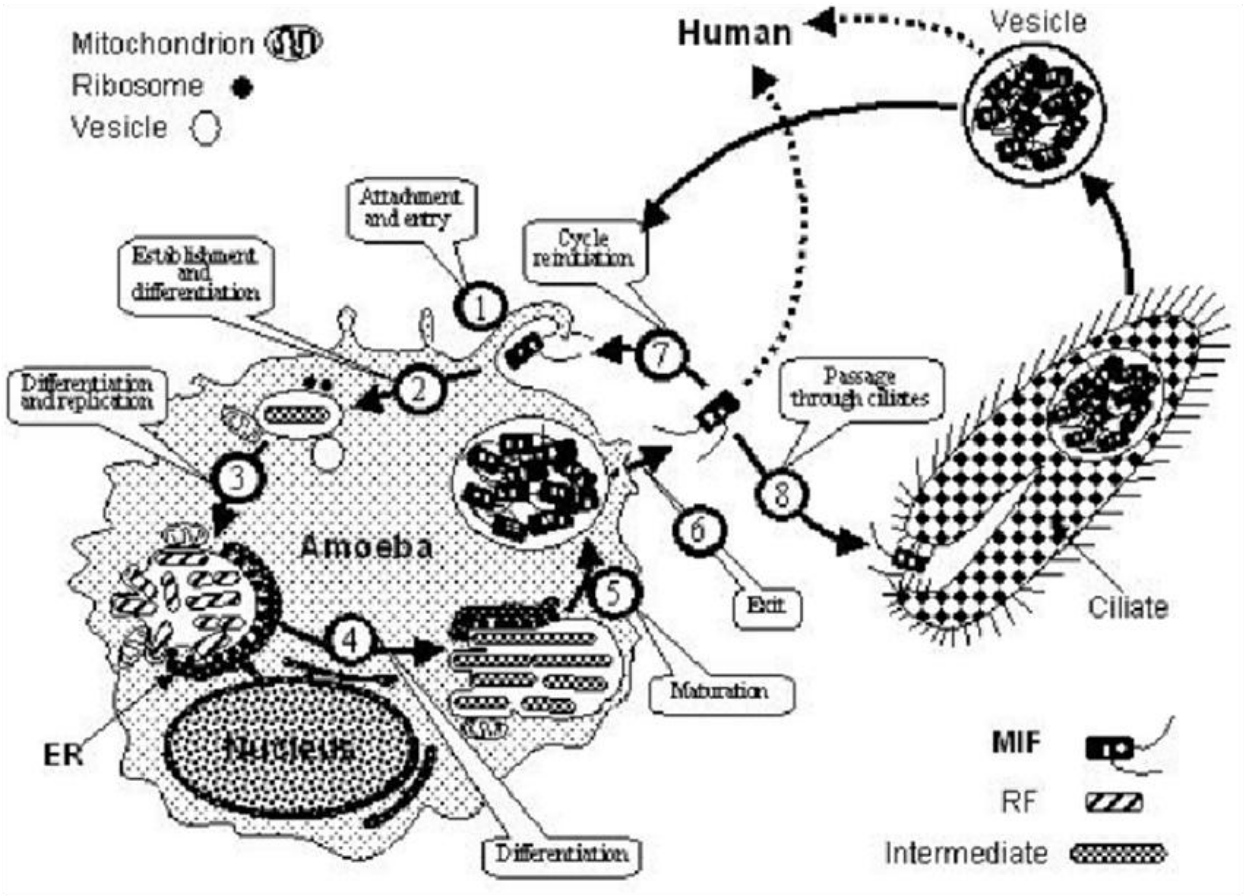

Figure 1.2 The life cycle of *L. pneumophila*. The cycle begins with the attachment to, and the invasion of an amoebal host. Post-internalization events include inhibition of phagosome-lysosome fusion and alteration of organelle traffic. *L. pneumophila* replicates in a ribosome-decorated vacuole that associates with the ER and acquires ER markers. After replication is finished the progeny exit the wasted amoeba to reinitiate the cycle. The life cycle of *L. pneumophila* is associated with bacterial differentiation. The two main morphological forms are the mature intracellular form, or MIF, and the replicative form, or RF, which differentiate into each other via intermediates. MIFs play a central role in the infection of amoeba and are the potential agents that spread Legionnaires's disease to humans, either free or packaged into vesicles. MIF-laden vesicles may be directly released by amoebae or indirectly by ciliates via an additional packaging step. Figure and the figure legend are taken from (Rowbotham, 1986).

indispensable virulence apparatus is a multi-protein system encoded by a set of highly conserved genes among *Legionella* species (Berger and Isberg, 1993; Brand et al., 1994; Marra et al., 1992). Most of the 27 Icm/Dot genes are required for establishment of the LCV and intracellular growth of *L. pneumophila*. Mutations in many of these genes disrupt ER-derived vesicle recruitment to the LCV and acquisition of late endosomal markers by the LCV (Berger et al., 1994; Isberg et al., 2009; Tilney et al., 2001).

The Icm/Dot T4BSS translocates an exceptionally high number of effector proteins into the host cell cytosol (Segal et al., 1998; Vogel et al., 1998). These translocated proteins modulate several host cell processes such as organelle trafficking, and contribute to the biogenesis of a “replication permissive” LCV (Shin and Roy, 2008; Vogel and Isberg, 1999).

Almost 300 protein substrates of the Icm/Dot translocation system have been identified (Altman and Segal, 2008; Burstein et al., 2009; Campodonico et al., 2005; Conover et al., 2003; de Felipe et al., 2008; Lifshitz et al., 2013; Luo and Isberg, 2004; Ninio and Roy, 2007; Shohdy et al., 2005; Zusman et al., 2007). The function of the majority of these translocated proteins is not yet known, but they are believed to modulate host cell vesicular trafficking, apoptosis, and immune responses to support LCV formation and *L. pneumophila* intracellular multiplication (de Felipe et al., 2008; Derre and Isberg, 2005; Hubber and Roy, 2010; Ingmundson et al., 2007; Machner and Isberg, 2006; Murata et al., 2006; Nagai et al., 2002; Shohdy et al., 2005). The majority of effector proteins are non-essential due to high functional redundancy, making function determination for each Icm/Dot substrate complicated. In fact, concurrent

deletion of more than 30% of Icm/Dot substrates only affects *L. pneumophila* in subtle ways in a mouse macrophage system (O'Connor et al., 2011). In addition to the redundancy among bacterial effector proteins, multiple host vesicular trafficking pathways may contribute to LCV formation. This may explain why virulence is preserved upon deletion of many bacterial effector genes (Dorer et al., 2006).

1.6 The life cycle of L. pneumophila

1.6.1 Attachment of L. pneumophila to host cells

The first step in *L. pneumophila* infection is attachment to the host cell surface. Both bacterial and host factors are involved in this attachment. Several *L. pneumophila* proteins including RtxA, PilEL, EnhC, MOMP, LadC, and Lcl have been implicated in the binding of *L. pneumophila* to host cells. RtxA and PilEL are involved in the attachment of the bacteria to both human macrophages and amoeba (Cirillo et al., 2002; Stone and Abu Kwaik, 1998). *L. pneumophila rtxA* and *pilEL* single mutants are defective in attachment to and entry into human epithelial and monocytic cell lines (Cirillo et al., 2002). Moreover, the major outer membrane protein (MOMP), a *L. pneumophila* collagen like protein (Lcl), and a putative *L. pneumophila*-specific adenylate cyclase in the bacterial inner membrane (LadC) are involved in the adhesion *L. pneumophila* to macrophages (Bellinger-Kawahara and Horwitz, 1990; Krinos et al., 1999; Newton et al., 2008; Vandersmissen et al., 2010).

On the other hand, *L. pneumophila* exploits different host factors to attach to their cell surface in a host specific manner. This is true even when *L. pneumophila* infects different species of amoeba. In *Hartmannella vermiformis* infection, the host surface lectin galactose/N-acetylgalactosamine (Gal/GalNAc) acts as a receptor for *L.*

pneumophila (Venkataraman et al., 1997). However, this molecule does not seem to play a role in the attachment of *L. pneumophila* to *Acanthamoeba polyphaga*. This implies that different mechanisms are involved in the attachment of *L. pneumophila* to different species of amoeba (Harb et al., 1998). *L. pneumophila* proteins MOMP and Lcl and the macrophages complement receptors CR1 (CD35) and CR3 (CD18/CD11b) on the macrophage surface participate in complement-mediated attachment of the bacteria to macrophages (Payne and Horwitz, 1987). In addition, non-complement-mediated attachment of *L. pneumophila* has also been reported (Elliott and Winn, 1986; Gibson et al., 1994; Lau and Ashbolt, 2009; Rodgers and Gibson, 1993). All the available data point to *L. pneumophila* adhesion to the host cell being a host-specific process.

1.6.2 Phagocytosis of *L. pneumophila* by host cells

L. pneumophila uptake is predominantly mediated by host-mediated phagocytosis. *L. pneumophila* is phagocytosed by macrophages through a unique process called “coiling phagocytosis” following attachment to the host cell surface (Horwitz, 1984) (Figure 3.1). Unlike the conventional symmetrical and circumferential (zipper-like) phagocytosis, in coiling phagocytosis, extracellular bacteria are asymmetrically engulfed and encircled by unilateral pseudopods (Rittig et al., 1998). The functional significance of coiling phagocytosis on the virulence of *L. pneumophila* is not clear, as other *Legionella* strains and species can be taken up through conventional phagocytosis by their host (Al-Quadan et al., 2012; Elliott and Winn, 1986; Molmeret et al., 2005; Rechnitzer and Blom, 1989). Uptake of *L. pneumophila* by amoebae is mediated by both coiling and conventional phagocytosis (Abu Kwaik, 1996; Bozue and Johnson, 1996). Although *L. pneumophila* internalization primarily occurs through host-

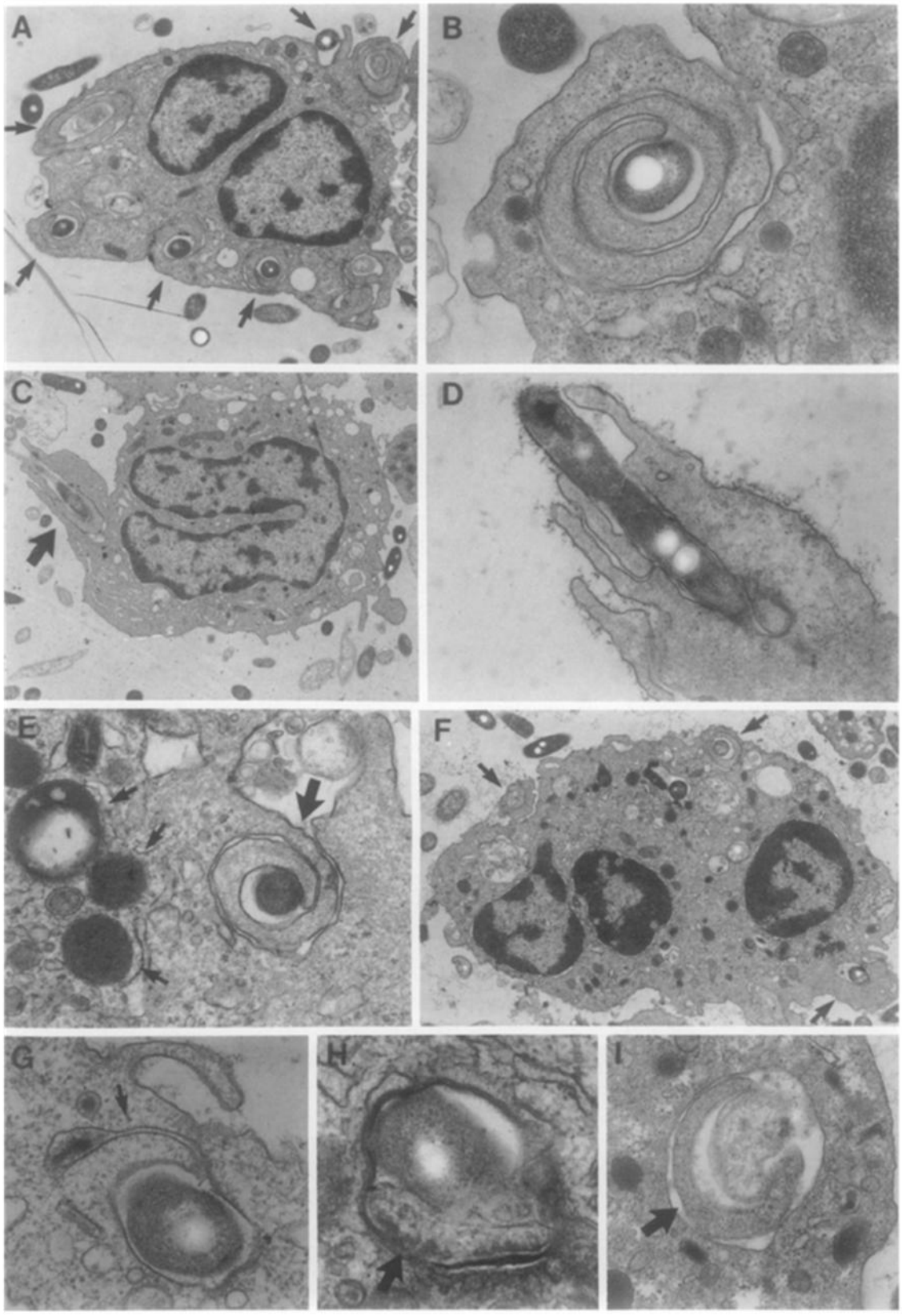
A
B
C
D
E
F
G
H
I

Figure 1.3 Phagocytosis of *L. pneumophila* by Human Phagocytes. *L. pneumophila* were mixed and then sedimented with monocytes (A-D, G, H), alveolar macrophages (E), or polymorphonuclear leukocytes (F, I) at 4° C, incubated for 3.5 min at 37 °C to allow phagocytosis to proceed, and rapidly fixed and processed for electron microscopy, as described in the text. (A) Cross-section through a monocyte showing the monocyte ingesting seven *L. pneumophila* (arrows), six of which are individually enclosed within a closed coiled monocyte pseudopod, (8650X). (B) Micrograph showing, at higher magnification, a monocyte ingesting a single *L. pneumophila*. The bacterium is located in the center of a coiled monocyte pseudopod. As is frequently the case, the bacterium contains a lucent fat vacuole, (28500X). (C) Cross-section of monocyte phagocytosis of *L. pneumophila* from a different perspective than in (A) and (B). The pseudopod coil (arrow) is sectioned along its axis so that bacterium is located between finger-like projections of monocyte membrane (5700X). (D) Higher magnification micrograph showing a monocyte ingesting *L. pneumophila* from the same perspective as in C. (22500X). (E) Cross-section through an alveolar macrophage showing the macrophage a *L. pneumophila* bacterium (large arrow). The alveolar macrophage contains numerous cytoplasmic inclusions characteristic of these cells (small arrows, (22500X). (F) Cross-section through polymorphonuclear leukocyte showing the phagocyte ingesting three *L. pneumophila* in pseudopod coils. (arrow), (7400X). (G) Late stage in monocyte phagocytosis of *L. pneumophila*. The monocyte has enclosed the bacterium in an intracellular vacuole. Incomplete fusion of monocyte plasma membrane about the bacterium has resulted in the creation of an intracellular sinus (arrow) continuous with the phagosome, (43000X). (H) and (I). Late stage in monocyte (H) and polymorphonuclear leukocyte (I) phagocytosis of *L. pneumophila*. The phagosomes contain what appear to be tucked-in protrusions of phagocyte membrane (arrow) caught in the vacuole during its formation. (H) (43000X), (I) (22500X) Figure and the figure legend are taken from (Horwitz, 1984).

driven phagocytosis, Icm/Dot translocated effectors such as LaiA/SdeA may mediate attachment and uptake of *L. pneumophila* as well (Bardill et al., 2005; Chang et al., 2005). *L. pneumophila laiA/sdeA* mutants are defective in attachment to and infection of epithelial cells. However, the biochemical mechanism behind how these effector proteins affect *L. pneumophila* adherence and uptake remains unknown.

on the host side, coronin and actin are implicated in *L. pneumophila* phagocytosis in both macrophages and amoebae (Escoll et al., 2013). In macrophages, the formation of a nascent phagosome is greatly actin-dependent and sensitive to the actin polymerization inhibitor drug cytochalasin-D during *L. pneumophila* uptake (Charpentier et al., 2009; Elliott and Winn, 1986; Hayashi et al., 2008; King et al., 1991). *L. pneumophila* uptake by the amoeba *Dictyostelium discoideum* is also actin-dependent (Lu and Clarke, 2005; Peracino et al., 2006; Weber et al., 2006). In addition, in both U937 macrophage-like cells and D*. discoideum* transient recruitment of the actin-binding protein, coronin, to the phagocytic cup and to the nascent phagosome have been shown during *L. pneumophila* uptake (Hayashi et al., 2008; Lu and Clarke, 2005). In summary, phagocytosis of *L. pneumophila* seems to be conserved at the molecular level between macrophages and amoebae.

1.6.3 Endocytic pathway and how *L. pneumophila* can avoid vacuole acidification

During phagocytosis, the nascent phagosomes go through an intracellular pathway that mirrors the endocytic pathway. The phagosome is transformed to a phagolysosome following serial fusion and fission events with endosomes, late endosomes, and lysosomes (Desjardins et al., 1994). The phagosome lumen becomes acidic and oxidative during the biogenesis of phagolysosomes, which then brings about

bacterial degradation (Birkeland and Stenmark, 2004; Vieira et al., 2004). However, *L. pneumophila* can evade the endocytic pathway and prevent phagosome-lysosome fusion after being internalized by the host cells. During infection, especially within 6 hours after bacterial uptake, the LCV lumen remains neutral (Horwitz, 1983b; Sturgill-Koszycki and Swanson, 2000; Swanson and Hammer, 2000). Around 18 h post-infection, the LCVs acquire endosomal markers such as lysosomal-associated membrane protein 1 (LAMP-1) and become acidic. Meanwhile, *L. pneumophila* bacteria residing in these late LCVs change from an acid-sensitive state to an acid-resistant one. (Sturgill-Koszycki and Swanson, 2000; Swanson and Hammer, 2000). In fact, the fusion of late replicative LCVs with the lysosomal compartment promotes *L. pneumophila* growth in macrophages (Swanson and Hammer, 2000).

Despite the ability of *L. pneumophila* to tolerate acidification of the LCV in macrophages at later stages of infection, maintaining neutral pH and avoiding vacuole acidification is necessary for successful infection during the early stages of the *L. pneumophila* life cycle. However, our knowledge of the molecular mechanisms governing how the LCV avoids vacuole acidification during early stages of infection is limited to a single study (Xu et al. 2010). Lumenal acidification of phagolysosomes is mainly mediated by ATP-dependent proton transporters, Vacuolar type H+-ATPases (V-ATPases) (Forgac, 2007). Interestingly, SidK, a *L. pneumophila* effector protein, inhibits the activity of the v-ATPase proton transporter through direct interaction with VatA, a key component of the proton pump that is responsible for ATP hydrolysis of the pump (Xu et al., 2010). Since avoidance of v-ATPase recruitment to the LCV is also known to be required for amoeba infection, it seems that v-ATPase activity at early stages of

infection is essential for successful *L. pneumophila* infection in both macrophages and amoeba (Escoll et al., 2013).

1.6.4 Remodeling of the LCV

Although formation of the LCV and avoidance of the endocytic pathway and vacuole acidification are essential for bacterial survival, remodeling the nascent LCV to a replication-permissive LCV by the host secretory pathway is required for bacterial growth in the host cells. In the process of remodeling, the LCV recruits host cell mitochondria. The LCV also recruits and fuses with the ER-derived small vesicles and rough ER (Horwitz, 1983a; Tilney et al., 2001). In addition, *L*. *pneumophila* also hijacks host polyubiquitinated (polyUb) proteins and decorates the LCV with them during LCV remodeling (Dorer et al., 2006; Lomma et al., 2010; Price et al., 2011). At the molecular level, LCV remodeling is very similar between amoeba and macrophages (Escoll et al., 2013).

Formation and maturation of the LCV occurs mostly in two phases through its interaction with the host secretory pathway. In the first phase, shortly after *L. pneumophila* uptake, the early "*legionella*-containing phagosome" intercepts vesicles exiting the ER and fuses with them. This process is dependent on the function of host Sar1 protein (small GTPase of the COPII), COPII protein (coat protein complex II), and the *L. pneumophila* Icm/Dot system. In this early phase, the LCV also recruits host mitochondria and polyUb proteins. In the second phase, ER membranes fuse with the LCV and deliver their content to the lumen of the LCV in a host Arf1 (ADP-ribosylation factor-1)-dependent manner (Kagan and Roy, 2002; Kagan et al., 2004) . Arf1 is a member of small guanine nucleotide-binding proteins (G-proteins) or small GTPase Arf

family that play essential roles in vesicular trafficking among different compartments (Donaldson and Jackson, 2000).

The LCV recruits ER-derived vesicles and fuses with them

Shortly after *L. pneumophila* uptake, during the early phase of LCV remodeling, the LCV interacts with the vesicles exiting the ER to exploit them for its own maturation. The host small GTPases Sar1, Arf1, and Rab1 have essential roles for LCV maturation. Small GTPases serve as molecular switches for many cellular events. Whether the GTPase is turned “on” or “off” depends on whether it is associated with GTP or GDP, respectively. While the GDP-bound GTPase is inactive and cytosolic, the active GTP-bound GTPase is membrane bound and capable of interacting with proteins that mostly regulate vesicular and membrane transport. Members of the Arf and Rab families of small GTPases play essential roles in eukaryotic vesicular trafficking. Sar1, Arf1, and Rab1 also play critical roles in LCV maturation, consistent with *L. pneumophila*’s ability to exploit the host secretory pathway.

Sar1 regulates COPII-coated vesicles formation. These vesicles are generated in ER exit sites (ERES) and facilitate cargo transportation from the ER to the Golgi complex (Sato and Nakano, 2007). Knockdown using siRNA, pharmacological inhibition, or dominant negative expression of Sar1 all show that Sar1 is essential for the formation of a “replication permissive” LCV(Dorer et al., 2006; Kagan and Roy, 2002). When cells expressing the dominant negative Sar1H79G mutant were infected with *L. pneumophila*, the LCV was not associated with the ER-derived vesicles. These results show that Sar1 function is important for recruiting vesicles from the ERES and tethering them to the LCV.

The small GTPase Rab1 is another host protein that is required for the early stages of LCV maturation. Rab GTPase family members regulate membrane transport and fusion in cells by recruiting cellular tethering factors and motor proteins (Stenmark, 2009). Rab1 is associated with host Golgi membranes and ER-derived vesicles and regulates protein transport from the ER to the Golgi apparatus by recruiting tethering factors (Moyer et al., 2001). Rab1 is recruited to the LCV in an Icm/Dot system-dependent manner and contributes to the recruitment of ER-derived vesicles to the LCV (Derre and Isberg, 2004; Kagan et al., 2004). The mechanism for this recruitment may be via Rab1's cooperation with *L. pneumophila* effector proteins that are involved in tethering of ER-derived vesicles (Machner and Isberg, 2006). *L. pneumophila* encodes a number of translocated effectors that regulate Rab1 activity and its recruitment to the LCV (Ingmundson et al., 2007; Machner and Isberg, 2007; Murata et al., 2006). SidM/DrrA has a substantial contribution to Rab1 recruitment to the LCV and its activation (Machner and Isberg, 2006; Murata et al., 2006; Nagai et al., 2002). SidM/DrrA is able to bind to PI(4)P through a novel 12 kDa C-terminally located P4M (PI(4)P-binding of SidM/DrrA) domain, which facilitates SidM/DrrA anchorage on the LCV. SidM/DrrA is a *L. pneumophila* Rab1 guanosine exchange factor (GEF) and a GDP dissociation inhibitor displacement factor (GDF) for Rab1. Both the GEF and GDF activities of SidM/DrrA are required for activation of Rab1. Thus, *L. pneumophila* uses a single effector protein, SidM/DrrA, to support recruitment of Rab1 and activate Rab1 by its GDF and GEF activities (Ingmundson et al., 2007; Machner and Isberg, 2007). Moreover, SidM lengthens the activation of Rab1 by functioning as an enzyme that catalyzes the covalently attaching of adenosine monophosphate (AMP) to Rab1, a post-

translational modification called “AMPylation” that limits GTPase activating proteins (GAPs) access to Rab1 (Muller et al., 2010).

In addition, another *L. pneumophila* PI-binding effector, LidA, enhances the SidM-driven recruitment of Rab1 (Machner and Isberg, 2006; Murata et al., 2006). LidA localizes to the cytoplasmic face of the LCV, activates SidM/DrrA, and therefore cooperates with SidM/DrrA for Rab1 recruitment to the LCV (Conover et al., 2003; Machner and Isberg, 2006). LidA preferentially binds to active Rab1 with an exceptionally high affinity and stabilizes this active form of Rab1 by blocking the interaction of Rab1 with GAPs. In addition, LidA stabilizes the active Rab1 by preventing de-AMPylation and dephosphocholination of Rab1 by two other bacterial effectors: SidD and Lem3, likely through steric hindrance (Neunuebel et al., 2012).

In contrast to SidM/DrrA, the *L. pneumophila* effector protein LepB, inactivates Rab1 by functioning as a GAP and facilitates removal of Rab1 from the LCV (Ingmundson et al., 2007). Thus, *L. pneumophila* encodes effector proteins that modulate Rab1 activity on the LCV by either activation or deactivation of Rab1 in diverse ways: through Rab1 GDI-displacement (GDF), nucleotide exchange (GEF), post-translational modifications (adenylylation, phosphocholination) or GTP hydrolysis (GAP). How all these effector proteins temporally coordinate their regulation of Rab1 on the LCV is a very interesting open question.

After being recruited to the LCV, the vesicles exiting the ER fuse with the LCV by exploiting the host protein Sec22b, a soluble NSF attachment protein receptor (SNARE) protein localized on the LCV-bound ER-derived vesicles, and syntaxins, which are PM-SNARES on the cytosolic surface of the LCV. SNARE proteins mediate membrane

fusion at all levels of the secretory pathway. In general, SNARE proteins are present in the donor and acceptor membranes and mediate the interaction between these membranes through the highly conserved four-helix bundle SNARE motifs that bring the membranes together and drive their fusion. The SNARE complex is composed of two types of proteins: v-SNAREs and t-SNAREs, which are the proteins, present on the donor and the target membranes, respectively (Sollner et al., 1993a; Sollner et al., 1993b; Weber et al., 1998). SNARE proteins also play a role in promoting ER-derived vesicle fusion with Golgi membranes. It is thought that Sec22b on ER-derived vesicles may play a role in their fusion with the LCV by non-canonical pairing with plasma membrane (PM) syntaxins that are integrated into the LCV during bacterial uptake. SidM/ DrrA effector proteins also play a role in this fusion by binding to PM-syntaxin and promoting pairing of Sec22b with PM syntaxins, which leads to fusion of ER-derived vesicles with LCVs (Arasaki and Roy, 2010; Arasaki et al., 2012).

Host polyubiquitinated proteins and their recruitment to the LCV

Host polyubiquitinated (polyUb) proteins are also recruited to the LCV during LCV remodeling. PolyUb proteins recruitment happens shortly after *L. pneumophila* infection in an Icm/Dot-dependent manner (Dorer et al., 2006; Lomma et al., 2010; Price et al., 2010a). The *L. pneumophila* effector AnkB plays a role in the recruitment of ubiquitinated proteins. AnkB anchors to the LCV through its CaaX motif that is farnesylated by the host farnesyltransferase. At the same time, AnkB attaches to host polyUb proteins through its ankyrin and an F-box domain, thereby functions as a platform onto which host polyUb proteins are recruited (Ivanov et al., 2010; Lomma et al., 2010; Price et al., 2010b). Besides remodeling the LCV, polyUb proteins have been

proposed to be proteasomally degraded during infection to increase host cellular levels of amino acids that can be used as carbon and energy sources for bacterial replication (Price et al., 2011). In both amoebae and macrophages, recruitment of polyUb proteins into the LCV by AnkB is required for intracellular multiplication (Al-Quadan and Kwaik, 2011; Lomma et al., 2010; Price et al., 2011). Thus, *L. pneumophila* exploitation of the host ubiquitination/proteasome machinery seems to be a conserved strategy in its infection of macrophages and amoebae.

Recruitment of host mitochondria to the LCV

Recruitment of at least one mitochondrion to the vicinity of LCVs has been reported in both human cells and amoeba shortly after infection with *L. pneumophila* (Horwitz, 1983a; Newsome et al., 1985). It is not clear why and how *L. pneumophila* recruits mitochondria, although it seems to be a Icm/Dot-dependent process, and *icm/dot* mutants defective in effector protein translocation do not recruit mitochondria in mammalian and amoebal hosts (Berger et al., 1994; Chong et al., 2009; Tilney et al., 2001). Translocated effectors like LncP (*Legionella* nucleotide carrier Protein) or LegS2/Spl have been found to be targeted to mitochondria (Degtyar et al., 2009; Dolezal et al., 2012); however, no translocated effector protein responsible for the recruitment of mitochondria to LCVs has been identified. Worth noting is that in contrast to mammalian and amoebal cells, in *Drosophila melanogaster* cells the recruitment of mitochondria near vacuoles doesn't seem to be Icm/Dot-dependent. In *dotA* mutant-infected cells, mitochondria accumulate around the LCV very similarly to the phenotype observed in wild type cells (Sun et al., 2013). Therefore, how *L. pneumophila* recruits

mitochondria is not yet clear and any functional consequences of the LCV's interaction with host mitochondria have not yet been identified.

Interaction of the LCV with the ER: the late phase event

Interaction of the LCV with rough ER and acquisition of ER proteins occur in the second phase of the LCV maturation. The fusion events in this phase are dependent on the host GTPase Arf1. In general, the regulatory function of Arf proteins is essential for vesicular trafficking between the ER and the Golgi. Arf GTPase proteins not only play critical roles in vesicular transport by recruiting and assembly of coat proteins that facilitate cargo sorting, but they also regulate many other proteins that play roles in the organization and trafficking of membrane vesicles. A large family of GEFs activates Arfs that all contain a conserved domain of almost 200 amino acids called the Sec7 domain. This domain is necessary and sufficient to activate Arf proteins by exchanging the Arf GDP to GTP (Donaldson and Jackson, 2000). Knockdown of Arf1 using siRNA, pharmacological inhibition of Arf1, and dominant negative expression of Arf1 in host cells (Dorer et al., 2006; Kagan and Roy, 2002) block intracellular multiplication of *L. pneumophila*. Thus, formation of a replication permissive LCV is dependent on the host Arf1. On the other hand, the *L. pneumophila* effector protein RalF is required for the recruitment of Arf1 to the LCV (Nagai et al., 2002). RalF contains a Sec7 domain at its N-terminus that has been shown to have GEF function for Arf proteins *in vitro* (Nagai et al., 2002). The GEF activity of RalF also seems necessary for recruitment of Arf1 to the LCV *in vivo* (Amor et al., 2005). Although inactivating host Arf1 protein inhibits intracellular bacterial growth, *L. pneumophila* mutants in which the RalF gene is deleted can still grow and replicate in host cells (Nagai et al., 2002). This suggests that host

Sec7 domain-containing proteins can activate Arf in the absence of RalF (Hubber and Roy, 2010). The crystal structure of RalF revealed two domains. The C-terminal domain forms a cap on the amino-terminal Sec7 domain and blocks the access of Arf1 to the Sec7 domain. Potentially RalF exists in both open and close forms and its interaction with membranes could play a role in regulating its activity by triggering a conformational switch (Amor et al., 2005).

The substrate of Icm/Dot transporter C (SidC) effector protein and its paralogue SdcA have been reported to anchor to the LCV through binding PI(4)P. SidC interacts with PI(4)P through a specific “PI(4)P-binding of SidC” (P4C) domain. P4C is a 20-kDa fragment near the C-terminus of SidC, which is unique to *L. pneumophila* and does not show similarity to eukaryotic PI(4)P binding domains. SidC and SidM compete with each other for binding on the LCV (Brombacher et al., 2009). SidC can promote ER-derived vesicle fusion to the LCV by binding ER vesicles and anchoring them to the LCV (Ragaz et al., 2008; Weber et al., 2006). A 70 kDa, N-terminally located predicted coiled-coil fragment of SidC is sufficient for binding to ER vesicles. It is also necessary for recruitment of ER vesicles to the LCV. SidC may function as a platform for host or other *L. pneumophila* interaction with the LCV.

The LCV harboring *L. pneumophila ΔsidC-sdcA* is impaired in acquiring the ER-resident protein calnexin, ER retention signal HDEL peptide, and lysosomal markers that are found in the wild-type LCV harboring *L. pneumophila*. Although deletion of SidC/SdcA may change organelle marker acquisition by the LCV compared to wild-type*L. pneumophila*, the membrane integrity of the LCV was not affected by deletion of SidC/Sdc. *L. pneumophila sidC-sdcA* deletion mutants do replicate at wild-type levels.

Therefore, the recruitment of ER is not essential for formation of a replication-permissive LCV. Alternative trafficking pathways may contribute to the LCV membranes acquisition that makes the LCV able to support bacterial replication, at which point they become replication-permissive LCVs (Ragaz et al., 2008; Weber et al., 2006).

L. pneumophila egress from host cells

After a few rounds of intracellular replication and following completion of the infection cycle, the *L. pneumophila* progeny in LCVs must escape the host cell and start a new cycle of infection in non-infected neighboring cells (Molmeret et al., 2004). Several *L. pneumophila* mutants defective in egress from both mammalian and amoebal host cells have been reported (Alli et al., 2000). However, the detailed molecular mechanisms and the proteins involved in *L. pneumophila* exit from the host cells are still unknown.

Several egress mechanisms have been proposed. Formation of a cytolysin/egress pore has been suggested to play a role in host cell lysis (Molmeret and Abu Kwaik, 2002). However, the *L. pneumophila* proteins that are involved in pore-forming activity and required for egress have not been identified (Alli et al., 2000; Molmeret and Abu Kwaik, 2002) . In addition, a non-lytic egress mechanism has been suggested in protozoan hosts. In this process, the intact LCV fuses with the plasma membrane of the protozoan host. Bacterial SNARE-like effectors LepA and LepB seem to be involved in this non-lytic process (Chen et al., 2004). LepB is a large protein that encompasses multiple domains and has Rab1-GAP activity. It has been suggested to function at different stages of *L. pneumophila* infection (Ingmundson et al., 2007). Although it is known that LepB associates with the LCV between 2-13 hours post

infection in mouse macrophages, the mechanism that LepA and LepB undertake to facilitate bacterial egress from protozoan cells remains to be found. *L. pneumophila* may use multiple egress strategies as a way for it to exit multiple host cell types under different conditions (Hubber and Roy, 2010).

1.7 *L. pneumophila* infection and PI metabolism

Similar to the above mentioned intracellular pathogens, *L. pneumophila* modulates host cellular signaling and PI metabolism to avoid degradation by the host cell. As exemplified by the pathogens *S. enteric, S. flexneri,* and *M. tuberculosis*, intracellular pathogens employ different strategies to exploit host PI signaling during infection. They encode PI metabolizing enzymes to hydrolyze the host cell PIs. They make proteins or lipids that affect host PI metabolizing enzymes. They produce effector proteins that bind to host PI kinases or phosphatases and directly recruit them to the LCV or take them away from their active site, as well as other effector proteins that activate small host GTPases. They generate PI binding effector proteins that bind host PIs located on the surface of PCVs or host cellular organelles and trigger or quench downstream signaling events that eventually benefit the bacteria (Hilbi, 2006a).

It seems that, in *L. pneumophila*, several effectors work together to shift the PI composition of the LCV into a PI composition similar to that found in the Golgi/ER membranes, which makes the LCV a PI(4)P-rich compartment. It stands to reason that the PI composition and lipid identity of the LCV play a significant role in LCV biogenesis and maturation to a replication-permissive compartment. Thus, unraveling the molecular mechanisms by which PIs are spatially and temporally regulated on the LCV is very important for understanding *L. pneumophila* pathogenicity. Identifying and studying *L.*

pneumophila effectors that subvert host PI lipid metabolism and the interplay between these effector proteins and their targets in the host cells are key to understanding *L. pneumophila* infection.

L. pneumophila translocates several PI-binding effector proteins to host cells during infection. Interestingly these effector proteins do not contain any known eukaryotic PI-binding domains. Several *L. pneumophila* effector proteins that can bind PIs and use this binding to anchor on the LCV membrane have been identified. 'Substrate of Icm/ Dot transporter C' (SidC) protein, its paralog SdcA, and the Rab1 guanine nucleotide exchange factor (GEF) SidM/DrrA all bind to PI(4)P (Brombacher et al., 2009; Ragaz et al., 2008; Weber et al., 2006). 'Lowered viability in the presence of dotA' (LidA) binds to both PI(3)P and PI(4)P (Derre and Isberg, 2005; Machner and Isberg, 2006). '*L. pneumophila* entry' LpnE, 'subversion of eukaryotic traffic A' SetA, and LtpD bind to PI(3)P (Harding et al., 2013; Heidtman et al., 2009; Newton et al., 2006). It is thought that *L. pneumophila* may use these LCV-anchored translocated effectors as facilitators to acquire host secretory vesicles and to promote LCV biogenesis and maturation (Brombacher et al., 2009; Ingmundson et al., 2007; Urwyler et al., 2009; Weber et al., 2006). Besides the previously described functions of these PI-binding bacterial effectors during the *L. pneumophila* life cycle, I will now discuss several other functions of these proteins relating to *L. pneumophila*'s ability to change the PI identity of LCVs.

SetA is secreted into the host cells and anchors on the cytoplasmic leaflet of the LCV through its binding with PI(3)P during infection. Once it binds to LCV, SetA can

glycosylate its substrates, which may be necessary for the early steps of LCV maturation (Heidtman et al., 2009; Jank et al., 2012).

LtpD localizes on the cytoplasmic face of the LCV through its PI(3)P binding domain during infection. It has been shown that LtpD is required for optimal intercellular *L. pneumophila* growth. Exogenous expression of LtpD in mammalian cells suggests that LtpD may play a role in helping the LCV avoid the endocytic pathway by interfering with host endosomal vesicle trafficking. However, LCVs that harbor *L. pneumophila* which lack or overproduce LtpD did not show any detectable differences in endosomal marker recruitment. The absence of phenotype may be because of functional redundancy by other T4SS effectors. (Harding et al., 2013). LtpD binds to the host cell enzyme inositol (*myo*)-1 (or 4)-monophosphatase IMPA1**,** an important phosphatase involved in the generation of phosphoinositides, as well as second messengers myoinositol 1,4,5-trisphosphate and diacylglycerol (McAllister et al., 1992). It seems that binding between LtpD and IMPA1 does not have any effect on modulation of IMPA1 enzymatic activity *in vitro*. The significance of the interaction between LtpD and IMPA1 during infection is still an open question, although it can be speculated that LtpD may facilitate IMPA1 interaction with other host or bacterial proteins (Harding et al., 2013).

Host PI metabolizing enzymes have also been shown to contribute to generating PI(4)P on the LCV. For example, the phosphatidylinositol 4-kinase (PI4K) PI4KIIIβ converts PI into PI(4)P (Brombacher et al., 2009) and human protein phosphatases dephosphorylate PI(4,5)P_2 to produce PI(4)P (Lowe, 2005). In fact, experiments involving depletion of host PI4-kinases by RNA interference suggest that PI4KIIIβ, but not PI4KIIIα contributes to the formation of PI(4)P on the LCV *(Brombacher et al.,*

2009). A few *L. pneumophila* effector proteins may modulate PIs on the LCV membrane through indirect interactions with (PI4K) PI4KIIIβ and OCRL1, a PI(4,5)P_2 5-phosphatase localized on the Golgi apparatus and known to be critical in regulating the endocytic pathway and retrograde traffic from the endosome to the trans-Golgi network (TGN), as well as in the maintenance of TGN (Lowe, 2005). The *L. pneumophila* effector protein LpnE binds to PI(3)P and anchors on the cytosolic surface of the LCV, and can also interact with the N-terminal domain of OCRL1 (Weber et al., 2009). LpnE might play a role in the regulation of PI composition on the LCV by recruiting OCRL1 which can hydrolyze PI(4,5)P_2 and increases PI(4)P levels on the LCV (Haneburger and Hilbi, 2013). Furthermore, LpnE has been shown to be critical for *L. pneumophila* entry into both mammalian and amoebal cells. LpnE mutants are defective in avoidance of LAMP-1 association, implying that LpnE plays a role in LCV formation and in regulating vacuolar trafficking in order to prevent the LCV from acquiring lysosomal characteristics (Newton et al., 2007).

The *L. pneumophila* effector RalF might also modulate the PI composition of the LCV through recruitment and activation of the host small GTPase Arf1 (Haneburger and Hilbi, 2013). RalF recruits Arf1 to the LCV (Nagai et al., 2002), thereby regulating ER to the Golgi vesicle trafficking (Donaldson and Jackson, 2000). In addition, It has been shown that Arf1 can recruit and activate PI4-kinase IIIβ and Arf1 can recruit and activate PI4-kinase IIIβ to trans-Golgi network (TGN) (Godi et al., 1999). Thus, Arf1 may play a role in PI(4)P formation on the LCV by recruiting and activating the PI4-kinase IIIβ to the LCV (Haneburger and Hilbi, 2013).

Similarly, the Icm/Dot substrate SidM/DrrA that has both GEF and GDF activities for Rab1 recruits and activates Rab1 on LCV membranes and lengthens Rab1 activation by Rab1 AMPylation. (Ingmundson et al., 2007; Machner and Isberg, 2007; Muller et al., 2010). Meanwhile, it has been shown that activated Rab1 (Hyvola et al., 2006) and activated Arf1(Lichter-Konecki et al., 2006) can recruit OCRL1 to endosomal membranes. Therefore, SidM/DrrA and RalF may indirectly contribute to the enrichment of PI(4)P on LCV membranes by facilitating recruitment of OCRL1 to LCVs (Haneburger and Hilbi, 2013).

Lastly, LpdA and LecE are Icm/Dot substrates that localize to the LCVs and their combined activity is thought to promote conversion of PC to DAG (Viner et al., 2012). DAG is a second messenger and its activity results in recruitment of protein kinase D (PKD) (Fu and Rubin, 2011) and protein kinase C (PKC) to the LCV membrane (Almena and Merida, 2011). PKC can phosphorylate and activate PKD that in turn will lead to PI4KIIIβ recruitment to the LCV. So far, *L. pneumophila* effector proteins LpnE, RalF, SidM/DrrA, LpdA and LecE are the only bacterial protein that may indirectly contribute to the production of PI(4)P on the LCV by exploiting the host PI metabolizing enzymes PI4KIIIβ and OCRL1. However, no *L. pneumophila* PI-metabolizing enzymes have been discovered to date, although as it was discussed earlier that other intracellular pathogens such as *S. flexneri*, *S. enterica* and *M. tuberculosis* encode bacterial phosphatases to target host cell PI metabolism and signaling during infection(Payrastre et al., 2012).

The presence of PI phosphatases in these pathogens further motivated our lab to try to identify genes that may encode PI phosphatases in *L. pneumophila.*

Thesis outline

In this dissertation, I will discuss my work, which focuses on the identification and characterization of a novel PI phosphatase in *L. pneumophila*, called SidP. An introduction to PI metabolism and their role in pathogenesis of intracellular pathogens is provided in chapter one. Chapter 2 will cover materials and methods used to perform the experiments described in this dissertation. Chapter 3 first describes the identification of this novel PI phosphatase by bioinformatics. It then lays out the in vitro and in vivo experiments demonstrating the PI phosphatase activity and substrate specificity of SidP as a PI(3)P phosphatase. I hypothesized that SidP may affect host cellular pathways that require PI(3)P, and therefore PI(3)P hydrolysis by SidP may be used as a pathogenicity factor by *L. pneumophila* compromising those pathways in host cells. The last part of chapter three covers the experiments that I have done to address the possible role of SidP in *L. pneumophila* pathogenicity.

Chapter 4 centers on crystal structure of the SidP in order to get insights into the substrate specificity of SidP. I first describe my efforts to obtain the various SidP protein constructs used in my attempts to crystallize SidP. Since none of our SidP protein variants resulted in any crystals, I eventually successfully crystallized the SidP orthologue from *L. longbeachae*. In the last part of this chapter, using the SidP orthologue structure determination, I discuss SidP substrate specificity. Finally, in chapter 5 I present a model that describes the possible contribution of SidP in *L. pneumophila* pathogenicity, and I suggest some future experiments related to the research presented in this dissertation.

CHAPTER 2

Materials and Methods

2.1 Protein expression and purification

All recombinant proteins were expressed in the *E.coli* Rosetta strain, which was grown in LB medium supplemented with 50 µg/mL kanamycin. Protein expression was induced at OD_{600} = 0.8 for overnight at 18 °C with 0.1 mM isopropyl- B-D-thiogalactopyranoside (IPTG). The selenomethionine-substituted proteins were expressed in M9 minimal media supplied with “Drop-out Mix Synthetic Minus Methionine w/o Yeast Nitrogen Base Powder” (US Biological). Selenomethionine powder (Affymetrix) was added with a final concentration of 120 mg/L of LB 15 min before IPTG induction. Harvested cells were resuspended in a buffer containing 50 mM Tris-HCl at pH 8.0, 500 mM NaCl, and protease inhibitor mixture (Roche) and were lysed by sonication. Soluble fractions were collected by centrifugation at 40,000 g for 40 min at 4 °C and incubated with cobalt resins (Clontech) for 2 hours at 4 °C. Protein bound resins were extensively washed with lysis buffer. The His-SUMO tag was removed by incubating the protein bound resin with the SUMO-specific protease Ulp1 at 4 °C for overnight. Eluted protein samples were further purified by FPLC size exclusion chromatography. The peak corresponding to SidP and the homologue were pooled and concentrated using Amicon ultra centrifugal filter units (EMD Millipore, MA, USA) to 7-8 mg/ml in a buffer containing 50mM HEPES at pH 7.4 and 150 mM NaCl.

2.2 Enzymatic assays

All diC8-phosphoinositides were purchased from Cell Signals, Inc. All reactions were performed in a polystyrene 96-well plate for 20 min at 37 °C with a total volume of

50 μl, which contains reaction buffer (50 mM Tris-HCl pH 8.0 and 150 mM NaCl, 1mM DTT), 1 nmol of lipids, and 0.1 μg of purified enzymes. Phosphate release was measured at OD_{620} absorbance with the addition of malachite green reagent as described (Maehama et al., 2000).

2.3 Cloning and mutagenesis

SidP (Lpg0130) gene and its *Longbeachae* orthologue were PCR amplified from the *L. pneumophila* strain Philadelphia 1 and *L. longbeachae* strain NSW150 genomic DNA, respectively. The PCR products were digested with BamH1 and Xho1 or Sal1 restriction enzymes and inserted into a pET28a-based vector in frame with an N-terminal His-SUMO tag. The same digested SidP fragments were inserted into pRS415-p*GPD*-GFP and pEGFP-C1 vectors (Parrish et al., 2005) for the expression of GFP fused SidP and its catalytically inactive mutant in yeast and mammalian cells, respectively. Point mutations were generated by site directed mutagenesis. All constructs were confirmed by DNA sequencing.

2.4 Yeast *in vivo* experiment and analysis

Yeast strain YTS1: SEY6210.1 *ymr1Δsjl2Δ sjl3Δ* harboring pRS415*ymr1*^{ts} (Parrish et al., 2004) and strain YCS215: *sac1*^{ts}*sjl2Δsjl3Δ* (Foti et al., 2001), which carries a temperature sensitive allele of the SAC1 gene and null alleles of SJL2 and SJL3, were transformed with indicated plasmids. For growth assay, yeast transformants were grown to midlog (OD_{600}=0.5) at permissive temperature (26 °C), adjusted to 10D/ml, serially diluted 1:10 3 times, spotted onto –Leu selection plates. The viability of these transformed cells was analyzed by incubating the plates in permissive and

restricted temperatures after 3-4 days. PI levels were analyzed as previously described (Stefan et al., 2002). Briefly, cells transformed with control empty vector or vector harboring WT or mutant SidP were grown to log phase. Cells (5 OD_{600}) were harvested, washed in media lacking inositol, and labeled with 50 μCi of myo-[2-^{3}H] inositol (Perkin Elmer) in synthetic media lacking inositol for 1 hour. Lipids were deacylated. [^{3}H] glycerophosphoinositides were extracted and 5 x 10^{6} cpm of samples were separated by HPLC.

2.5 Crystallization and preliminary X-ray crystallographic analysis

Initial crystallization trials were set up with a PHOENIX liquid handling system (Art Robbins Instruments). SidP crystals were improved by hanging drop vapor diffusion at 4 °C by mixing 1 µl of protein (7.5mg/ml) with an equal volume of reservoir solution containing 0.1M succinic acid, 0.1M HEPES at pH 7.0, 6.5% (wt/vol) PEG3350, 5 mM DTT. Plate shape crystals were formed within 7-10 days. Selenomethionine substituted SidP crystals were grown under similar conditions. For data collection, SidP crystals were transferred step-wise into the same solution supplemented with 20% glycerol before flash cooling to 100 K in liquid nitrogen. The crystal diffracted up to 2.58 Å at the Cornell synchrotron light source MacCHESS beam line A1. All data sets were indexed, integrated and scaled with HKL-2000 (Otwinowski and Minor, 1997). The crystals belong to space group $P2_1$ with unit cell parameters of a = 89.28 Å, b = 119.65 Å, c = 133.53 Å, $\alpha = 90^0$, $\beta = 101.33^0$, $\gamma = 90^0$ (Table 4.3). The calculated Matthews coefficient V_m= 3.9 and with 68.4% of solvent in the crystal and two protein molecules in an asymmetric unit (Matthews, 1968).

2.6 Structure determination and refinement

Twenty selenium sites were identified in the asymmetric unit by SAD method using the program HKL2MAP (Pape and Schneider, 2004). The initial phase was calculated by single anomalous scattering (SAD) method and was improved by solvent flattening in HKL2MAP. The *ab initio* protein model was then built with COOT (Emsley and Cowtan, 2004). Iterative cycles of model building and refinement were carried out with refmac5 (Murshudov et al., 1997) in the CCP4 suite (Collaborative Computational Project, 1994) to complete the final model. The final SidP structure consists of 1-825 amino acids with excellent stereochemistry and good crystallographic statistics (Table 4.3).

2.7 Small angle X-ray scattering (SAXS) data collecting and processing

SAXS experiments were done at the Cornell High Energy Synchrotron Source (CHESS, beam line F2) at X-ray of 9.881 keV at 25 °C on monodisperse and homogeneous samples. Protein was expressed and purified as described before in the protein expression and purification procedure. Protein concentrations were determined using the Bradford protein assay (Bio-Rad). Freshly purified proteins were centrifuged at 13,200 rpm and 4 °C for 10 min prior to loading into a flow cell. Scattering data were collected in triplicate at four different protein concentrations ranging (0.6, 1.25, 2.5, and 5 mg/mL in a buffer containing 20 mM Tris-HCl pH 7.4, 150 mM NaCl, 5mM DTT. In order to avoid concentration-dependent scattering, protein concentrations higher than 5 mg/ml were not used for data collection. The BioXTAS RAW program (http://sourceforge.net/projects/bioxtasraw/) was used for data reduction, averaging, and scaling to provide one-dimensional intensity profiles as function of q ($4\pi sin\theta/\lambda$, where

2θ is the scattering angle). Data were collected and used for further analysis, only if the data did not show any sign of radiation damage or aggregation based on examining of Guinier plots. Background scattering was collected from buffer and subtracted from the scattering data (Figure 4.10A). Program package ATSAS was used for further analysis, and free-atom modeling of the SAXS data (Petoukhov, 2007). Only scattering data with Smax Rg < 1.3, calculated from low-angle regions of Guinier plots r, were qualified for the more analysis. Kratky plots were used to evaluate data quality and get information about the folded state of the proteins (Figure 4.10B). CRYSOL (Svergun et al., 1995) was used to calculate the theoretical scattering for the two possible models in the LLO_3270 crystal and was compared to the experimental scattering data (Figure 4.9B).

The final averaged scattering profile, covering a q-range from 0.01 to 0.25 $Å^{-1}$ was further analyzed using the programs GNOM (Semenyuk, 1991; Svergun, 1992) to calculate distance distribution function *P(r)* (Figure 4.10C). Low resolution shapes were calculated and averaged from solution scattering data using the programs DAMMIF (Franke and Svergun, 2009) and DAMAVER (Volkov and Svergun, 2003). The crystal structure of LLO_3270 was docked in the low resolution solution structure using SUPCOMB (Figure 4.9C) (Kozin and Svergun, 2001).

2.8 Bacterial strains and growth conditions

E. coli strains were grown in LB supplemented with the appropriate antibiotics. All *Legionella* strains that I used in my experiments were derivatives of the *L. pneumophila* Philadelphia-1 wild-type strain, and received from Zhao-Qing Luo lab, Department of Biological Sciences, Purdue University, IN, USA. The *L. pneumophila* strains were grown on charcoal-yeast extract (CYE) plates or in ACES-buffered yeast

extract (AYE)(Feeley et al., 1979). *L. pneumophila* strains were considered being in the post-exponential phase when the optical density of the cultures were (OD_{600} = 3.3-3.8) and there was an increase in bacterial motility.

2.9 Thin Layer Chromatography

For each reaction, 0.1 µg of purified enzyme and 1 µg of the green fluorophore, Bodipy-FL labeled diC6 PI lipid substrates (Echelon Research Laboratories) were added to 20 µL of buffer containing 50 mM ammonium carbonate at pH 8.0 and 2 mM DTT then incubated for 20 min at 37 °C. If two enzymes needed to be added to a reaction, the first reaction was allowed to be completed and then the second enzyme was added and the reaction was incubated for another 20 min at 37 °C. When the reactions were completed, the products were dried in Speed-Vac for 30 min at 45 °C. 10 µL of methanol/isopropanol/acetic acid (5/5/2) was used to resuspend the pellet from each reaction. Resuspended samples were spotted on the bottom of a TLC Silica gel 60 F254 (EMD). Prior to sample loading the TLC Silica plate was soaked in methanol/water (3:2) containing 1% potassium oxalate and then dried in a 65 °C oven for one hour. Samples were loaded at the bottom of the TLC plate, which was then placed in a shallow pool of a solvent mixture of 1-propanol / 2 M acetic acid (65%:35%) in a developing chamber, with only the bottom of the plate covered in solvent. The solvent slowly moved up on the TLC and when it reached to the spotted samples, it carried out the soluble components of each sample and separate them based on their mobility and solubility. When the solvent reached the top of the plate, the plate was removed from the developing chamber, and using a Bio-Rad Gel dock system Fluorescent PIs were visualized under UV light.

2.10 Cell culture and transfection

RAW 264.7 macrophage cell line were cultured in Dulbecco's modified Eagle medium (DMEM) supplemented with 10% heat-inactivated FBS (PAA Laboratories) and penicillin-streptomycin solution (Cellgro) at 37 °C in 5% CO_2 . RAW 264.7 macrophage cells were used for infection, as described later.

HEK293T cells were maintained and grown in Dulbecco's modified Eagle medium (DMEM) supplemented with 10% FBS (Cellgro) and 1% penicillin-streptomycin solution (Cellgro) at 37 °C in 5% CO_2. For transient transfection, HEK293Tcells were grown to about 60% confluence and the appropriate plasmid DNA were transfected into cells using polyethylenimine (PEI) reagent at 1:5 ratio of DNA:PEI (Vancha et al., 2004). 24 hours after transfecting cells, they were fixed with 3.7% formaldehyde, 20% sucrose in PBS for 15 minutes at room temperature, or were collected with the addition of Laemmli sample buffer (100 mM Tris-HCl, pH 6.8, 2% SDS, 10% glycerol, 6% ß-mercaptoethanol, 0.0025% Bromophenol Blue) , followed by sonication and boiling. For microscopy, cells were plated on 12 mm sterile cover glasses coated with poly-(L)-lysine in 24-well plates. For some assays, cells were treated with drugs, starved or infected after transfection, and then fixed or lysed.

2.11 Bacterial Infection

RAW 264.7 macrophages constitutively expressing GFP-2XFYVE were seeded on coated cover glasses one day before infection and were grown in an antibiotic-free medium. The *L. pneumophila* Philadelphia-1 strains expressing DsRed also were inoculated early in the morning on the day before infection so they would be grown to

the post-exponential phase and ready for infection on the day after. The plated macrophages were infected with relevant strains at a multiplicity of infection (MOI) of 1. The plates were spun at 1000 rpm for 5 minutes to let bacteria settle down, and then the infected macrophages were incubated at 37 °C. 1 hour post-infection the cells were washed 3 times with 37 °C PBS, to remove a majority of bacteria that had not started internalization into the host cells, thereby synchronizing the infection. Medium was added to the wells and the samples were placed in a 37 °C incubator for indicated time periods and fixed in 10% sucrose in paraformaldehyde/lysine/periodate (PLP) fixative (McLean and Nakane, 1974). For earlier time points, the washes were done right before the fixation.

2.12 Immunofluorescence Microscopy

The fixed HEK293T cells transfected with GFP or m-cherry tagged proteins were directly mounted with Fluoromount-G (Southern Biotech, Birmingham, AL, USA).

Fixed RAW 264.7 macrophages were blocked in PBS containing 4% normal donkey serum (NDS) for 15 minutes in in 37 °C , followed by incubation with the primary rabbit-anti- *L. pneumophila* antibody diluted 1:10000 in PBS containing 4% NDS for 30 minutes in 37 °C. This antibody would interact with the non-internalized bacteria allowing us to distinguish internalized from the non-internalized bacteria. Extensive washing with PBS followed the primary antibody incubation. Then cells were incubated with secondary antibodies conjugated to CF405S Goat Anti-Rabbit IgG (H+L), (1: 500) (Biotium, Hayward, CA, USA) for an hour in 37 °C and washed extensively with PBS after secondary incubations, and then mounted with Fluoromount-G.

For both RAW 264.7 macrophages and HEK293T cells Images were collected using the 63X objective on a Zeiss LSM 700 confocal microscope (Carl Zeiss).

2.13 Western blot

Protein samples in Laemmli sample buffer containing β-mercaptoethanol were boiled for 5 minutes, resolved by SDS-PAGE, and then transferred to polyvinylidene fluoride (PVDF) membranes (Millipore Corporation, Bedford, MA, USA). After blocking the membrane with 5% non-fat milk in Tris-buffered saline (TBS) (in 20 mM Tris, 135 mM NaCl) or Odyssey Blocking Buffer (LI-COR Biosciences) for 2 hours at room temperature or overnight at 4 °C, the membranes were incubated with the indicated primary antibodies diluted in TBST (in 20 mM Tris, 135 mM NaCl, and 0.1% Tween-20) and then washed extensively with TBST. The primary antibodies were detected with secondary antibodies. Secondary antibody incubation for 2 hours at room temperature was followed by extensive washing and imaging using an Odyssey Infrared Imaging System (LI-COR Biosciences, Lincoln, NE, USA). If necessary, intensity of the bands in the resulting blots were quantified by using LI-COR software and normalized to a corresponding reference band.

2.14 Antibodies, drugs, special reagents

The following antibodies were used for western blot, and immunofluorescence. Rabbit polyclonal antibody against full length GFP (1:1000), mouse anti-GAPDH (1:750), and goat anti-LC3 (1:200), all were purchased from Santa Cruz Biotechnology, Inc. Antisera against rabbit-anti- *L. pneumophila* (1:10000), and rabbit-anti-isocitrate dehydrogenase (ICDH) (1:10000) were gifts from from Zhao-Qing Luo lab. (Department

of Biological Sciences, Purdue University, IN, USA). Full length recombinant SidP protein were used as an antigen to produce a specific rabbit polyclonal antibody against SidP following a standard protocol (Covance, Princeton, NJ, USA). Serum from the final bleed was diluted 1:10000 times and used. The specificity of SidP antibody was confirmed via western blot using the purified SidP protein as the control.

HBSS (Hank's Balanced Salt Solution) plus calcium, magnesium, and no phenol red (GIBCO® HBSS Cat# 14025) was used for starving the cells, when it was needed. Bafilomycin A1 was purchased from LC Laboratories.

2.15 Yeast TCA Whole Cell Extracts

Yeast cells were grown to mid-log phase. 5 OD_{600} equivalents of cells were collected by centrifugation and washed with 20% trichloroacidic acid (TCA) from Acros Organics. The cell pellets were frozen in –80 °C. The frozen cells were thawed on ice and resuspended in 20% TCA. Then cells were mechanically lysed with glass beads in 4 °C.

Cell lysates and precipitates were spun down in 4 °C and the pellets were washed with 100% EtOH (-20 °C). Precipitates were resuspended in 40 μl of 1 M Tris HCl pH8.0 and 80 μl of 2X Laemmli sample buffer. Samples were boiled for 5 minutes, followed by spinning at 14 K, for 5 minutes at RT. Supernatants were collected and 5-10 μl were analysed by SDS–PAGE and immunoblotting.

CHAPTER 3

Identification of a *L. pneumophila* Effector that Functions as PI Phosphatase[1]

3.1 Introduction

PIs can undergo catabolism through phospholipase-dependent mechanisms or PI phosphatase-dependent dephosphorylation at the D-3, D-4 and/or D-5 positions of the inositol ring. PI phosphatases are highly conserved throughout the eukaryotes. There are seven known PI phosphatases in yeast that are categorized in three subgroups based on their catalytic domain properties: the SAC-domain phosphatases; the inositol polyphosphate 5-phosphatase domain enzymes; and the myotubularin ortholog Ymr1 (Strahl and Thorner, 2007).

Mammalian PI phosphatases are divided into two superfamilies: the inositide polyphosphate 5-phosphatase superfamily, and the protein tyrosine phosphatase (PTP) superfamily. Each of these two superfamilies is further categorized into a few families.

PI-5-phosphatase family enzymes dephosphorylate the D-5 position of the inositol head group of PI(3,5)P_2, PI(4,5)P_2, PI(3,4,5)P_3, Ins(1,4,5)P_3 and, Ins(1,3,4,5)P_4. The PI-5-phosphatase superfamily is divided into four families: group I only hydrolyzes soluble inositol polyphosphates(InsP)s: Ins(1,4,5)P_3 and Ins(1,3,4,5)P_4; group II (e.g. OCRL1) hydrolyzes both PI and soluble InsP substrates; group III enzymes (e.g.SHIP1 and SHIP2) preferably hydrolyze PIs; and group IV exclusively hydrolyzes PI(4,5)P_2 ,PI(3,4,5)P_3 (Liu and Bankaitis, 2010; Mitchell et al., 1996). This family is characterized by having a central catalytic domain consisting of almost 300 residues that contains two signature motifs: WXGDXN(F/Y)R and P(A/S)W(C/T)DRIL separated by about 60–75

[1] Starting from this chapter till the end, the majority of results that has been presented in this thesis have been published previously as Toulabi L, et al. (2013) *J Biol Chem* 288: 24518-27

residues (Majerus et al., 1999). The PI-5-phosphatases have a similar structural fold to those of magnesium-dependent endonucleases, and functions similar to these endonucleases as well, showing phosphomonoesterase activity in a magnesium-dependent manner. Bioinformatics methods and mutagenesis studies suggest that inositide polyphosphate-5-phosphatases use the same catalytic mechanism that the apurinic/apyrimidinic base excision repair endonucleases use to hydrolyze their substrates (Liu and Bankaitis, 2010).

The PI phosphatases of the PTP-superfamily are divided into four primary families. One family is the PI- 4-phosphatases type I and II whose primary substrate is $PI(3,4)P_2$ (Norris et al., 1997; Nystuen et al., 2001). PTEN (phosphatase and tensin homolog) family of PI-3-phosphate phosphatases is included in this superfamily. PTEN, a tumor suppressor gene, hydrolyzes $PI(3,4,5)P_3$. The tumor suppressor activity of PTEN is believed to arise from hydrolyzing the membrane-bound $PI(3,4,5)P_3$, which is a signal in the regulation of cell proliferation, cell migration, and apoptosis. A third member of the PTP-superfamily is the myotubularins family of PI-3-phosphatases. Myotubularin (MTM1) is the founding member of this family, which was discovered by isolation of a gene mutated in X-linked centromyotubular myopathy. Mutations in several genes of this family are associated with human diseases. The Sac1-like PI phosphatases that contain a SAC domain (Suppressor of ACtin) also belong to the PTP superfamily. The Sac1-like PI phosphatases can hydrolyze a diverse range of PI substrates. This family is subdivided into two subgroups. One group contains only a Sac domain (e.g. human and yeast Sac1 protein) and the other group contains a SAC-

domain appended to PI-5- phosphatase domains (e.g. the synaptojanins)(Liu and Bankaitis, 2010).

PTP-superfamily PI phosphatases are metal-independent enzymes that use the signature sequence "CX_5R" catalytic motif to dephosphorylate PI substrates (Denu and Dixon, 1998). The PTP-like signature sequence "CX_5R" is the signature sequence of the catalytic residues in a number of enzymes, including lipid phosphatases (Begley et al., 2006), protein tyrosine phosphatases (PTPs) (Barford et al., 1998), and arsenate reductases (Mukhopadhyay and Rosen, 2002). The "CX_5R" containing enzymes are a diverse group of enzymes found in both eukaryotes and prokaryotes, which hydrolyze phosphoryl groups from protein substrates, specifically, phosphotyrosine, threonine and serine containing peptides (Denu and Dixon, 1995; Zhang, 2002) or/and from PIs and, inositol polyphosphates (IPP)s (Deleu et al., 2006; Maehama and Dixon, 1998).

3.2 Results

3.2.1 Identifying PI phosphatase candidates using a bioinformatics approach

The main goal of my project was identifying and characterizing *L. pneumophila* proteins that function as PI phosphatases. For this purpose, we initially took a bioinformatics approach and searched the genome of *L. pneumophila*, strain "Philadelphia". In this search, we used a sequence pattern-based method and searched for the "CX_5R" motif. We considered the "Cx_5R" motif as a strong screening tool for identifying PI phosphatases, since it is the catalytic motif of four major families of PI phosphatases: PTEN, MTM/MTMR, Sac and, 4-Ptase (Liu and Bankaitis, 2010). Moreover, the "CX_5R" motif is the catalytic motif of *S. enterica* SopB/SigD phosphatase,

S. flexneri IpgD phosphatase and *M. tuberculosis* MptpB phosphatase (Payrastre et al., 2012).

Using this bioinformatics approach, our lab identified 400 open-reading frames containing the "CX_5R" motif, of which 29 are believed to be substrates of the Icm/Dot secretion system (Hsu et al., 2012; Zhu et al., 2011). When I started my thesis research project, I expressed recombinant proteins of four of these 29 candidates, and tested them for phosphatase activity. Two of them showed phosphatase activity. Then, I focused on characterizing one of these candidates, the *L. pneumophila* effector Lpg0130, which we have named SidP (Substrate of Icm/Dot phosphatase). Our discovery and characterization of this novel *L. pneumophila* phosphatase brings new emphasis to the role of host PI metabolism subversion during intracellular pathogen infection, and significantly advances the field.

3.2.2 *L. pneumophila* effector SidP is a PI-3-phosphatase

SidP is an 822 amino acid protein with the peptide sequence "CVSGKDR" located between residues 553 and 561, which led me to believe that it is a potential PI phosphatase (Figure 3.2A). In order to determine whether this "CX_5R" motif, also called P-loop, functions as a PI phosphatase, I expressed recombinant SidP in the Rosetta (DE3) E. coli strain, then purified it to homogeneity using affinity chromatography followed by size exclusion chromatography (Figure 3.1A, B). I then examined the purified SidP for *in vitro* PI phosphatase activity by a malachite green based assay (Maehama et al., 2000).

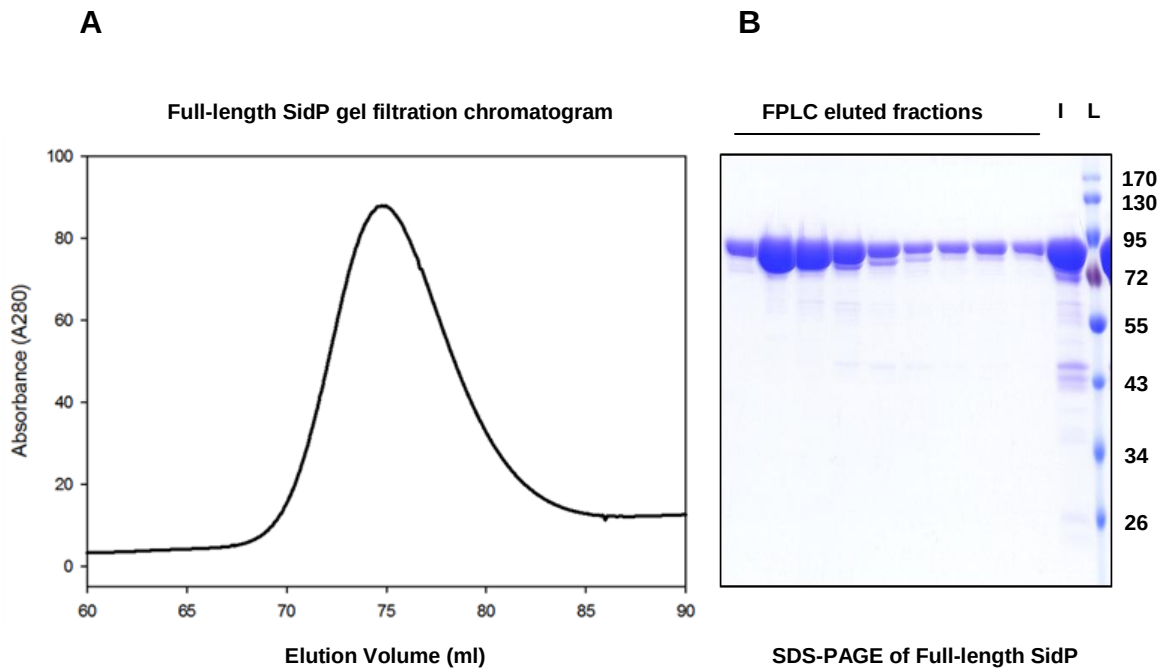

Figure 3.1 Gel filtration and SDS-PAGE of SidP. (A) Untagged-SidP elutes off the size-exclusion column as a single peak after approximately 70 mL. (B) The injected protein (I) has a little lower molecular weight contaminants or degraded protein, but these are removed from the eluted fractions. The (L) lane on the right is the molecular weight ladder (in kDa).

Based on this assay, recombinant SidP protein specifically hydrolyzes PI(3)P and PI(3,5)P_2 *in vitro* (Figure 3.2B, C). To determine whether the phosphatase activity of SidP is dependent on the "CX_5R" motif, I made several mutations in this motif and the catalytic activity of the mutant recombinant SidP proteins were tested using the same assay. When the invariant catalytic cysteine was mutated to serine (C554S), phosphatase activity was completely abolished. Mutations of conserved residues in the catalytic P-loop such as D559N and R560K also abrogated the catalytic activity of SidP (Figure 3.2B, C). These findings show for the first time that *L. pneumophila* encodes a novel Icm/Dot effector that functions as a PI-3-phosphatase.

3.2.3 SidP rescues the growth defect phenotype of a yeast strain defective in PI(3)P metabolism

Knowing that SidP is a PI phosphatase prompted me to further examine the phosphatase activity of SidP *in vivo*. I chose *Saccharomyces cerevisiae* as the initial model system to test the enzymatic activity of SidP because of the availability of yeast strains, which carry temperature sensitive alleles for specific PI phosphatases and therefore have a growth defect phenotype at non-permissive temperatures. These strains provided a read-out for the phosphatase activity of SidP *in vivo. S. cerevisiae* encodes three PI(3)P phosphatases: myotubularin-related phosphatase Ymr1p and synaptojanin-like phosphatases Sjl2p and Sjl3p. I chose the YTS1 strain of *S. cerevisiae* to examine the PI-3- phosphatase activity of SidP *in vivo*. The genotype of the YTS1 strain is: *ymr1^{ts}sjl2Δsjl3Δ*, meaning that it is null for both Sjl2p, Sjl3p, and the only remaining PI(3)P phosphatase-encoding gene is a temperature sensitive allele of YMR1. Ymr1p is the myotubularin 3-phosphatase ortholog (Parrish et al., 2005). Therefore, the

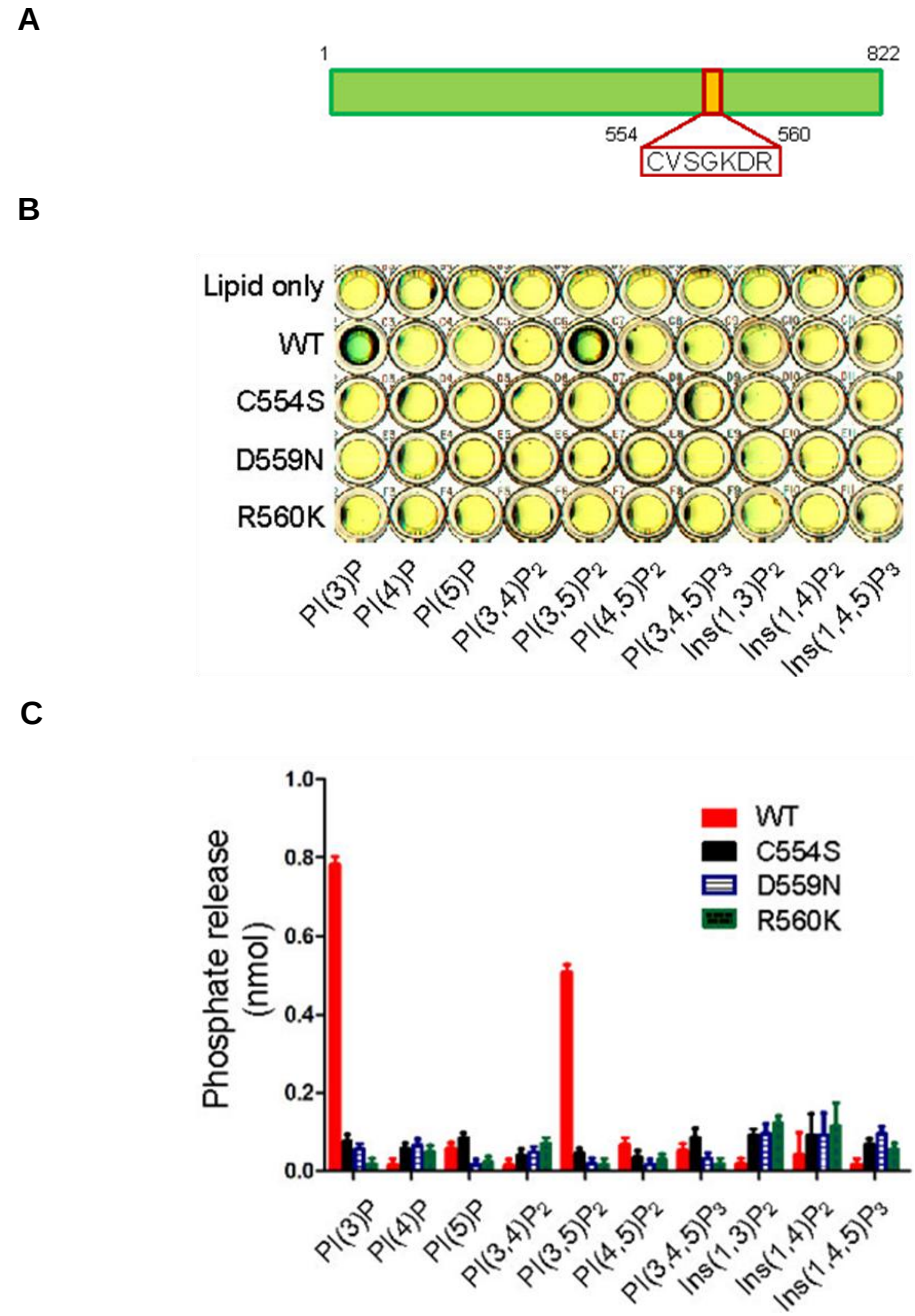

Figure 3.2 *L. pneumophila* effector SidP is a PI phosphatase. (A) Schematic structure of SidP (Lpg0130). The "CX_5R" is highlighted. (B) PI substrate specificity of purified wild type and C554S, D559N, R560K mutants SidP as determined by the malachite green assay (green color indicates the release of free phosphate). PI(3)P and $PI(3,5)P_2$ are the preferred substrates. (C) Quantification of the amount of released phosphates. Data are from three replicate experiments (mean ± S.E.M.).

strain does not grow at non-permissive temperature due to increased levels of PI(3)P, which are toxic to the cell.

To exogenously express SidP in yeast cells, I transformed YTS1 yeast cells with a plasmid harboring either (i) GFP, (ii) N-terminally GFP- tagged wild type SidP, or (iii) N-terminally GFP-tagged catalytically inactive mutant SidP(CS) (C554S), in which the conserved catalytic site cysteine is mutated (Figure 3.3). Exogenous expression of wt GFP-SidP rescued the growth defect phenotype of YTS1 at the non-permissive temperature at levels similar to when wt yeast Ymr1p is expressed. This suggests that when transformed into yeast, SidP is capable of hydrolyzing PI(3)P. However, exogenous expression of GFP alone or catalytically inactive GFP-SidP(CS) was not able to complement the growth defect phenotype at the non-permissive temperature (Figure 3.4A). Taken together, these data suggest that SidP can function as a PI(3)P phosphatase in yeast cells, and its phosphatase activity is dependent on the catalytic "CX_5R" peptide sequence.

3.2.4 PI-3-phosphatase activity of SidP decreases cellular levels of PI(3)P and $PI(3,5)P_2$ in yeast cells

In order to confirm that rescue of the growth defect phenotype in YTS1 by SidP is a result of PI(3)P hydrolysis, I directly measured the cellular levels of PIs inYTS1: *ymr1*^{ts}*sjl2Δsjl3Δ* transformed with N-terminally GFP- tagged wild type SidP plasmids and control plasmids at the non-permissive temperature. Exogenous expression of SidP decreased cellular PI(3)P levels almost three fold when compared to cells expressing empty vector or the catalytic inactive SidP CS mutant (Figure 3.4B) and (Table 3.1). In fact, expression of SidP reduced the levels of PI(3)P to levels similar to that found in

YTS1: *ymr1^{ts}sjl2Δsjl3Δ* at 27

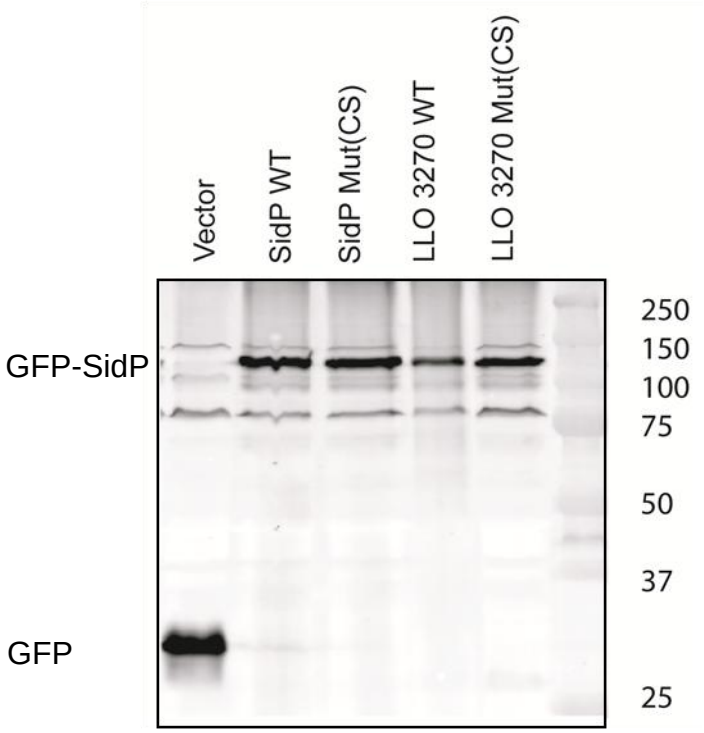

Figure 3.3 Exogenous expression of N-terminally GFP-tagged *L. pneumophila* SidP and SidP ortholog from *L. longbeachae* (LLO_3270) in *S. cerevisiae* YTS1: *ymr1^{ts}sjl2Δsjl3Δ* at 27 °C. Tested yeast transformants were grown to mid log phase (OD_{600}=0.5) at permissive temperature (26 °C), identical amounts of yeast cells were used for TCA acid extraction of the yeast proteins. The whole cell denatured proteins were resuspended in resuspension buffer, and protein samples were separated by SDS-PAGE. After being transferred to membranes, proteins were probed with antibody specific for GFP. Relevant molecular mass standards are shown on the right (in kDa).

yeast expressing wild type Ymr1p. Meanwhile, SidP expression did not affect the PI(4)P and PI(4,5)P_2 levels in these cells, but it decreased the levels of PI(3,5)P_2. These results verified that SidP specifically functions as a PI-3-phosphatase that hydrolyzes PI(3)P and PI(3,5)P_2 *in vivo* (Figure 3.4B, Table 3.1).

3.2.5 SidP is not able to rescue the growth defect phenotype of a yeast strain defective in PI(4)P metabolism

To further confirm the substrate specificity of SidP for PI(3)P *in vivo*, I used another strain of yeast that is deficient in all enzymes that hydrolyze PI(4)P at the non-permissive temperature, resulting in lethality at the non-permissive temperature due to elevated levels of PI(4)P. In the YCS215: *sac1^{ts}sjl2Δsjl3Δ* strain, all three genes that encode PI(4)P phosphatases are deleted and it can only produce a temperature sensitive Sac1p phosphatase (Foti et al., 2001). Exogenous expression of SidP in YCS215: *sac1^{ts}sjl2Δsjl3Δ* strain did not rescue the growth defect phenotype in these cells (Figure 3.5), indicating that PI(4)P is not a substrate for SidP.

3.2.6 SidP is constantly produced by *L. pneumophila* during its entire extracellular growth cycle in AYE broth

When *L. pneumophila* enters post-exponential growth phase, expression of many virulence factors is considerably induced in order to increase the survival rate of bacteria in the host cells in this phase (Byrne and Swanson, 1998). Consistently, when *L. pneumophila* cultures reach post-exponential phase too, expression levels of several substrates of the Icm/Dot system such as RalF and SidC are increased (Conover et al., 2003; Luo and Isberg, 2004; Nagai et al., 2002). In order to gain insights into the biological function of SidP, I wanted to see how the expression of SidP is regulated in

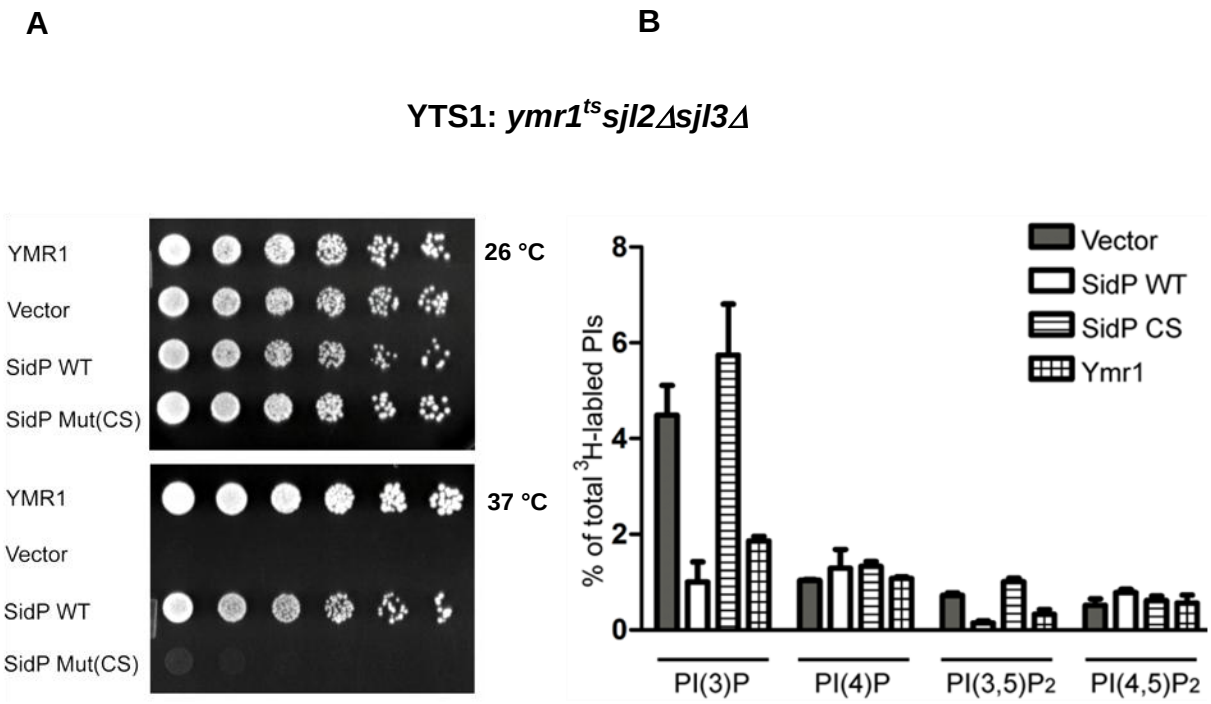

Figure 3.4 Functional assay of SidP in yeast. (A) *In vivo* growth rescue assay of SidP. *ymr1*^{ts}*sjl2Δsjl3Δ* cells were transformed with indicated constructs or vector control. The cells were spotted onto selection plates with four serial of 10x dilutions from left to right, and grown at the indicated temperatures for three days. (B) Quantitative analysis of *in vivo* PI levels. *ymr1*^{ts}*sjl2Δsjl3Δ* cells were transformed with vectors expressing GFP (negative control), wild type SidP, SidP C554S mutant, or YMR1 (positive control) and labeled with ^{3}H-*myo*-inositol for one hour at 37 °C. Total lipids were extracted and analyzed by HPLC.

Table 3.1: Quantitative PI level analysis in yeast strains transformed with vectors expressing SidP or control proteins.				
Vectors transformed	**PI levels (% of total ^{3}H-labeled PIPs/total phosphoinositol)**			
	PI(3)P	PI(4)P	PI(3,5)P_2	PI(4,5)P_2
pRS415-GPD-GFP	4.49 ± 0.44	1.04 ± 0.01	0.72 ± 0.03	0.52 ± 0.09
pRS415-GPD-GFP-SidPWt	1.00 ± 0.29	1.29 ± 0.28	0.15 ± 0.03	0.78 ± 0.04
pRS415-GPD-GFP-SidPCS	6.80 ± 1.81	1.33 ± 0.07	1.01 ± 0.05	0.61 ± 0.06

Table 3.1 Quantitative PI level analysis in transformed yeast strains. Yeast strains were labeled with ^{3}H-*myo*-inositol at 37 °C for 1 hour. Lipids were extracted and deacylated and were used for HPLC analysis as described (Botelho et al., 2008). The mean peak area (cpm) of each PIP species is reported as a percentage of the total ^{3}H-labeled lipids.

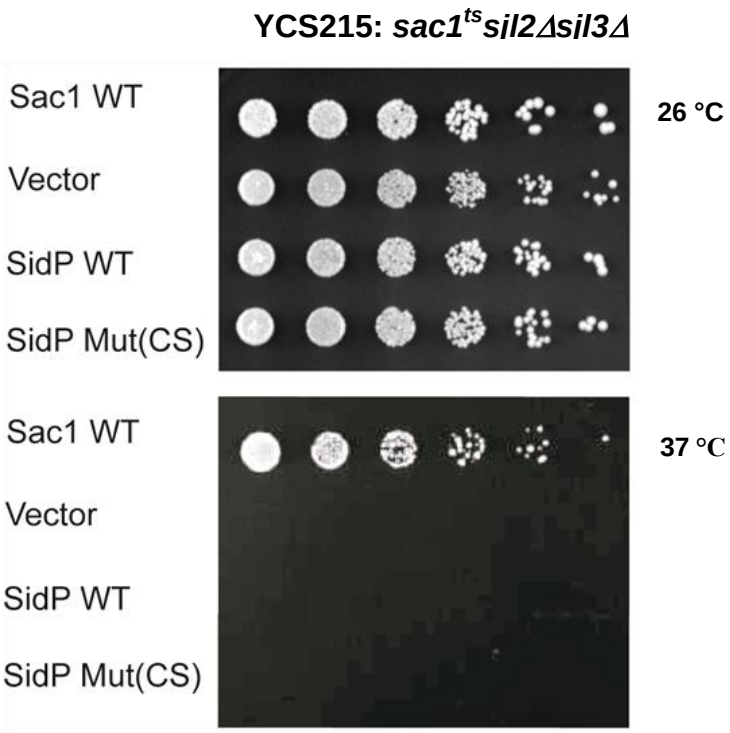

Figure 3.5 Functional assay of SidP in yeast. *In vivo* growth rescue assay of SidP. *sac1*^{ts}*sjl2Δsjl3Δ* cells were transformed with indicated constructs or vector control. The cells were spotted onto selection plates with four serial of 10x dilutions from left to right, and grown at the indicated permissive temperature (26 °C) and non-permissive temperature (37 °C) for three days.

L. pneumophila during infection. Non-specific signals from immuno-staining prevented me from probing the *in vivo* localization of SidP during *L. pneumophila* infection using the polyclonal antibodies that we generated against SidP. Therefore, I analyzed the SidP protein level in cell lysates of *L. pneumophila* grown in AYE culture at different phases. Interestingly, unlike RalF, and SidC whose expression is highly induced in the post-exponential phase, the level of SidP protein is elevated in the exponential phase of *L. pneumophila* growth. SidP is expressed throughout the growth cycle of *L. pneumophila* in AYE culture with a rise of expression in exponentially replicative phase in culture (Figure 3.6) (Conover et al., 2003; Luo and Isberg, 2004).

The expression pattern of SidP in the culture may reflect the SidP expression dynamics during infection. Therefore, continuous expression of SidP through the infection assures that LCVs will not acquire PI(3)P, since during the exponential growth phase the LCV needs to be protected from degradation. This suggests that SidP may be continuously expressed and translocated into infected cells during the entire cycle of intracellular growth with a rise of expression in the exponential phase of intracellular growth.

3.2.7 Deletion of SidP in *L. pneumophila* does not cause any significant defect in its pathogenicity

Considering the critical role of PI(3)P in phagosome maturation (Flannagan et al., 2009; Vergne et al., 2003a), I speculated that removal of PI(3)P may contribute to eliminating the endosomal-like identity of the LCV and disruption of the regular phagosome maturation pathway. In other words, removal of PI(3)P by SidP from the

A

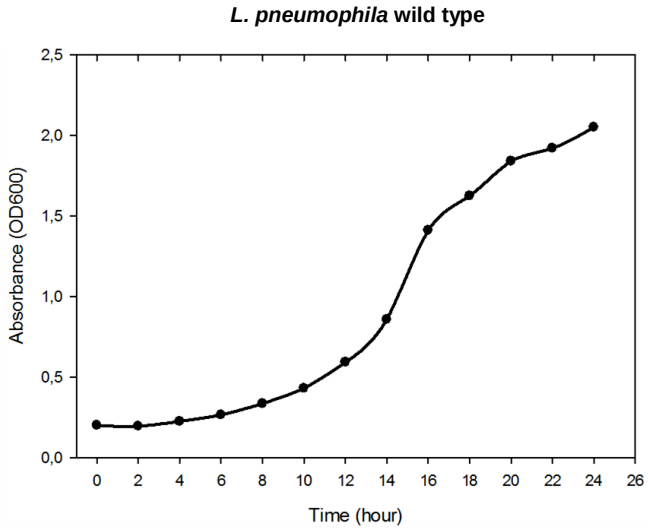
L. pneumophila wild type
Absorbance (OD600)
2,5
2,0
1,5
1,0
0,5
0,0
0 2 4 6 8 10 12 14 16 18 20 22 24 26
Time (hour)

B

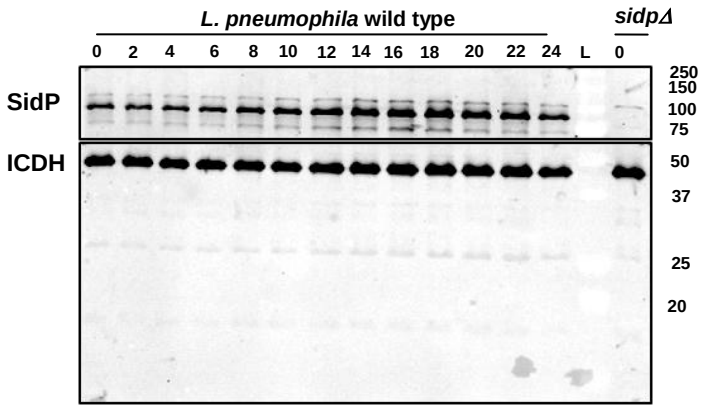
L. pneumophila wild type
sidpΔ
0 2 4 6 8 10 12 14 16 18 20 22 24 L 0
SidP
ICDH
250
150
100
75
50
37
25
20

C

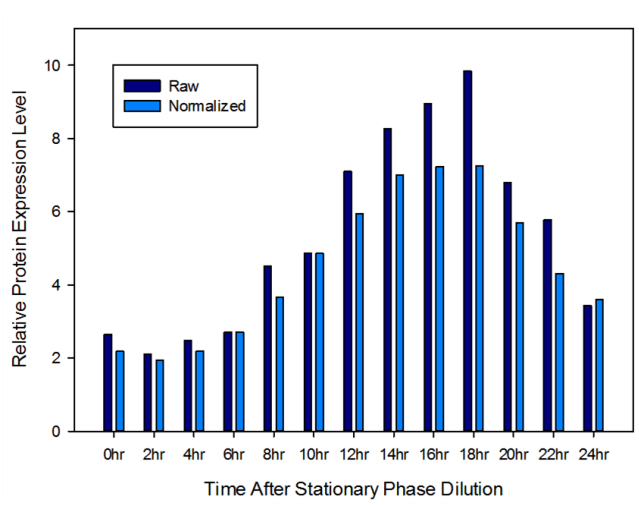
L. pneumophila wild type
Raw
Normalized
Relative Protein Expression Level
10
8
6
4
2
0
0hr 2hr 4hr 6hr 8hr 10hr 12hr 14hr 16hr 18hr 20hr 22hr 24hr
Time After Stationary Phase Dilution

Figure 3.6 Dynamic of SidP expression in *L. pneumophila* grown in AYE culture. SidP is produced by *L. pneumophila* constitutively during its growth cycle. (A) Cultures grown in AYE at stationary phase were diluted 1:20 into fresh medium at time zero and the growth of bacteria was monitored by measuring OD_{600} at indicated time points. (B) The expression of SidP at different bacterial growth phases. Total proteins from equivalent amount of bacteria at the indicated time points after dilution were resolved by SDS-PAGE and probed with an anti-SidP, and anti-isocitrate dehydrogenase (ICDH) specific antibody. The *L. pneumophila* metabolic protein ICDH was used as a loading control. Relevant molecular mass standards ladders (L) are shown on the right (in kDa). Lp02 *sidp*Δ sample at time 0 was loaded as a negative control for anti-SidP antibody. (C) Quantified and normalized SidP protein expression levels in panel (B).

early phagosome may prevent fusion of the LCV with host late endosomes or lysosomes and block the degradation of *L. pneumophila* in the host phagocytic pathway. This scenario would be similar to the function of PI-3- phosphatases SapM and MptpB in *M. tuberculosis* infection that block phagosome maturation by depleting PI(3)P from *Mycobacterium*-containing vacuoles (MCV) (Beresford et al., 2007; Vergne et al., 2005).

Accordingly, I speculate that in the absence of SidP, phagosome maturation would not be prevented; thus, LCVs harboring *L. pneumophila* carrying a *sidP* deletion mutation would not be able to avoid lysosomal fusion. As a result, *sidP* deletion mutant bacteria would not be able to multiply intracellularly in host cells and instead they would be degraded through the phagocytosis pathway. In order to test this hypothesis, I infected a murine RAW 264.7 macrophage cell line with wild-type *L. pneumophila*, an Icm/Dot deficient mutant, or a *sidP* deletion mutant. Similar to the wild-type *L. pneumophila*, the *sidP* deletion mutant was able to form “replication permissive” LCV, while the Icm/Dot deficient mutant was not able to replicate in the RAW 264.7 cells (Figure 3.7). Therefore, it seems that deletion of SidP in *L. pneumophila* did not cause any significant bacterial growth defect of the bacteria in the macrophage cells. Although the result of this experiment did not prove my hypothesis, it did not disprove it, since it is very common that deletion of one or several genes does not cause a growth defect because of functional redundancy among *L. pneumophila* effector proteins. There may be other PI(3)P phosphatases in *L. pneumophila*.

3.2.8 Examining SidP phosphatase activity during infection using a PI(3)P probe

At the same time, I took another approach to visualize the contribution of SidP in

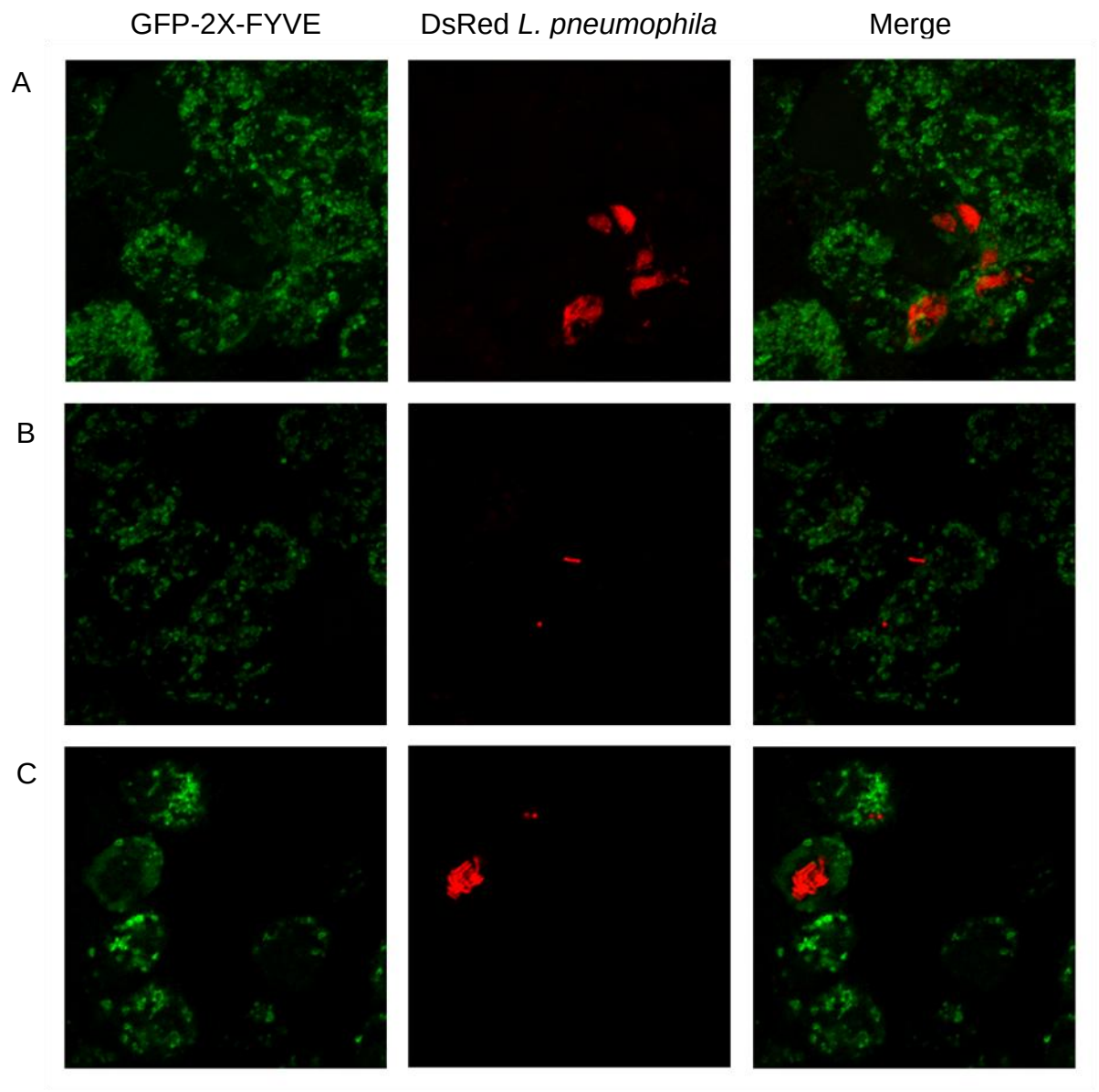

Figure 3.7 Deletion of SidP in *L. pneumophila* did not cause any significant bacterial growth defect of the bacteria in the macrophage cells. RAW 264.7 cell line containing a GFP-fusion-2X-FYVE domain infected with indicated *L. pneumophila* strains at an MOI of 1 for 18 hours. *L. pneumophila* Philadelphia-1 wild type strain Lp02 (A) Icm/Dot deficient strain Lp03(dotA-)(B), or strain *ΔsidP* strain: the *sidP* deletion mutant Lp02 strain (C). Note, wild type and *ΔsidP* replicated inside RAW 264.7 cell (red patches), but Icm/Dot deficient strain was not able to replicate intracellularly.

hydrolyzing and removing PI(3)P from the LCV during infection. In this experiment, I used a PI(3)P probe, GFP-tagged 2X tandem FYVE domain of early EEA1, as a molecular tool to monitor the levels of PI(3)P on the LCV and as a read-out for the PI-3-phosphatase activity of SidP during infection. To circumvent the technical difficulty of transiently transfecting macrophage cell lines, I made a stable RAW 264.7 cell line containing a GFP-fusion-2X-FYVE domain. I infected these cells with wild type, Icm/Dot deficient, or *sidP* deficient mutant *L. pneumophila* and analyzed the levels of the PI(3)P probe using confocal microscopy and immunohistochemistry staining. Considering the PI-3-phosphatase activity of SidP in the wild type strain, I expected to see a higher GFP signal around LCVs in the Icm/Dot deficient *sidP* deletion mutant bacteria, when compared to the signal around LCVs harboring wild type *L. pneumophila*. Because of the variability of the PI(3)P signal in LCVs, even within the same *L. pneumophila* strain, I was not able to definitively assign any signal differences based on *L. pneumophila* strain (data not shown). Since PI(3)P enrichment on a phagosome happens at the early stages of phagocytosis (within 5 minutes of phagocytosis initiation) (Cosio and Grinstein, 2008), it is possible that the difference of PI(3)P levels on the LCVs of these different *L. pneumophila* strains would be detectable only in the earlier stages of the infection. Therefore, it is likely that by the time I had synchronized the bacteria and fixed the cells, the peak time of PI(3)P accumulation on the LCV carrying mutant *L. pneumophila* had already passed.

3.2.9 Investigating the possible role of SidP in disruption of recognition of the LCV by the host autophagy system

Another process that has been proposed to be manipulated by *L. pneumophila*

is autophagy (Dubuisson and Swanson, 2006). It is known that the generation of PI(3)P by the Vps34 kinase complex during the early stages of autophagy is essential for autophagosome (AP) formation. PI(3)P mediates recruitment of PI(3)P binding proteins such as DFCP1 and WIPI2 that are important for autophagosome formation and autophagy (Vergne and Deretic, 2010). Considering the critical role of PI(3)P in initiating autophagy, I wanted to address the question of whether SidP may interrupt autophagosome formation via hydrolysis of PI(3)P and therefore contribute to *L. pneumophila's* avoidance of the host autophagy pathway.

Furthermore, according to a recent study, *L. pneumophila* effector protein RavZ inhibits the host autophagy pathway during infection by functioning as a cysteine protease, which irreversibly deconjugates the host lipid-conjugated Atg8 proteins covalently attached to phosphatidylethanolamine (PE) on the autophagosomal membrane. Since attachment of Atg8 is essential for autophagosome formation, RavZ interferes with host autophagy by directly targeting Atg8 proteins (Choy et al., 2012). However, a *ravZ* deletion mutant is still able to establish replication permissive LCVs that can avoid the host autophagy system. This suggests that *L. pneumophila* encodes other effectors that can mediate the LCV's avoidance of the host autophagy system (Choy et al., 2012). Based on these previous findings, I tested the role of SidP in autophagy inhibition during infection. Since *sidP* deletion mutants are still infectious, and given the high likelihood that there are other bacterial effectors that can manipulate the host autophagy system, I did not look at autophagy during *L. pneumophila* infection. Rather, I investigated the possible effects of exogenous expression of SidP on the process of autophagy in transfected cells by Western blotting for LC3I and II complexes.

However, by looking at levels of endogenous and over expressed LC3I and II complexes using western blotting and confocal microscopy analysis, respectively, I concluded that SidP expression did not affect the autophagy pathway in mammalian cells (Figure 3.8 and 3.9). It is worth noting that simultaneous deletion of *ravZ and sidP* did not affect the *L. pneumophila* pathogenicity.

3.3 Discussion

Bacterial and host PI kinases, PI phosphatases, and PI-binding proteins can potentially regulate the PI identity of the LCV. Although our knowledge of the PI components of the LCV as well as the host proteins and bacterial effectors that target PIs has greatly increased in recent years, (Weber et al., 2006), to date, there has been no report of a *L. pneumophila* effector protein that hydrolyzes host PIs.

Taken together, my findings show for the first time that *L. pneumophila* encodes a PI-3-phosphatase that specifically hydrolyzes PI(3)P and PI(3,5)P_2 *in vitro* and *in vivo*. SidP contains the PTP-like signature sequence "CX_5R", which indeed hydrolyzes phosphoryl groups from PIs. The *in vitro* enzymatic activity of SidP was confirmed with several pieces of independent *in vivo* evidence, indicating that exogenously expressed SidP can also function as PI phosphatase in *S. cerevisiae* cells.

Moreover, my results indicate that endogenous SidP is constantly expressed throughout the entire extracellular growth cycle of *L*. *pneumophila* in AYE broth. This implies that SidP is also expressed during the entire cycle of *L*. *pneumophila* infection.

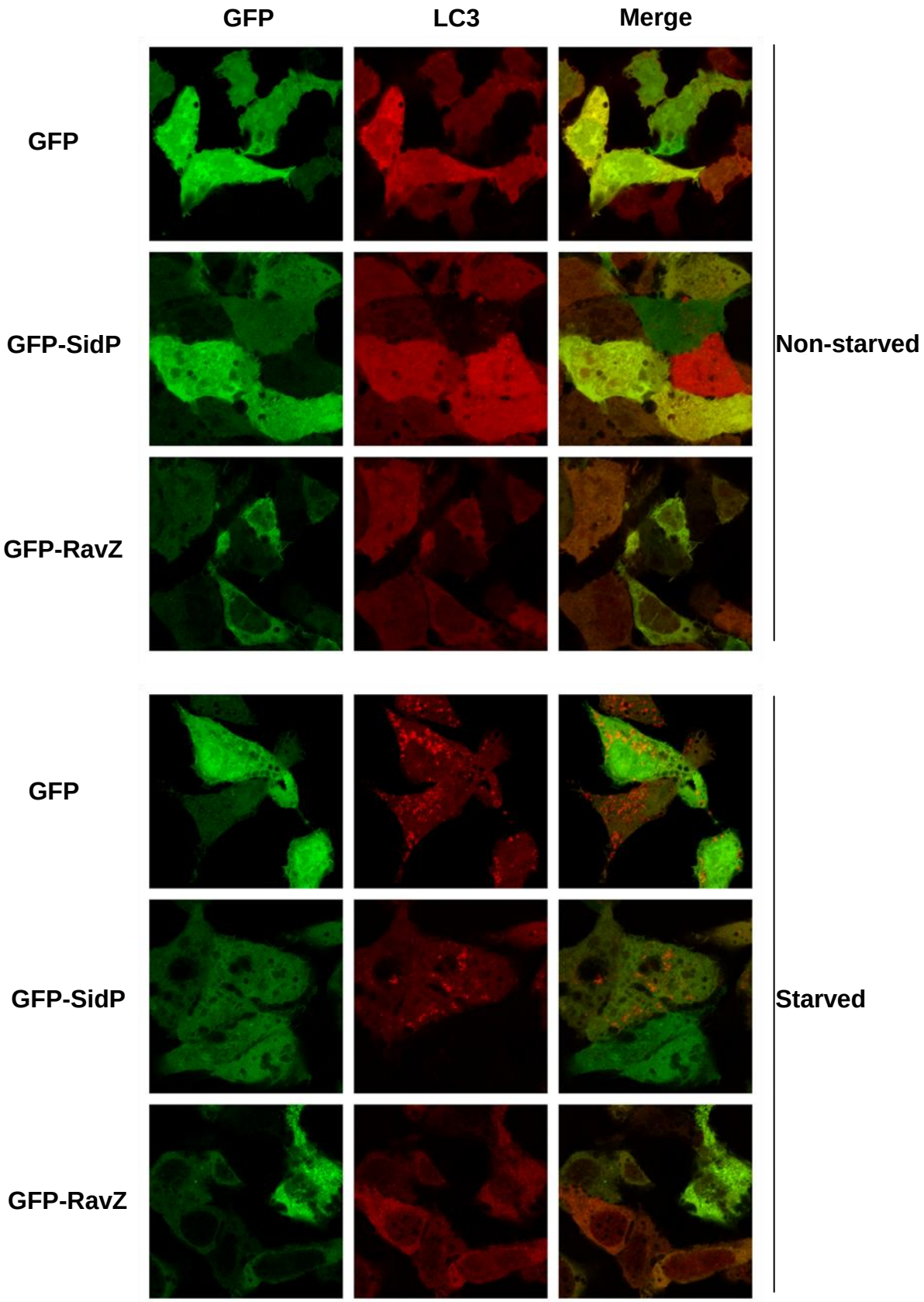
GFP
LC3
Merge
GFP
GFP-SidP
GFP-RavZ
Non-starved
GFP
GFP-SidP
GFP-RavZ
Starved

Figure 3.8 SidP does not inhibit LC3 puncta formation in HK293T cells under starvation condition. HK293T cells co-transfected with GFP, GFP-SidP, and GFP-RavZ together with mCherry tagged LC3 were starved by replacing the media with HBSS in the presence 160nM Bafilomycin A1 (for blocking the fusion of autophagosomes with lysosomes) for 1 hour. Under starvation condition, red channel images show LC3 puncta in cells transfected with SidP-GFP, as well as the control cells transfected with GFP but not in the cells transfected with GFP-RavZ.

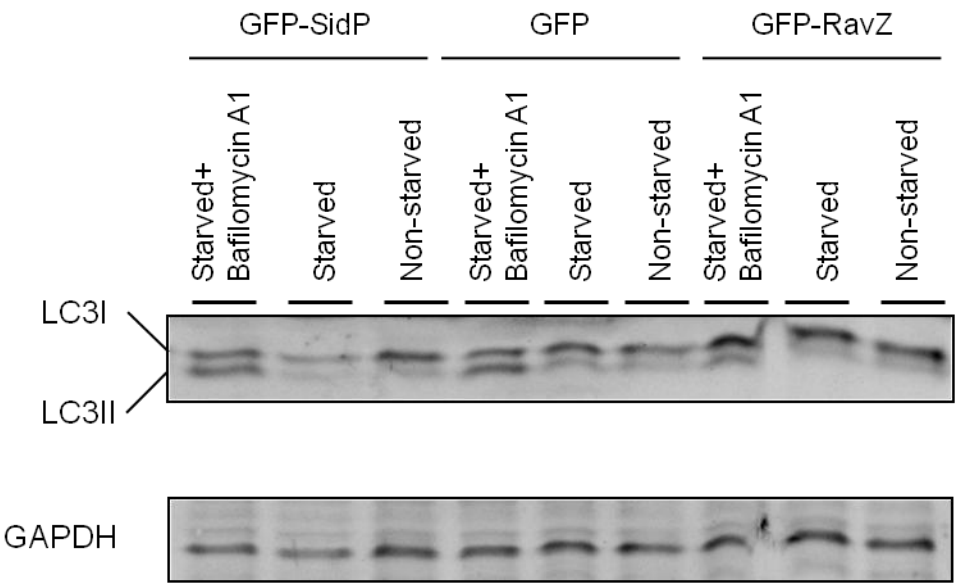

Figure 3.9 Exogenous expression of SidP did not inhibit the formation of LC3II in HEK293T cells. Immunoblot analysis of endogenous LC3I and LC3II levels in HEK293T cells transfected with plasmids encoding GFP, GFP-SidP, and GFP-RavZ. 24 hours post-transfection cells were starved by replacing the media with HBSS in the presence or absence of 160 nM Bafilomycin A1 (for blocking the fusion of autophagosomes with lysosomes) for 1 hour prior to collecting and lysing the cells.The whole cell lysates were collected with the addition of Laemmli sample buffer, and protein samples were separated by SDS-PAGE. After being transferred to membranes, proteins were probed with antibody specific for LC3. GAPDH protein was used as a loading control. Relative conversion of LC3I to LC3II under starvation condition is more in the cells expressing GFP, GFP-SidP compare to the cells expressing GFP-RavZ.

This speculative view about SidP expression during infection suggests that the catalytic activity of SidP and removing PI(3)P from LCVs may play a role in the formation of LCVs at the very early stages of infection, and even more important for intracellular replication of the bacteria in the exponential phase. It also implies that although SidP is expressed in lower quantities after the exponential phase, expression of SidP continues until later stages of infection, presumably to keep the integrity of LCVs and to help avoidance of LCVs fusion with the host lysosomes until late stages of infection.

During *L. pneumophila* infection, early phagosomes enriched with PI(3)P transform into LCVs enriched with PI(4)P (Vieira et al., 2002). The subversion of a PI(3)P-enriched early phagosome to a PI(4)P-enriched LCV, combined with the continuous expression of SidP during the whole cycle of L. *pneumophila*, led me to think that there is a strong likelihood that SidP plays a role in the PI identity change of the LCV and eliminating the endosomal-like identity of the LCV. This change of identity contributes to blocking phagosome maturation and the degradation of *L. pneumophila* in the host lysosomes.

However, my experimental results suggest that SidP is not the only player in this transformation, yet SidP's enzymatic activity suggests that it could be one the players. Although the results from my experiments showed that deletion of SidP in *L. pneumophila* does not cause any significant intracellular bacterial growth defect in the macrophage cells, they do not exclude the role of SidP in inhibition of phagosome maturation by depleting PI(3)P from the LCV. Because of functional redundancy among *L. pneumophila* effector proteins, only a small number of single deletions impair its

pathogenicity. It is possible that *L. pneumophila* encodes other PI phosphatases that have not been identified yet. In fact, our bioinformatics screen revealed 28 more PI phosphatase candidates besides SidP. Furthermore, the SidP deletion mutant's lack of phenotype may be the result of bacterial compensation by exploiting host proteins. The lack of phenotype does not disprove my hypothesis that SidP's enzymatic activity removes PI(3)P from early *Legionella* containing phagosomes, and helps these phagosomes acquire LCV PI identity.

In support of the idea that *L. pneumophila* encodes other PI metabolizing enzyme such as SidP to establish the LCV composition, recently our lab reported that the Icm/Dot substrate SidF functions as a PI-3-phosphatase (Hsu et al., 2012). According to this study, SidF anchors on the LCV membrane and hydrolyzes PI(3,4,5)P_3 and PI(3,4)P_2 to PI(4,5)P_2 and PI(4)P. Therefore, SidF and SidP can synergistically contribute to regulation of the PI composition of the LCV by making PI(4)P and removing PI(3)P, respectively. Furthermore, SidF can indirectly prevent PI(3)P accumulation on the LCV by hydrolyzing PI(3,4,5)P_3 to PI(4,5) P_2 . PI(3,4,5)P_3 can be hydrolyzed by host 5p- or 4p- phosphatases, such as SHIP-1 and Inpp4A, to PI(3)P during endocytic processes (Shin et al., 2005). Thus, SidF by consuming the substrate PI(3,4,5)P_3 prevents the accumulation of PI(3)P by these enzymes.

In summary, this part of my research led to discovery of a *L*. *pneumophila* PI-3-phosphatase that hydrolyzes PI(3)P and PI(3,5)P_2 . The enzymatic activity of SidP strongly suggests that SidP may contribute to the lipid identity of the LCV and its escape from lysosomal fusion. However, additional experimental data are needed to support this hypothesis.

CHAPTER 4

Crystal Structure Determination and Overall Structure of SidP

4.1 Introduction

The PTP-superfamily PI phosphatases consists of metal-independent enzymes that use their signature "CX_5R" motif to dephosphorylate PI substrates (Denu and Dixon, 1998). The PTP-like phosphatases share a common mechanism of catalysis and a conserved catalytic core structure (Andersen et al., 2001; Zhang, 2003). The conserved catalytic core structure of most if not all the PTP-like phosphatases contains a central parallel ß-sheet with flanking α-helices and the catalytic pocket which contains the "CX_5R" signature sequence at its bottom. The active site pocket of these enzymes varies in shape and size, most likely resulting from the structural components peripheral to the conserved catalytic core. This diversity may be responsible for the various substrate specificities found in these enzymes. Non-catalytic regions that flank the catalytic core of these enzymes, especially in the PTP superfamily, often play a role in their diverse cellular functions (Andersen et al., 2001; Mauro and Dixon, 1994; Tonks and Neel, 2001). Regardless of their substrate specificity and the size or shape of the catalytic pocket, all "CX_5R" containing enzymes seem to use a similar catalytic mechanism for executing their phosphate monoester hydrolysis.

The phosphate-binding loop called (P-loop) is located at the bottom of the active site of these enzymes and contains the signature sequence "CX_5R" (Denu and Dixon, 1998). Site-directed mutagenesis studies and chemical modification experiments showed that the conserved cysteine residue present in the P-loop is vital for the phosphatase activity of these enzymes. These enzymes use a double displacement reaction as their

catalytic mechanisms. The SH group of cysteine, a strong nucleophile, displaces the leaving alcohol group and binds to the phosphate monoester of the substrate forming a thiol-phosphate (phospho-enzyme) intermediate (Barford et al., 1998; Guan and Dixon, 1991; Pannifer et al., 1998). The nitrogens in the main chain of the P-loop residues and the guanidinium group of the conserved arginine side chain have been proposed to position the oxygens of the substrate phosphate group into an optimal orientation and stabilize its highly negative charge (Barford et al., 1994). In fact, mutational studies indicate that the conserved arginine in the CX_5R signature sequence is required for catalysis, most likely for stabilizing the transition state. This arginine can play a role in substrate binding to a lesser degree (Zhang et al., 1994b). The transition state is resolved when an acceptor water molecule displaces the PO_3 group from the phospho-enzyme intermediate. The PTP superfamily enzymes use a general acid-base mechanism for catalysis. It has been suggested that they employ an aspartic acid residue located in an adjacent structural loop as the general acid. This Asp promotes the phosphoester bond cleavage by donating a proton to the ester oxygen of the substrate leaving group and reconstituting an uncharged hydroxyl group at the position from which the PO_3 group is removed (Fauman and Saper, 1996; Fauman et al., 1996; Jia et al., 1995; Zhang et al., 1994a).

4.2 Results

4.2.1 Full length and truncated SidP proteins did not crystallize

Sequence alignment shows that SidP is fairly well conserved in all genome sequenced *Legionella* species, as well as some related pathogenic bacterial species

such as *Fluoribacter dumoffii* and *Rickettsiella grylli* (Figure 4.1). However, SidP has no significant sequence homology to any known prokaryotic and eukaryotic PI phosphatase. This prompted me to investigate the existence of novel structural or mechanistic features in SidP. To further characterize the molecular mechanism and structure of this newly characterized PI-3-phosphatase, we set out to determine the atomic structure of SidP by X-ray crystallography.

In order to obtain atomic level structural information of SidP, I first tried to crystallize SidP. As described in chapter 3, the recombinant full-length protein of SidP from *L. pneumophila* strain Philadelphia 1 was highly expressed in Rosetta cells. I was able to purify relatively large quantities of SidP to high purity and homogeneity and concentrate it to > 8mg/ml. However, SidP did not crystallize in any of the 480 conditions I used in my crystallization screen, where sitting drops were dispensed using the PHOENIX liquid handling system (Art Robbins Instruments).

After several unsuccessful crystallization screen trials using full-length SidP, the next logical step was to attempt to crystallize truncated SidP proteins that were still enzymatically active. The rationale was that the truncated SidP proteins would be more amenable to crystallization because of their smaller size. There are several commonly used methods used to identify the boundaries of distinct domains in a protein such as limited proteolysis and sequence conservation. One such method identifies blocks of sequence conservation among protein homologous to a protein of interest to estimate the domain boundaries (Wilson et al., 2000).

I used sequence conservation comparison and the predicted secondary structure

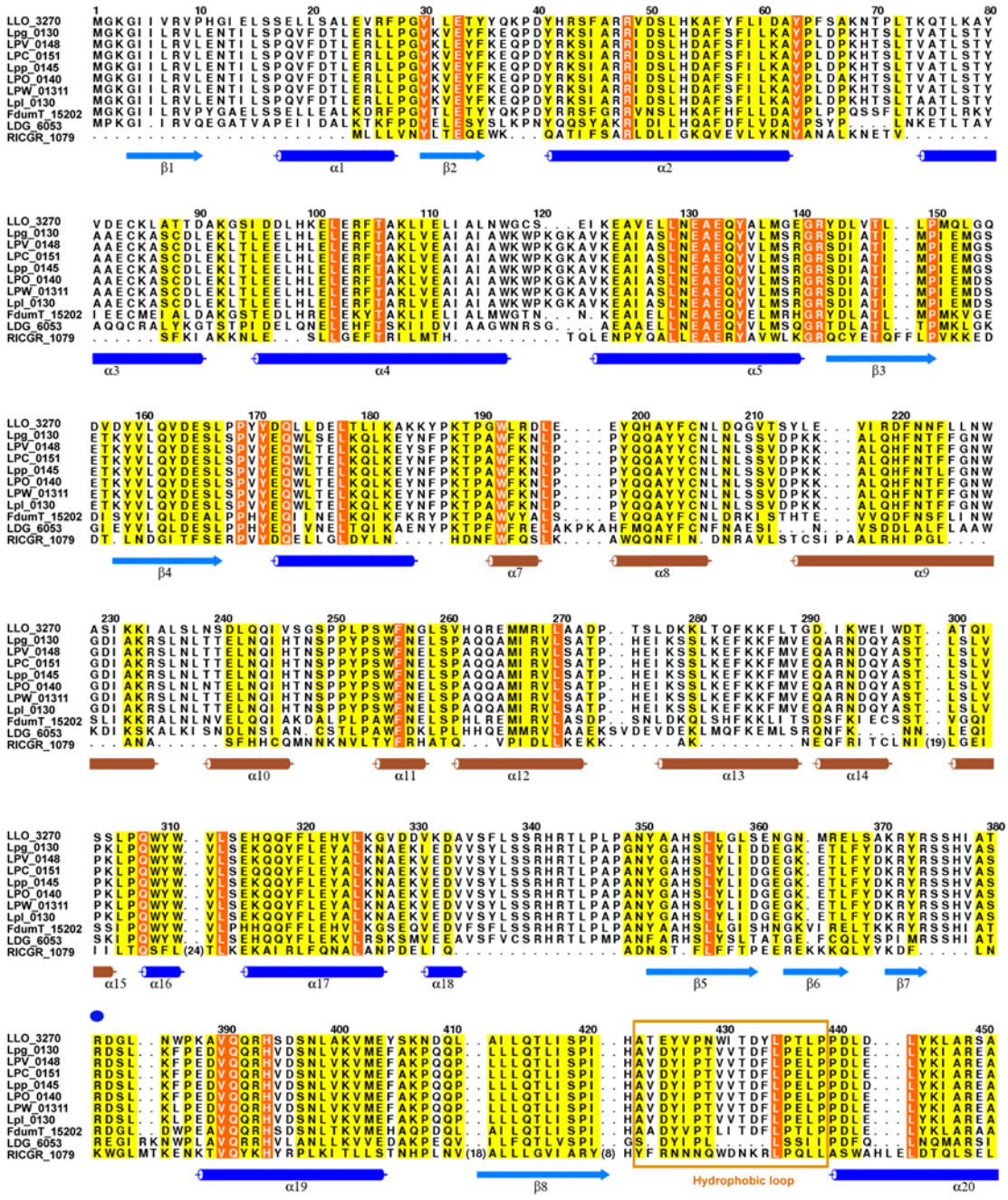
LLO_3270
Lpg_0130
LPV_0148
LPC_0151
Lpp_0145
LPO_0140
LPW_01311
Lpl_0130
FdumT_15202
LDG_6053
RICGR_1079
β1
α1
β2
α2
α3
α4
α5
β3
β4
α7
α8
α9
α10
α11
α12
α13
α14
α15
α16
α17
α18
β5
β6
β7
α19
β8
Hydrophobic loop
α20

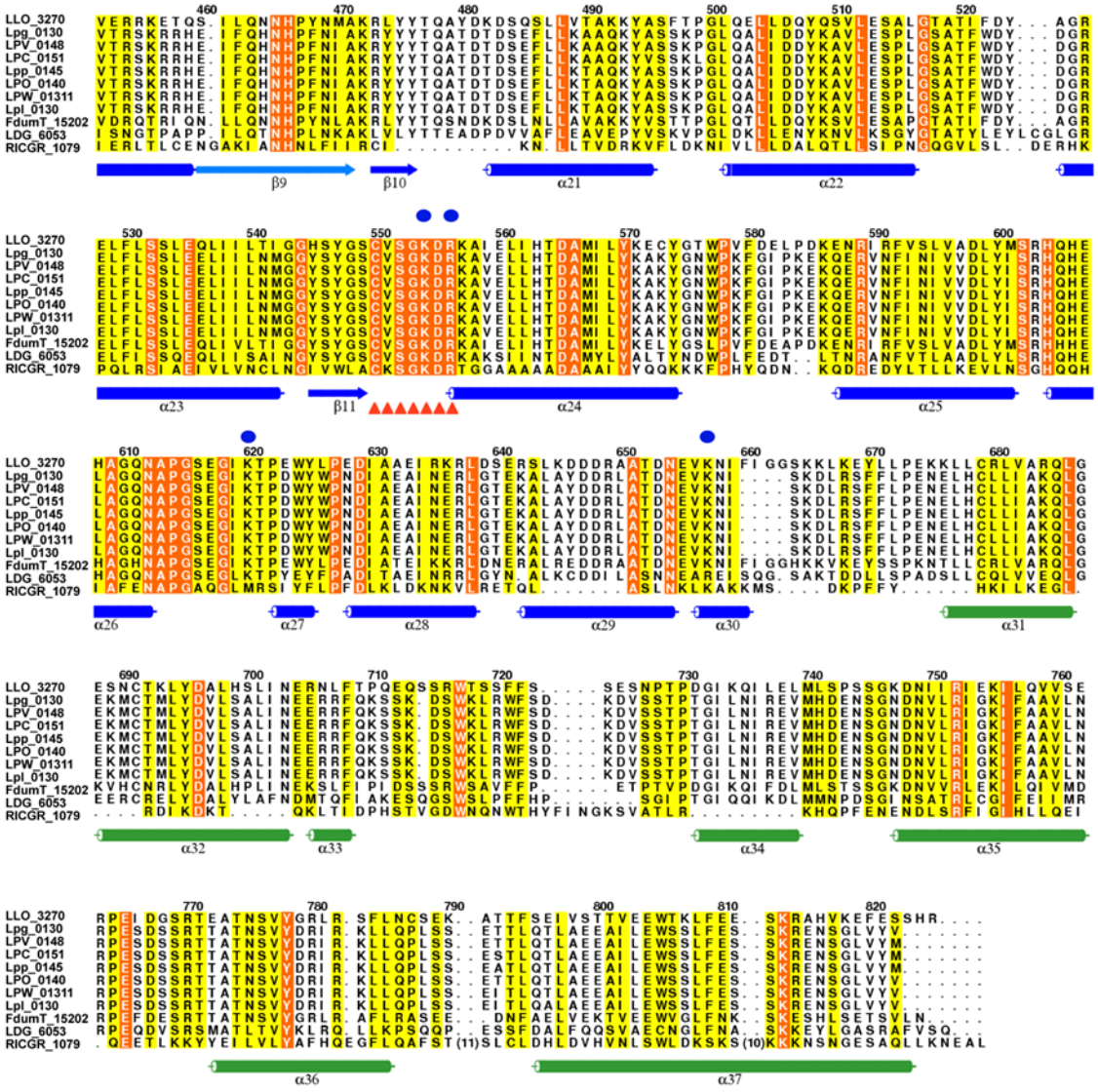

Figure 4.1 Multiple sequence alignment of SidP. The sequences of SidP from pathogenic bacteria were aligned by the Clustal Omega server (Sievers et al., 2011) and colored by ALSCRIPT program (Barton, 1993). Residues numbers are labeled according to the LLO_3270 sequence. The conserved residues are shaded in yellow and identical residues are shaded in red. Secondary elements of SidP are draw under the alignment. The catalytic CX_5R motif is marked by red triangles. Five conserved cationic residues that contribute the positive charges at the catalytic site are marked by blue dots. The hydrophobic loop is highlighted by a brown box. Entrez database accession numbers are as follow: LLO_3270: gi: 289166576; Lpg_0130: gi: 52840385; LPV_0148: gi : 397665762; LPC_0151: gi: 148358289; Lpp_0145: gi: 54296126; LPO_0140: gi : 397662684; LPW_01311: 307608875; Lpl_0130: gi: 54293092; FdumT_15202: gi: 388457923; LDG_6053: gi: 374261093; RICGR_1079: gi: 160871888.

obtained from PsiPred (http://bioinf.cs.ucl.ac.uk/psipred/) to design and express several recombinant truncated SidP proteins. These truncated SidP proteins were cloned, expressed, and purified using the same procedures used for the full length SidP cloning and expression. Then, I tested the purified proteins for PI-phosphatase activity. The truncated protein variants that were found to be catalytically active were screened for crystallization. Similar to full-length SidP, none of these pure and homogenous truncated proteins crystallized despite extensive crystallization trials. (Figure 4.2 and Table 4.1). This finding is not uncommon and can result from low protein stability, protein degradation, and misfolding (Smialowski and Frishman, 2010). To check whether this was the case, I compared the differences in size and purity between freshly purified protein samples and proteins that had been left at 4 °C for 5-7 days using SDS-PAGE. I found that neither full-length nor truncated SidP proteins are stable. The appearance of a smaller (almost 40 KDa, compared to 90 kDa for full-length SidP) band in the older samples of both full-length and truncated SidP indicated that proteolytic cleavage of the protein takes place near either the amino or carboxyl terminus

Since none of the truncated SidP proteins crystallized, perhaps because of proteolytic cleavage, I took an experimental approach of “limited proteolysis” as a complementary method to identify SidP domains suitable for structural analysis. This method is based on the fact that in general, inter-domain regions of proteins are more accessible to proteases than folded regions within a structural domain. Therefore, inter-domain regions are more susceptible to protease digestion than the structured domains. The stable limited proteolytic products corresponding to individual protein domains can be identified using mass spectroscopy (Koth et al., 2003).

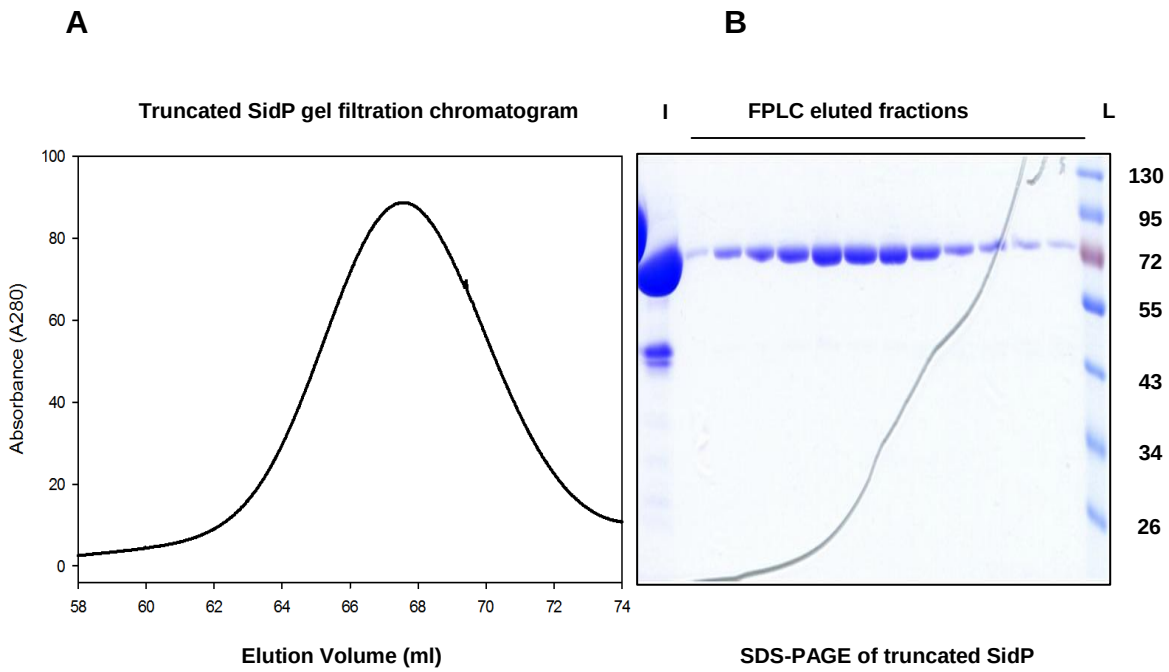

Figure 4.2 Gel filtration and SDS-PAGE of truncated SidP (residues 1-689). (A) Untagged-SidP elutes off the size-exclusion column as a single peak after approximately 60 mL. (B) The injected protein has lower molecular weight contaminants or degraded protein (Lane I) but these are removed from the eluted fractions. The “L” lane is the molecular weight ladder.

SidP	Enzymatic activity
aa 1-822 Wt	Y
aa 123-822 Wt	N
aa 1-762 Wt	Y
aa 123-762 Wt	N
aa 1-711 Wt	Y
aa 123-711 Wt	N
aa 1-689 Wt	Y
aa 123-689 Wt	N
aa 1-666	N
aa 123-666	N
aa 1-822 Mutant (C 554S)	N

Table 4.1 List of recombinant SidP proteins that were cloned and tested for PI phosphatase activity.

I used two different proteases, trypsin and chymotrypsin, for limited digestion of full-length SidP. The trypsin digestion was less informative, since SidP appeared completely digested over a very narrow range of trypsin concentrations. However, when I used chymotrypsin for limited digestion of the full-length SidP and two truncated SidP versions, the digestion profile of all three SidP proteins showed a similar pattern with a few stable fragments (Figure 4.3). The biggest stable fragment was around 30 kDa, which is one-third the size of full-length SidP. Since the fragment was too small, I decided not to analyze it using mass spectroscopy.

4.2.2 *Legionella longbeachae* strain NSW150 LLO_3270 is a PI-3-phosphatase

Following the previous set of experiments, I decided to turn my focus to crystallizing SidP orthologues from other *Legionella* species. I cloned SidP from *Legionella longbeachae* strain NSW150 (locus tag LLO_3270), which has 54% sequence identity and 68% sequence similarity to SidP from *L. pneumophila* in Rosetta cells. It is worth noting that the primary sequence of the catalytic loop of LLO_3270, “CVSGKDR”, is identical to the catalytic motif of SidP. Using the same methods described for full-length and truncated *pneumophila* SidP proteins, the *L*. *longbeachae* SidP orthologue LLO_3270 was expressed and purified to homogeneity (Figure 4.4).

Before trying to crystallize LLO_3270, I tested its PI- phosphatase activity *in vitro*. Based on results from the malachite green test, LLO_3270 specifically hydrolyzes PI(3)P while it does not show any detectable activity with PI (3,5) P_2 (Figure 4.5).

4.2.3 LLO_3270 can rescue the growth defect of yeast cells defective in generating PI 3-phosphatase

To confirm the similarity between SidP and its ortholog LLO_3270, I analyzed the

A

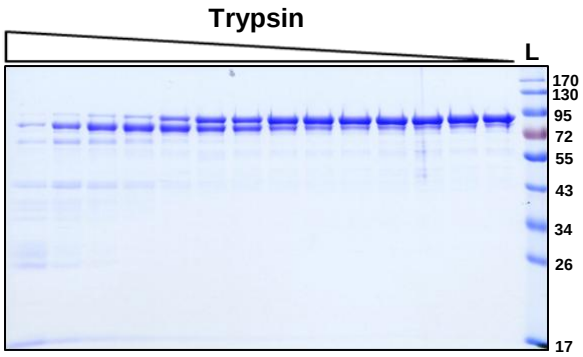
Trypsin
L
170
130
95
72
55
43
34
26
17

B

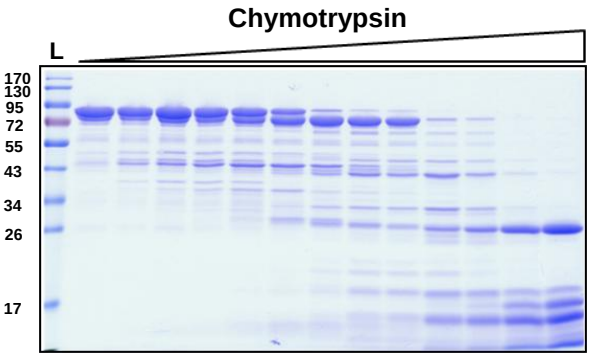
Chymotrypsin
L
170
130
95
72
55
43
34
26
17

C

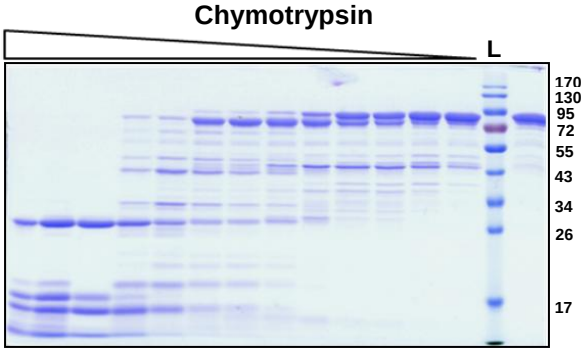
Chymotrypsin
L
170
130
95
72
55
43
34
26
17

D

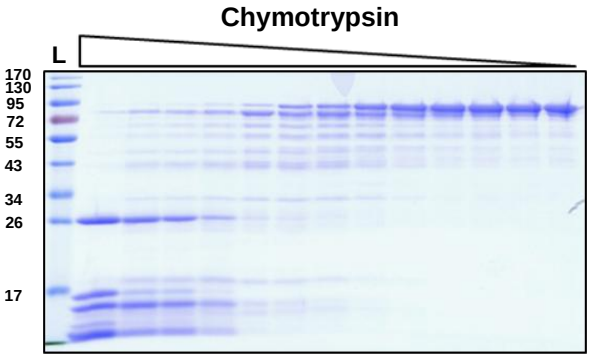
Chymotrypsin
L
170
130
95
72
55
43
34
26
17

Figure 4.3 Limited proteolysis of recombinant full length and truncated SidP proteins by trypsin and chymotrypsin. (A, B) 4 µg purified full length SidP was incubated with two fold serial dilutions(1 µg) of trypsin(A) and chymotrypsin (B) on ice for 1 hour and immediately boil in loading buffer, following with analysis by SDS-PAGE . (C,D) Limited proteolysis of truncated SidP(aa 1-762) panel (C) and SidP(aa 1-711) panel (D) by chymotrypsin in the same way it was done for full length SidP. All polyacrylamide gels were developed by coomassie Brilliant Blue G-250 staining. The undigested sample of each protein has been labeled “U”.The (L) lane is the molecular weight ladder (in kDa).

in vivo phosphatase activity of LLO_3270 by complementation assays in *Saccharomyces cerevisiae***.** Similar to SidP, exogenous expression of GFP-tagged LLO_3270 in the PI(3)P phosphatase deficient YTS1: *ymr1^{ts}sjl2Δsjl3Δ* strain that only encodes a temperature sensitive Ymr1p phosphatase, rescued the growth defect phenotype resulting from the elevated levels of PI(3)P at the non-permissive temperature (Parrish et al., 2005). In contrast, transformation of the PI(4)P phosphatase deficient YCS215: *sac1^{ts}sjl2Δsjl3Δ* strain with the same LLO_3270 expression vector did not rescue the growth defect resulting from toxic levels of PI(4)P at the non-permissive temperature (Figure 4.6) (Foti et al., 2001). These findings show that *L. longbeachae* substrate of Icm/Dot effector *LLO*_3270 also functions as a PI-3-phosphatase both *in vitro* and *in vivo*.

4.2.4 Crystal structure determination and overall structure of *L. longbeachae* SidP ortholog LLO_3270

To attempt to crystallize LLO_3270, highly pure and homogenous full-length LLO_3270 protein was concentrated to 7.5 mg/ml and subjected to an initial crystallization screen of 480 conditions, as set up by the ARI Phoenix robot. In my first crystal trial, I found several conditions that promoted the formation of diamond-shaped crystals (Table 4.2). To get larger crystals, I manually set up crystal trays using the initial conditions and the hanging drop vapor diffusion method at room temperature. LLO_3270 formed large diamond-shaped crystals within a relatively short time range, anywhere from overnight to a few days after I set up the crystal trays (Figure 4.7A).

When we took the diamond-shaped crystals to the Cornell High Energy Synchrotron Source (CHESS) for X-ray diffraction, the crystals produced low quality

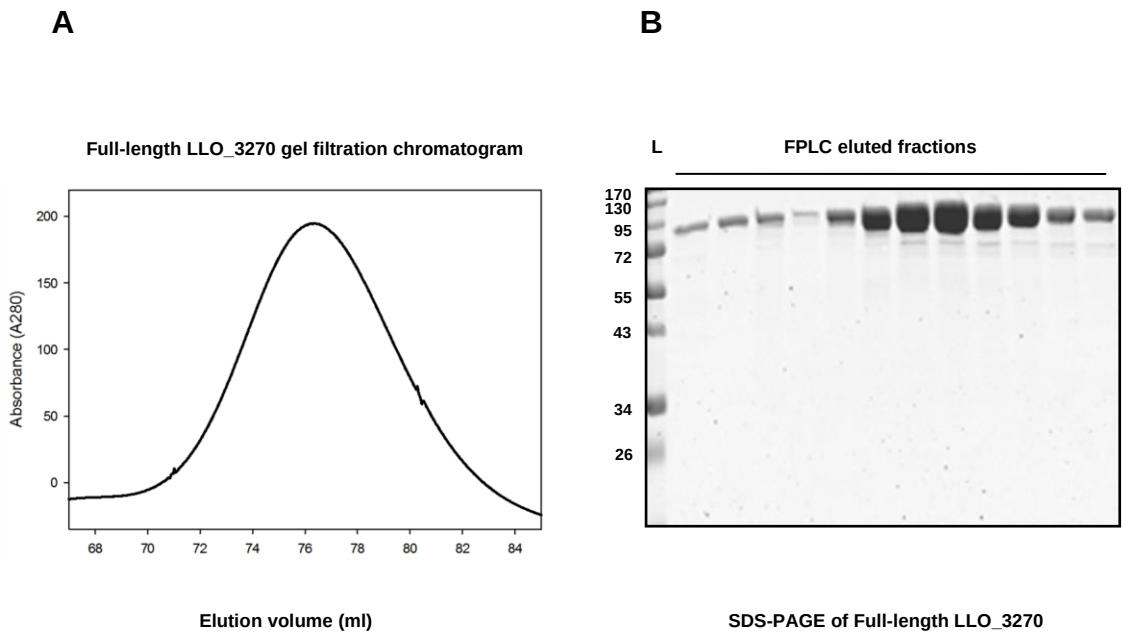

Figure 4.4 Gel filtration and SDS-PAGE of LLO_3270. (A) Untagged-LLO_3270 elutes off the size-exclusion column as a major single peak after 70 mL. (B) Eluted fractions on a SDS-PAGE. The “L” lane is the molecular weight ladder in kDa.

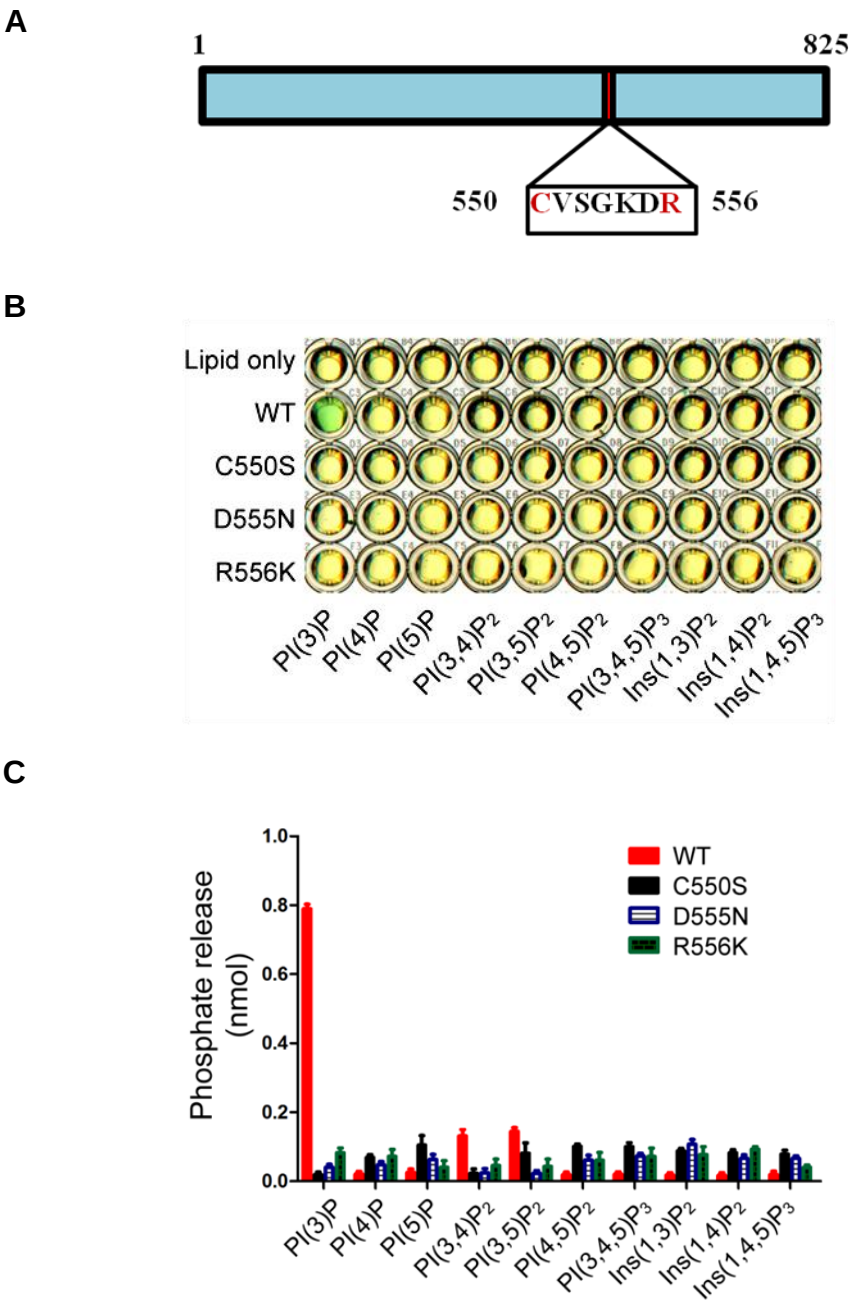

Figure 4.5 SidP *Legionella longbeachae* orthologue, LLO_3270 is a PI phosphatase. (A) Schematic structure of LLO_3270. The "CX_5R" is highlighted. (B) PI substrate specificity of purified wild type and C550S, D555N, and R556K mutants LLO_3270 as determined by the malachite green assay (green color indicates the release of free phosphate). PI(3)P is the preferred substrates. (C) Quantification of the amount of released phosphate. Data are from three replicate experiments (mean ± S.E.M).

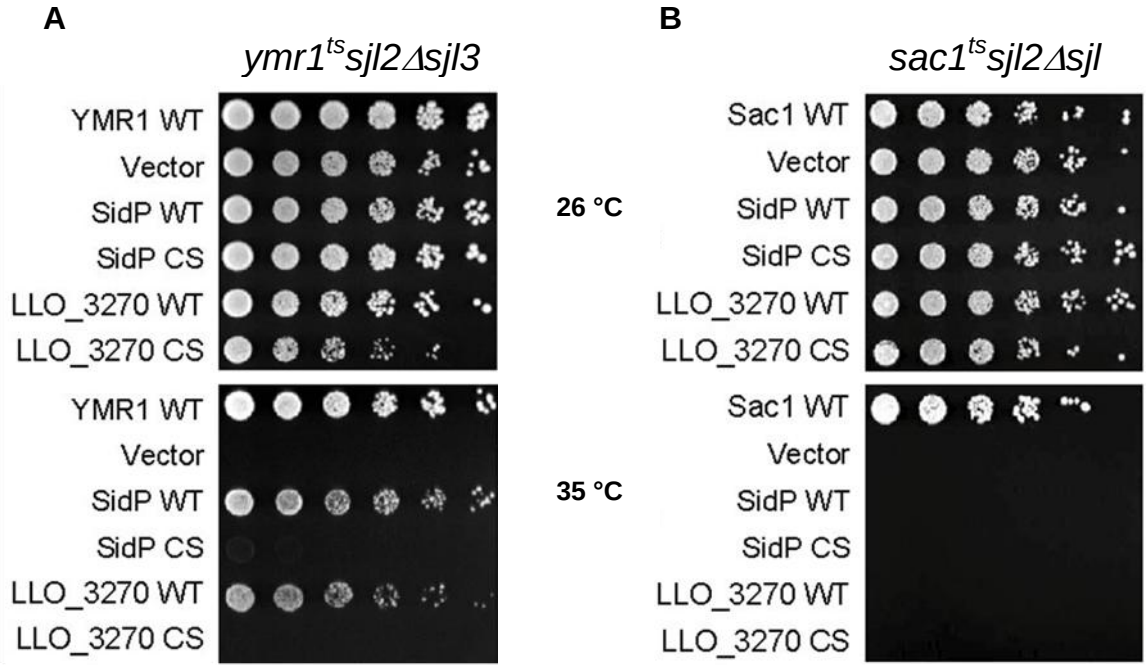

Figure 4.6 Functional complementation assays of SidP and its *L. longbeachae* orthologue (LLO_3270) in yeast. (A) *In vivo* growth rescue assay of SidPs in *ymr1^{ts}sjl2Δsjl3Δ* stain. (B) *In vivo* growth rescue assay of SidPs in *sac1^{ts}sjl2Δsjl3Δ* strain. In both (A) and (B), corresponding yeast cells were transformed with indicated constructs or vector control. The cells were spotted onto selection plates with four serial of 10x dilutions from left to right, and grown at the indicated temperatures for three days.

diffraction patterns that were non-analyzable and unusable for structure determination. The diffraction pattern resembled a twinned crystal diffraction pattern, although the crystals were not visibly twinned. This likely happened because the protein crystallized too quickly. Therefore, I worked on identifying the conditions to produce crystals at a slower rate or with different shapes.

I re-examined my initial screening trays and looked for crystals with morphologies different from the initial diamond shape. Of fifteen 24 well plates (288 conditions), only one well had a few tiny plate-shaped crystals. Fortunately, their diffraction pattern looked promising and analyzable. However, reproducing these plate crystals proved difficult. I carried out extensive optimizations trials by varying pH, buffer, salt, precipitant, temperature, drop size as well as concentration of the protein. Finally, it became apparent that these plate crystals form only in a very narrow range of conditions at temperatures around 4 degree centigrade. The best plate-shaped crystals were obtained using hanging drop vapor diffusion method at 4 degrees centigrade, with a reservoir solution containing 0.1M HEPES (pH 7.0), 0.1M succinic acid, and 6.5% (wt/vol) PEG3350. The crystals formed a few weeks after I set up the tray (Figure 4.7B).

The detectors that are used to measure and visualize the x-ray diffraction pattern of a crystal can only measure the intensity and therefore can only give information about the amplitude of a diffracted X-ray. Thus, phase information of each diffracted X-ray is systematically lost during data collection. Meanwhile, both amplitude and phase information are required to obtain the electron density distribution in a crystal. The lost phase can be recovered using a few methods including multi-wavelength anomalous diffraction (MAD), multiple isomorphous replacemnet (MIR), and single-wavelength.

Screen name	Well	Condition
Hampton Index	H3	0.2 M sodium malonate pH 7.0, 20% PEG-3000
Hampton Index	H4	0.1 M Citric acid pH 3.5, 25% PEG-3000
Hampton Index	H7	0.15 M DL-Malic acid pH 7.0, 20% PEG-3350
JCSG-Plus	B12	0.2 M tri-potassium citrate, 20 % w/v PEG 3350
JCSG-Plus	F7	0.8 M succinic acid pH 7.0
JCSG-Plus	F10	1.1 M sodium malonate, 0.1 M HEPES pH 7.0, 0.5 % v/v Jeffamine ED-2001
JCSG-Plus	F11	1.0 M succinic acid, 0.1 M HEPES pH7.0, 1 % w/v PEG 2000 MME 2.0
JCSG-Plus	G2	0.02 M magnesium chloride, 0.1 M HEPES pH 7.5, 22 % w/v polyacrylic acid 5100 sodium salt
PACT Premier	E11	0.2 M sodium citrate, 20 % w/v PEG 3350
PACT Premier	E12	0.2 M sodium malonate, 20 % w/v PEG 3350
PACT Premier	F12	0.2 M sodium malonate, 0.1 M Bis Tris propane pH 6.5, 20 % w/v PEG 3350
PACT Premier	G1	0.2 M sodium fluoride, 0.1 M Bis Tris propane pH 7.5 ,20 % w/v PEG 3350
PACT Premier	G12	0.2 M sodium malonate 0.1 M Bis Tris propane pH 7.5,20 % w/v PEG 3350
PACT Premier	H12	0.2 M sodium malonate 0.1 M Bis Tris propane pH 8.5, 20 % w/v PEG 3350

Table 4.2 Initial screen hits for LLO_3270 diamond crystals

anomalous dispersion (SAD).

SAD method was used for initial phase calculation I expressed LLO_3270 in Rosetta cells that were grown in media where methionine was replaced by selenomethionine (Se-Met). Since LLO_3270 has 10 methionine residues, incorporation of Se-Met should produce enough anomalous signal to be used for initial phase calculation.

I collected X-ray diffraction data from the Se-Met substituted plate crystals of LLO_3270 at CHESS (Figure 4.7C). All data sets were indexed, integrated and scaled with HKL-2000 (Otwinowski and Minor, 1997). The crystals belong to space group $P2_1$ with unit cell parameters of a = 89.28 Å, b = 119.65 Å, c = 133.53 Å, $\alpha = 90^0$, $\beta = 101.33^0$, $\gamma = 90^0$ (Table 4.3). Each asymmetric unit contains two molecules. The structure was solved using the selenium single wavelength anomalous diffraction (SAD) method with the help of the program HKL2MAP (Pape and Schneider, 2004). The final structure was refined against a 2.58 Å resolution data set with R_{work} = 19.8 and R_{free} =23.7, respectively (Table 4.3).

4.2.5 Crystal structure and overall domain configuration of LLO_3270

Full length LLO_3270 contains 825 amino acids. The crystal structure indicates that LLO_3270 is composed of three distinctive domains (Figure 4.8). The catalytic domain (alpha helices are colored in blue and beta-strands are in pink) and the appendage domain (I-domain – depicted in brown), which is inserted within the catalytic domain between residues 189 and 306, are both found at the N-terminus between residues 1 - 666. The C-terminus (residue 667-825) folds into an entirely α helical domain (CT-domain - colored in green).

A

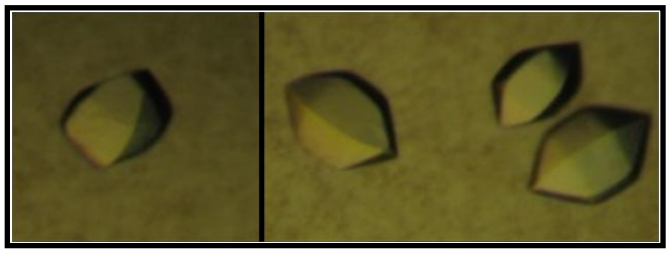

B

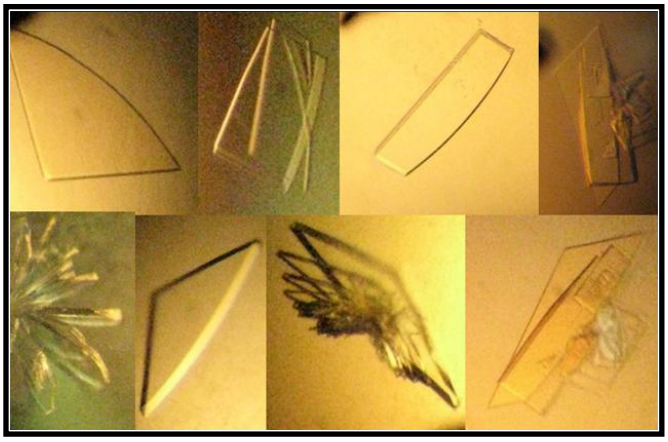

C

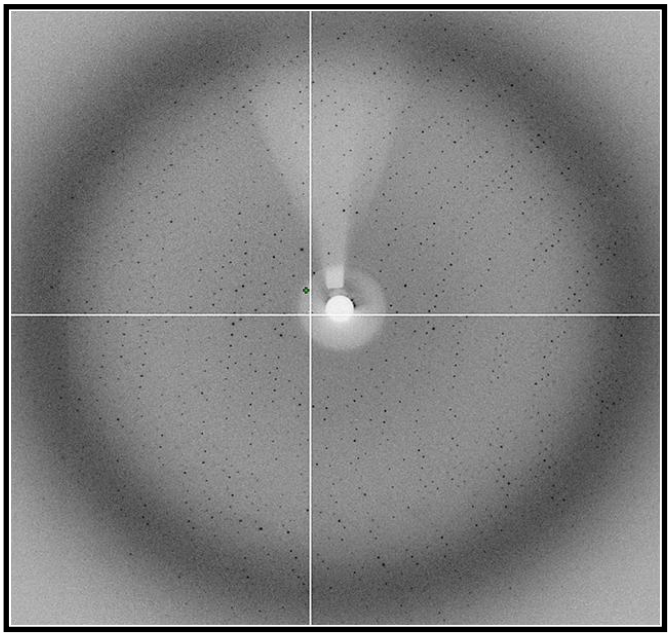

Figure 4.7 Crystallization and X-ray crystallography of LLO_3270. (A) Diamond shape crystals were the first observed crystals but did not diffract well. (B) After optimizing the condition, the plate shape crystals were formed that diffracted well. (C) Diffraction pattern of plate-shaped LLO_3270 crystals.

Data collection	
Space group	$P2_1$
Cell dimensions	a = 89.28 Å, b = 119.65 Å, c = 133.53 Å, $\alpha = 90^0$, $\beta = 101.33^0$, $\gamma = 90^0$
Synchrotron beam lines	CHESS A1
Wavelength (Å)	0.978
Resolution (Å)[a]	49.44-2.58 (2.65-2.58)
Unique reflections	164,803
Completeness (%)[a]	98.5 (95.5)
R_{sym}[a,b] (%)	9.9
$\langle I \rangle / \langle \sigma \rangle$[a]	10.96 (1.21)
Number of molecules in an ASU	2
Refinement statistics	
R_{crys} / R_{free} (%)[a,c]	19.8/23.7 (30.8/37.5)
Rms bond length (Å)	0.016
Rms bond angles (°)	1.729
Most favored/Allowed (%)	97.04/2.96
Outliers (%)	0
[a]Values in parenthesis are for the highest resolution shell	
[b]$R_{sym} = \Sigma_h \Sigma_i \lvert I_i(h) - \langle I(h) \rangle \rvert / \Sigma_h \Sigma_i I_i(h)$	
[c]$R_{crys} = \Sigma(\lvert F_{obs} \rvert - k \lvert F_{cal} \rvert) / \Sigma \lvert F_{obs} \rvert$. R_{free} was calculated for 5% of reflections randomly excluded from the refinement.	

Table 4.3 X-ray data collection, and structural refinement statistics

Since the electron density for the linker peptide between the catalytic domain and the C-terminal domain is missing, the C-terminal domain can be assigned to either one of the two LLO_3270 molecules in the asymmetric unit in two possible ways (Figure 4.9 A). In order to definitively assign the correct domain organization of LLO_3270, I used small-angle X-ray scattering (SAXS) method to obtain information about the solution properties of LLO_3270, including its overall shape.

SAXS can give information about the scattering intensity of a particle. In an ideal dilute monodisperse solution, where there are no interactions between the particles, the scattering intensity from the entire solution is proportional to the average of the scattering intensities of a single particle in all orientations. The scattering intensity of a particle can be transformed to scattering density of that particle. Scattering density reflects the number of electrons of that particle as well as the distribution of the electrons around the particle and can be used to reconstitute the electron density and its distance distribution in the particle. Thus, SAXS can be used to determine size, shape, and internal structure of a particle at low resolution (10-100) Å. in-solution scattering data that are complementary to high-resolution crystal X-ray diffraction data. In general, SAXS data can give us information about overall shape, conformational changes, folding and assembly, flexibility of a structures, quaternary structure, complex formation, and oligomerization behavior, and even more information about macromolecules (Svergun, 1992; Svergun, 1995; Svergun et al., 2001).

The SAXS data allowed me to reconstruct a low-resolution three-dimensional (3D) structural model of the LLO_3270. I used CRYSOL (described in chapter 2) program to position and fit two possible atomic models from crystallography into the

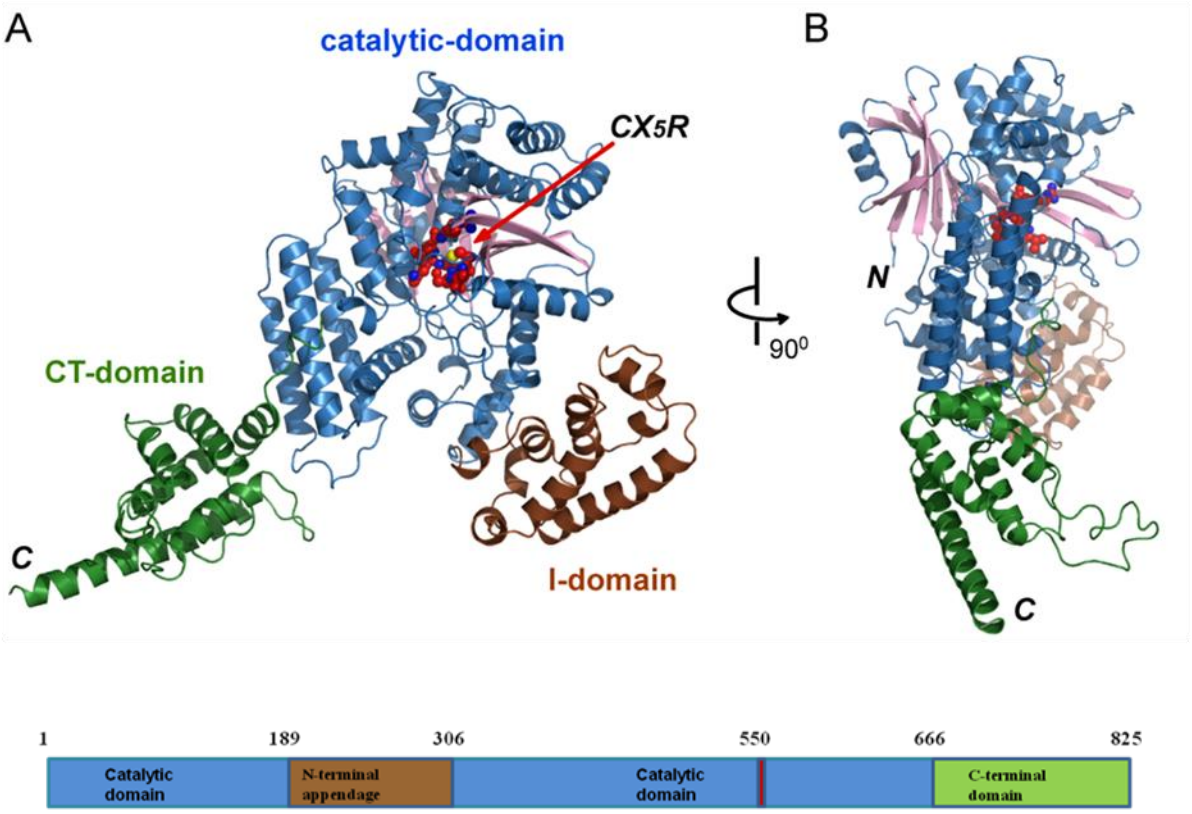

Figure 4.8 Crystal structure of LLO_3270. (A) and (B) Two orthogonal views of the crystal structure of SidP represented in ribbons. The catalytic "CX_5R" motif is shown in spheres and indicated by an arrow. LLO_3270 consists of three domains. The N-terminal catalytic domain is colored in blue and the I-domain, which is inserted within the catalytic domain, is shown in brown. The C-terminal (CT) domain is colored in green.

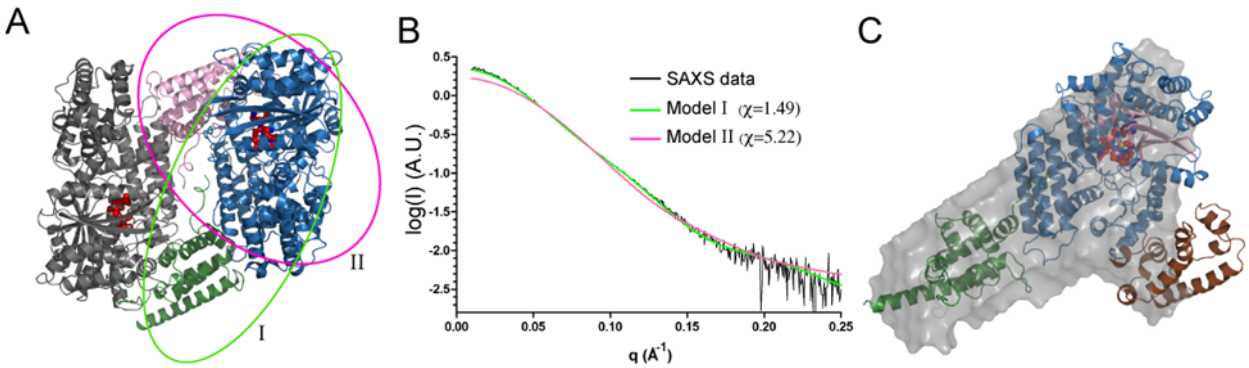

Figure 4.9 BioSAXS analysis of LLO_3270. (A) The two protein molecules in the asymmetric unit of the LLO_3270 crystal. The green (model I) and pink (model II) colored ovals indicate two distinct monomer models of LLO_3270. (B) CRYSOL fitting of LLO_3270 crystal structure models to the experimental data (black curve) on a plot of intensity versus q. The theoretic scattering from the LLO_3270 crystallographic model I is shown in green and in pink for model II. The Chi ($\sqrt{\chi^2}$) values are 1.49 and 5.22 for the fitting of Model I and II, respectively. The Chi values indicate that model I is acceptable and has a significant better fit with the experimental data than model II. (C) SAXS-based shape reconstruction for LLO_3270. The crystal structure of Model I is docked in the low-resolution envelope using the SUPCOMB program.

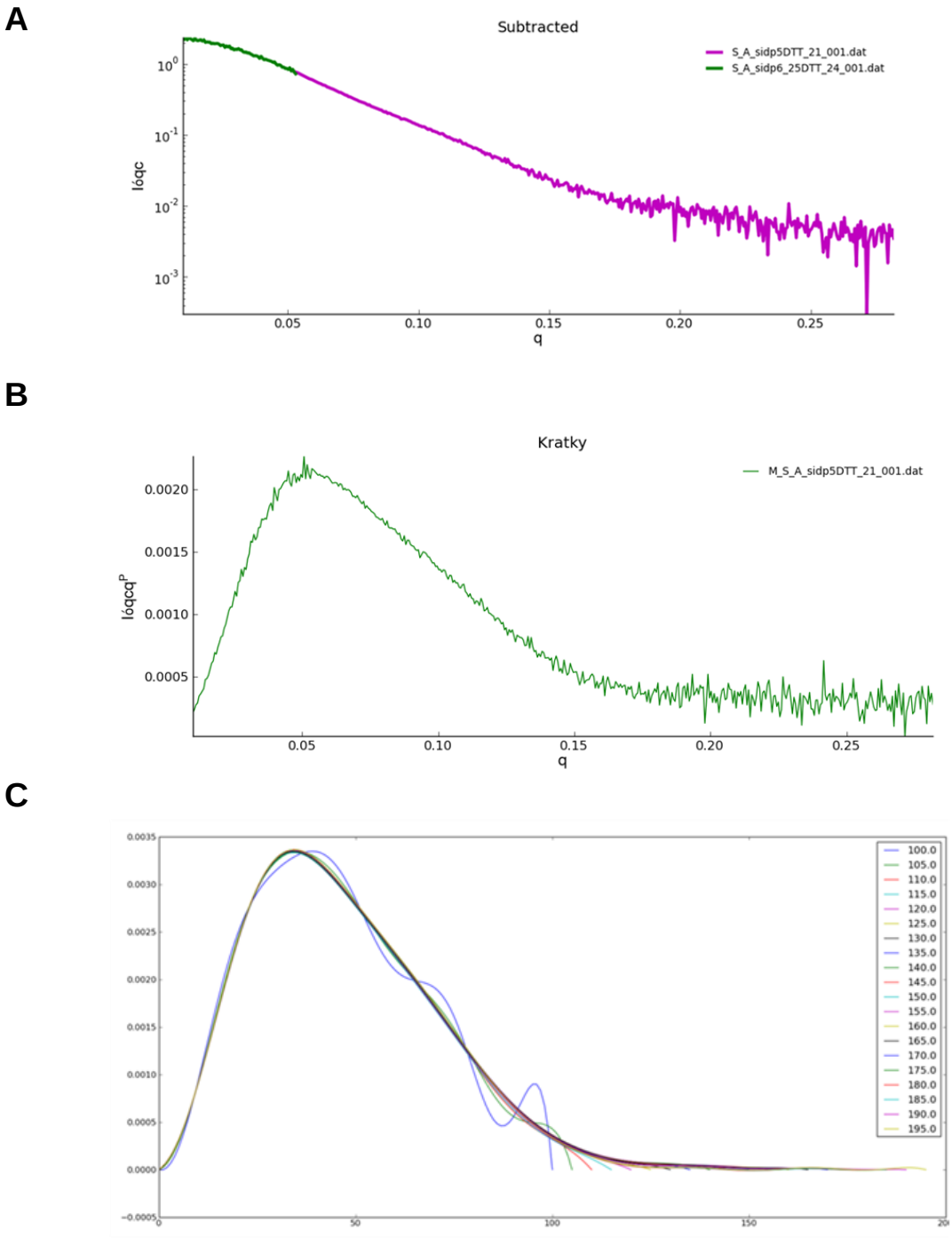

Figure 4.10 Background scattering subtraction and data quality evaluation. (A) Background scattering was collected from buffer and subtracted from the scattering. Green shows the lowest concentration, and purple shows the highest concentration. (B)Kratky plots were used to evaluate data quality and get information about the folded state of the proteins (C) Distance distribution function *P(r).*

SAXS data. Using the SAXS model, I was able to select the correct atomic model from the two possible atomic models obtained from the crystal structure. The model presented in (Figure 4.11C) (labeled as model I in Figure 4.9A) had a significantly better fit with the SAXS data than the alternative model (model II) (Figure 4.9B).Therefore, information that I obtained using X-ray crystallography combined with SAXS enabled me to construct the overall shape and domain configuration of LLO_3270 (Figure 4.9C, Figure 4.8).

4.2.6 The catalytic domain of LLO_3270

The catalytic domain of LLO_3270 is composed of a structural core consisting of 11 pleated β-sheets surrounded by 18 α-helices. These secondary structure elements group in a bird nest-like structure with a deep invaginated pocket at the center of the catalytic domain (Figure 4.11). Like other PI phosphatases, the bottom of this deep pocket, where the catalytic CX_5R motif (residue 554-560 or catalytic P-loop) is located, is highly positively charged (Figure 4.11B, D). A number of conserved arginine and lysine residues (labeled with blue oval in Figure 4.1) and the electric dipole of the α-helix, where the catalytic P-loop ends, contribute in part to the positive electrostatic potential of the catalytic site. Similar to other CX_5R containing phosphatases, this positively charged pocket is perfect for the recognition and accommodation of the negatively charged head group of PIs.

Intriguingly, a long loop between β8 and α20 enriched with hydrophobic residues (colored in gold in Figure 4.11, 4.12 and in the brown box Figure 4.1) works like a cap that closely covers the catalytic pocket of LLO_3270. This structural architecture

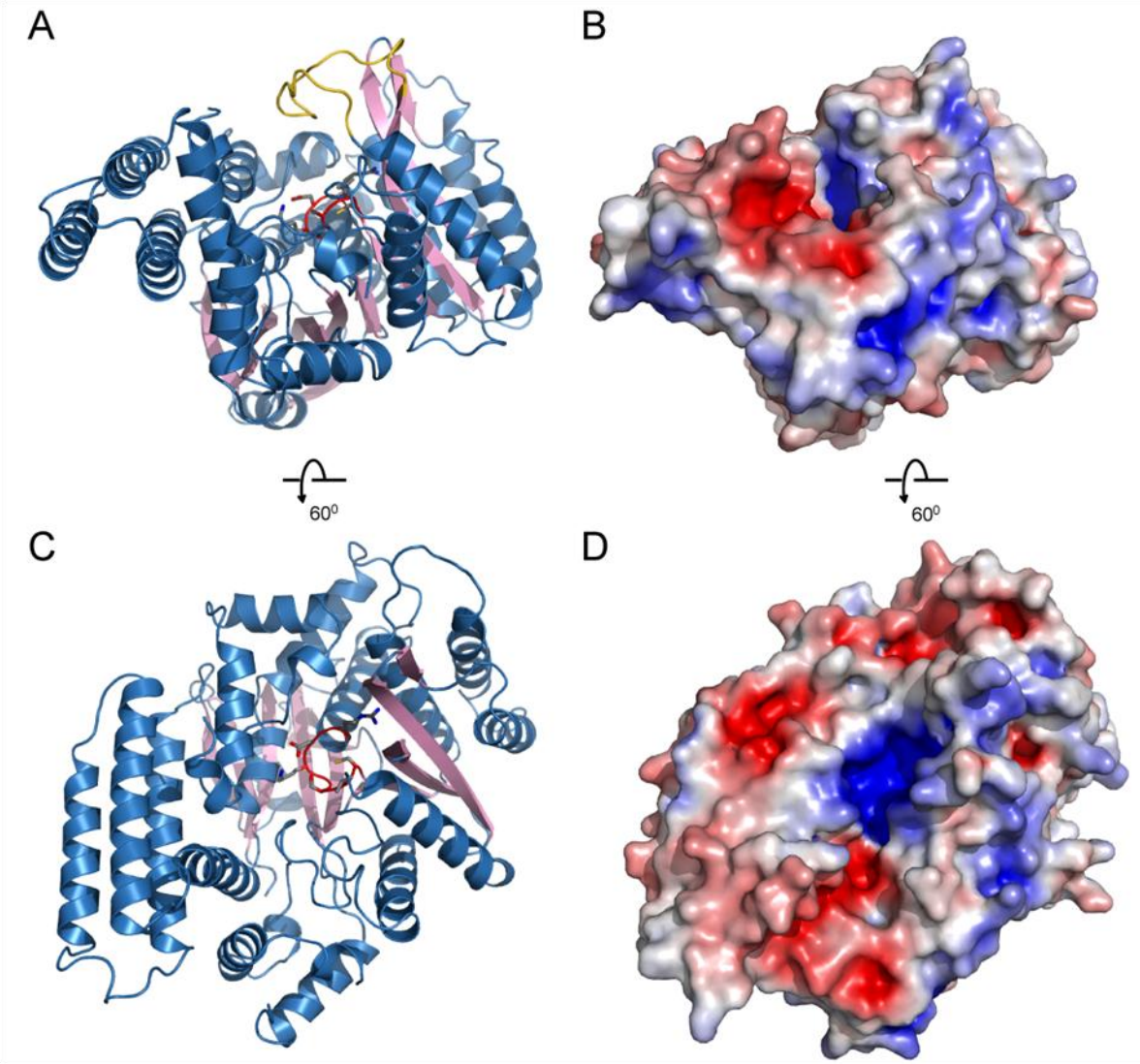

Figure 4.11 The catalytic domain of LLO_3270 . (A) Ribbon diagram of the catalytic domain of LLO_3270. the catalytic motif is shown in red in sticks. The catalytic pocket is covered by a hydrophobic loop, colored in gold. (B) The catalytic domain at the same orientation as in (A) represented in surface. The surface is colored based on electrostatic potential with positively charged regions in blue (+4 kcal per electron) and the negatively charged regions in red (-4 kcal per electron). Surface potential calculations were determined using APBS plug-in on PyMol (DeLano Scientific, LLC). (C) Ribbon diagram of the catalytic domain of SidP viewed with 60^0 rotation along the horizontal axis compared in *(A).* The hydrophobic loop is removed for a better view of the catalytic pocket. (D) Surface representation of the catalytic domain of SidP. The surface has a same orientation as (C) and is colored with the scheme as in (B). Again, the hydrophobic loop is removed to demonstrate the deeply invaginated and highly cationic catalytic site.

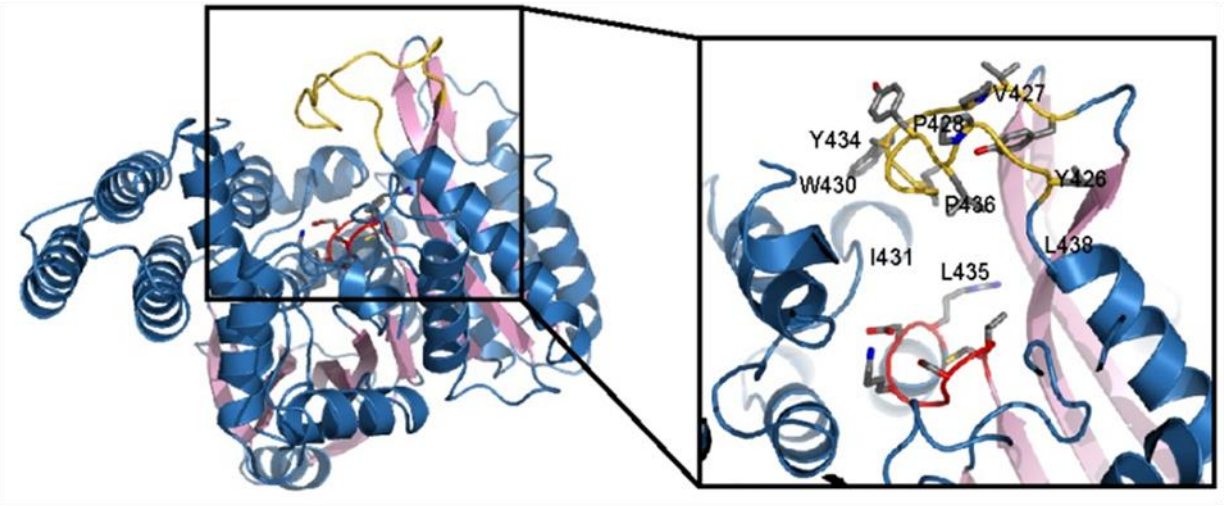

Figure 4.12 The catalytic domain of LLO_3270. Ribbon diagram of the catalytic domain of LLO_3270. The catalytic motif is shown in red in sticks. A hydrophobic loop that covers the catalytic pocket, is colored in gold and is showed in sticks in the zoomed-in view. A close view of the catalytic P-loop of LLO_3270 on the right.

suggests a regulatory role for the hydrophobic loop by controlling the accessibility of substrates to the catalytic pocket.

Close examination of the crystal structure of catalytic domain of LLO_3270 revealed another exceptional feature of its catalytic loop a unique conformation of the conserved arginine (Arg556) within the CX_5R loop. Arg556 faces away from the catalytic cysteine (Cys550) and the hydrophobic part of its side chain is inserted between two hydrophobic residues, Tyr625 and Leu417. Meanwhile, the guanidinium group of Arg556 makes hydrogen bonds with the main chain carbonyl group of His466 and interact with Glu528 through electrostatic attraction (Figure 4.13A). In contrast, this conserved catalytic arginine residue adopts a very different conformation in SidF, the other *L. pneumophila* PI phosphatase that our lab recently reported to specifically hydrolyze $PI(3,4)P_2$ and $PI(3,4,5)P_3$ (Hsu et al., 2012). The conserved catalytic Arg645 of the SidF CX_5R loop adopts a conformation that seems to facilitate the catalytic reaction of SidF by proper positioning the target phosphate group of the substrate and making it ready for the nucleophilic attack by the conserved catalytic cysteine (Cys 645). The conformation of SidF Arg651 is enforced by four hydrophobic residues (Val360, Val418, Phe624, and Phe718) that are located close to one another in the vicinity of the catalytic loop of SidF to create a hydrophobic fence that restricts the Arg651 in this conformation (Figure 4.13B).

It may be necessary for the Arg556 of LLO_3270 to switch its conformation to one similar to that of Arg645 of SidF to facilitate its substrate binding and catalytic activities. The question then is: why has LLO_3270 adopted a conformation that need to be changed to activate its catalytic activity? Although there is no obvious functional

advantage for Arg556 to have a different conformation than Arg645, it may play a regulatory role in the activity of LLO_3270. In fact, a conformational change in the. catalytic “CX5R” P-loop of Sac1 PI-phosphatase has been proposed to play a role in the regulation of the enzymatic activity of Sac1(Zhong et al., 2012).

4.2.7 Comparison of the catalytic domain of LLO_3270 and substrate specificity

The primary amino acid sequences of SidP and its orthologue LLO_3270 do not show any significant similarity to other known PI phosphatases. My structure of LLO_3270 revealed that its catalytic domain has the same conserved structural core seen in other PI phosphatases. The catalytic core of LLO_3270 comprises one α-helix and a central β-sheet with four parallel β-strands. The catalytic CX_5R is part of a loop that connects the carboxyl end of one of the β-strands to the amino terminus of the α-helix (Figure 4.11A and Figure 4.12) (Barford et al., 1994; Lee et al., 1999; Manford et al., 2010; Stuckey et al., 1994).

In addition, I performed a structural homology search using the **d**istance-matrix **ali**gnment (Dali) server (Holm and Rosenstrom, 2010; Holm and Sander, 1993). Dali server is a network service routinely used by crystallographers for comparing tertiary structure of proteins. By submitting coordinates of a query protein structure to Dali server, the 3D structure of the query protein will be compared against the protein structures available in protein data bank (PDB). Dali search of SidP revealed that the catalytic domain of LLO_3270 is strikingly similar to the catalytic domain of SidF. The Dali Server calculated the 3D structural superposition of these two structures and yielded a Z-score of 20.3 and a root-mean-square deviation (rmsd) of 2.9 Å for 421 aligned residues. Z-Score is a statistical measurement that reflects the distance of a

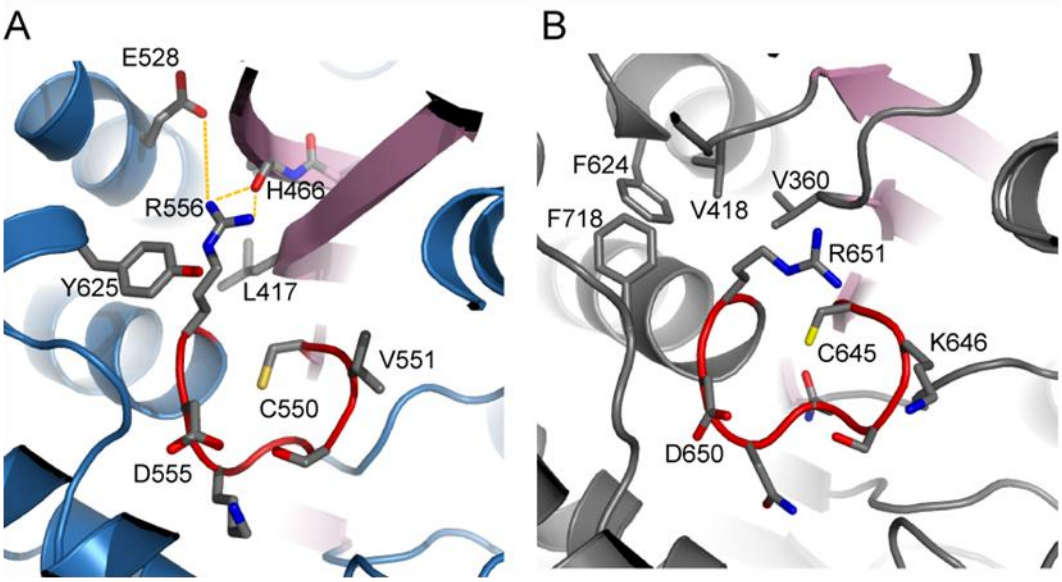

Figure 4.13 Structural comparison of the catalytic site between SidP and SidF. (A) The catalytic site of SidP. Note that CX_5R arginine is away from the catalytic cysteine (Cys550). The hydrophobic part of Arg556 side chain is sandwiched between two hydrophobic residues Tyr625 and Leu417, while the guanidinium group interacts with the main chain carbonyl group of His456 through hydrogen bonding and residue Glu528 through electrostatic attraction. (B) The catalytic site of SidF. The presence of a cluster of hydrophobic residues (Val360, Val418, Phe624, and Phe718) retains the CX_5R arginine Arg651 in a conformation that its guanidinium group is close to the catalytic cysteine.

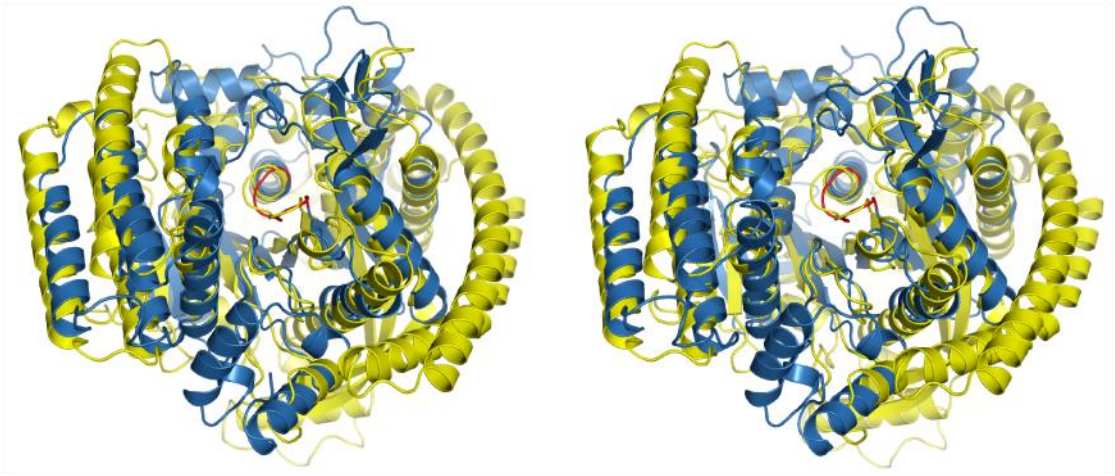

Figure 4.14 Stereo view of superposition of the catalytic domain of LLO_3270 with SidF. LLO_3270 is colored in blue and SidF (PDB ID: 4FYG) is in yellow. The CX_5R motif is shown in red.

data point from the mean in a group of data set, and the higher z-score means the further from the mean. Thus, the very high Z-score resulting from Dali comparison of catalytic domain of SidP and SidF indicates their similarity is very significant (Figure 4.14).

Although LLO_3270 and SidF have very similar catalytic domain structures and both have PI-3-phosphatase activity, SidF hydrolyzes PI(3,4)P_2 and PI(3,4,5)P_3. These are distinct from LLO_3270, which hydrolyzes PI(3)P. This prompted us to investigate whether there are fine structural features in these phosphatases that may contribute to their distinct substrate specificity. To this end, I closely compared the catalytic sites of SidP, SidF and other PI phosphatases, such as the myotubularin phosphatase (Begley et al., 2006; Begley et al., 2003) and the tumor suppressor PTEN (Lee et al., 1999). This analysis revealed differences in both the overall shape of the active site pocket and in the primary sequence of the catalytic P-loop.

A primary sequence comparison of the catalytic P-loops revealed an interesting pattern. It seems that all the phosphatases that can hydrolyze substrates with two adjacent phosphate groups have a lysine residue immediately after the conserved catalytic cysteine of the CX_5R motif (orange boxes)(Figure 4.15A). It is possible that the presence of a lysine residue after the catalytic cysteine could be a determining factor for the substrate specificity of these phosphatases. A lysine residue in this position in PI phosphatases such as SidF and IpgD, SopB, PTEN, and INPP4B, causes the preferable hydrolysis of the PI species with two consecutive phosphate groups. In contrast, enzymes such as SidP, Sac1 and MTMR2 those have a non-lysine residue after

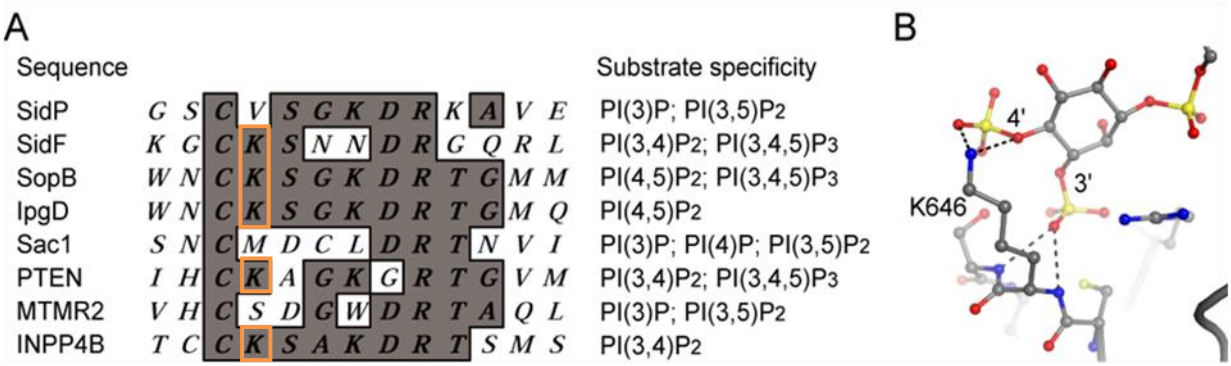

Figure 4.15 Enzymes with a non-lysine residue following the catalytic cysteine seem to hydrolyze mono- or non-consecutively di-phosphorylated PI species. However, enzymes with a lysine residue after the cysteine (orange boxes) can hydrolyze lipids with two consecutive phosphate groups. (B) A close view of the catalytic site lysine (K646) in SidF. The main chain amide group forms hydrogen bond with the D3 phosphate, while the epsilon amide group interacts with the D4 phosphate. A lysine residue at the second position of the "CX_5R" motif provides the specificity for PI substrates with two consecutive phosphate groups.

the catalytic cysteine preferably hydrolyze mono- or non-consecutively di-phosphorylated PI species. Thus, the presence or absence of a lysine residue after the conserved cysteine in the CX_5R motif is a likely determining factor for the substrate specificity of these enzymes. Based on the crystal structure of SidF in complex with its substrate $PI(3,4)P_2$ (Begley et al., 2006; Hsu et al., 2012; Luo and Isberg, 2004), the adjacent phosphate groups by "sensing" the distance between the phosphate groups. We can imagine this lysine as a "molecular ruler" for consecutively di-phosphorylated PI species. Therefore, the lack of this lysine residue in LLO_3270, as well as in Sac1 and MTMR2, could in part be the reason why these enzymes do not hydrolyze PI species with two adjacent phosphate groups.

Furthermore, structural comparison of the catalytic pocket of LLO_3270 with other phosphatases revealed that the size of the catalytic pocket in LLO_3270 is considerably smaller (Figure 4.11B, D) than the catalytic pocket of SidF (Hsu et al., 2012). This spatial restriction may also restrict the accessibility of bulky PIs with multiple phosphate groups.

4.3 Discussion

Structure determination of LLO_3270 revealed that this phosphatase contains two additional novel domains, the I-domain and the CT-domain, in addition to its main catalytic domain. The crystal structure allowed me to see for the first time several unique and interesting features of the catalytic domain of LLO_3270 that may play roles in the regulation of the enzymatic activity and substrate specificity of this enzyme.

Furthermore, the structure of LLO_3270 shows that both the I-domain and CT-domain are entirely made up of α-helices. Interestingly, neither of these two domains showed any considerable structural homology to any known protein structures, as

determined using a search on the Dali server. It is possible that these domains will function as protein-protein interaction domains during infection and mediate the interaction of LLO_3270 with host proteins or other *Legionella* effector proteins. These interactions may be important for the proper targeting of LLO_3270 during infection.

Since only 10% of *L. pneumophila* encoded proteins are transferred to the host cells during infection by the Icm/Dot secretion system, it has been proposed that these secreted effector proteins may carry some special molecular signature and structural features. In addition to the substrates' intrinsic properties such as the presence three hydrophobic amino acids at the very C-terminal end of some set of substrates like RalF (Nagai et al., 2005), or large stretches of glutamic acid in other subset of substrates (Lifshitz et al., 2013), other factors have been proposed to play roles in the proper transfer of the Icm/Dot substrates, including chaperones that may help correctly fold the substrates so that their molecular signature can be exposed to the Icm/Dot transporter. Molecular features on the substrates that can be recognized by the Icm/Dot secretion system, such as stretches of residues with similar physicochemical properties at the carboxyl terminal part of the protein, seem to play an important role in substrate translocation. It has been suggested that these determinants for substrate recognition and transfer may be found on the carboxyl terminus of substrate proteins, but the mechanism of substrate recognition is poorly understood (Luo and Isberg, 2004). Therefore, a more detailed study of the structure of the CT-domain may reveal a structural signature recognizable by the Icm/Dot secretion apparatus.

Consistent with our hypothesis that CT-domain may play a role in LLO_3270 transfer, we found a glutamate cluster called "E-block" in the CT-domain. E blocks are

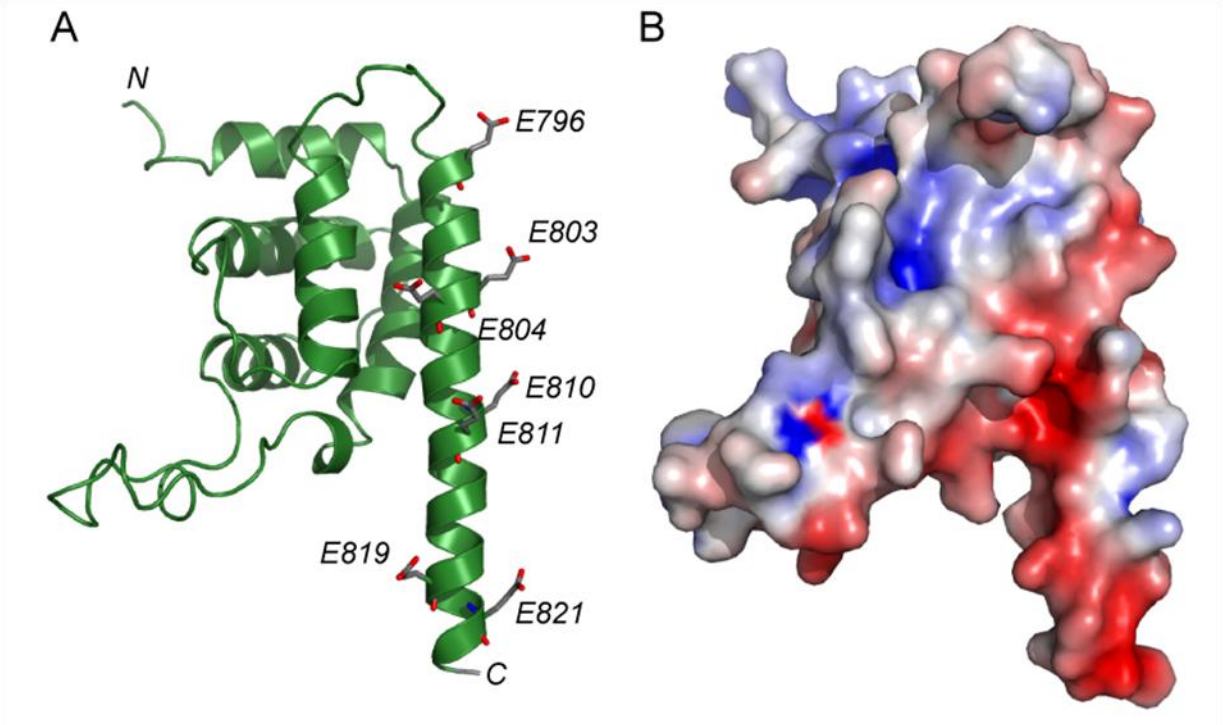

Figure 4.16 The CT-domain of LLO_3270. (A) Ribbon diagram of the CT-domain of LLO_3270. The very C-terminus of LLO_3270 assumes a long α-helix structure. This α-helix is enriched with glutamate residues (shown in sticks). (B) Surface representative of the CT domain. The same color scheme applied in Figure 4.8 is used in this figure. Note that the C-terminal α-helix is negatively charged due the cluster of glutamate residues.

regions of 6-8 glutamate residues that have been reported to act as an important element for the transfer of many effectors (Huang et al., 2011; Lifshitz et al., 2013). Intriguingly, the C-terminal residues of LLO_3270 form a long α helix containing 29 residues that is rich in glutamate and has an overall negative charge (Figure 4.16A and B). The seven glutamate residues found in this helix make an “E block”. Interestingly, although the glutamate residues in the C-terminal α helix are not completely conserved among SidP homologues in different species, it seems that having an overall negative surface potential at the C-terminus is a conserved physico-chemical property, as SidP proteins from other *Legionella* species are all enriched with glutamate residues at their C-termini (Figure 4.1).

L. pneumophila chaperones may facilitate exposure of the substrate translocation signature to the Icm/Dot transporter system. Small, acidic *L. pneumophila* proteins such as IcmS, IcmW, and LvgA have been shown to make stable IcmS/IcmW and IcmS/LvgA complexes (Coers et al., 2000; Vincent and Vogel, 2006) that interact with a large numbers of effector proteins and facilitate their transfer by an unknown mechanism, possibly by inducing conformational changes in the effectors. It is not understood why these chaperones only improve the transfer of a subset of effector proteins. Likely, these chaperones are required for transfer of the substrates that require chaperone binding to achieve the optimal conformation for recognition by the Icm/Dot system (Cambronne and Roy, 2007; Lifshitz et al., 2013; Qiu and Luo, 2013). Investigating the possible interaction of the CT-domain with IcmS/IcmW and IcmS/LvgA complexes *in vitro* may help us understand the mechanism of how *L. pneumophila* chaperones facilitate efficient transfer of effector proteins into the host.

Finally, SidP and LLO_3270 do not contain trans-membrane domains or membrane binding domains. Furthermore, my *in vitro* liposome-binding assay showed that neither the full-length proteins nor the catalytic domains were able to bind directly to membranes (data not shown). Therefore, it is plausible that either the I-domain, or the CT-domain, or both may be involved in protein-protein interactions that help LLO_3270 anchor onto the LCV membrane through binding to other yet unidentified host or *Legionella* proteins.

CHAPTER 5

Conclusions and perspectives

5.1 SidP and SidF may actively regulate the LCV lipid composition

Taking into consideration the critical roles that PIs play in cellular vesicle trafficking, PI composition and lipid identity of the LCV is expected to play a significant role in LCV biogenesis and maturation. Therefore, unraveling the molecular mechanisms that regulate the PIs on the LCV spatially and temporally during infection is very important for understanding *L. pneumophila* pathogenicity.

During *L. pneumophila* infection early phagosome transition to LCV is accompanied with a PI(3)P enriched organelle transformation to a PI(4)P enriched organelle. Enrichment of PI(4)P on the LCV membrane makes it a trans-Golgi-like compartment. This Golgi-like identity of the early LCV may make it a more appropriate organelle to recruit, interact with and fuse with ER-derived secretory vesicles. Consistent with this idea, PI(4)P-binding *L. pneumophila* effector proteins SidC and SidM anchor on the LCV membrane through PI(4)P and presumably aid in the recruitment and fusion of ER-derived vesicles with the LCV (Luo and Isberg, 2004; Machner and Isberg, 2006; Murata et al., 2006; Ragaz et al., 2008).

The following model depicts how the non-overlapping PI-3 phosphatase activities of SidP and SidF may actively regulate the LCV lipid composition and consequently contribute to the LCV programming for *L. pneumophila* multiplication. SidP dephosphorylates and depletes PI(3)P on the LCV. This may contribute in blocking the fusion of host endosomes or lysosomes with the LCV, which prevents bacterial degradation via the phagolysosomal pathway (Figure 5.1, and 5.2). According to this

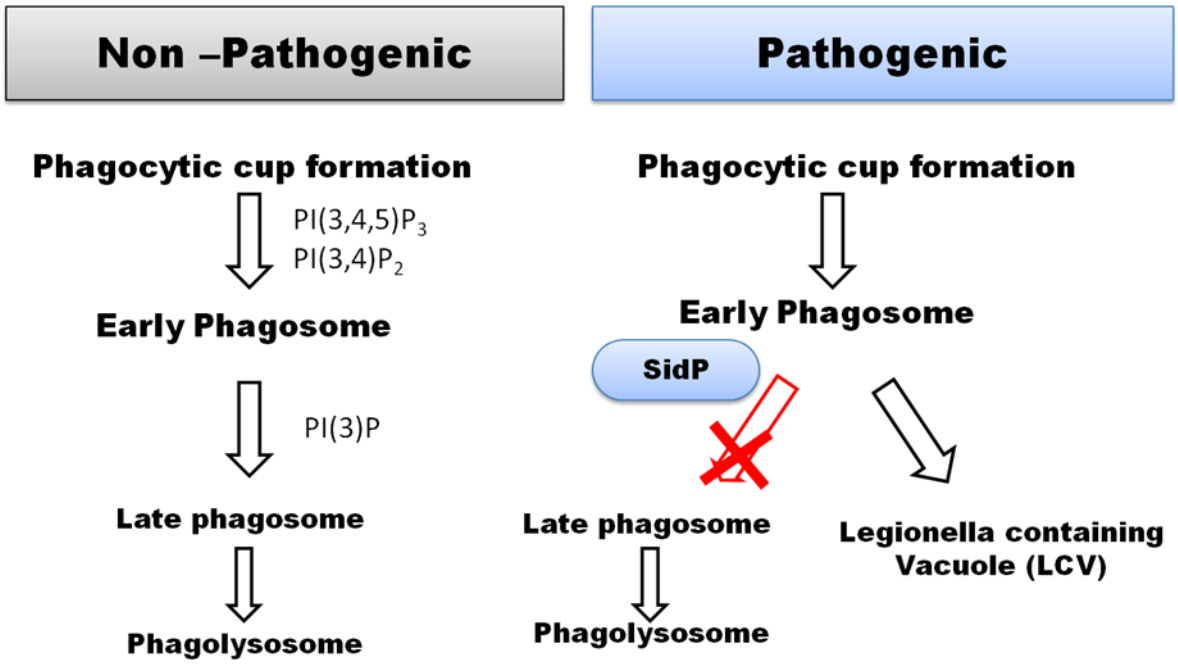

Figure 5.1 SidP may block phagocytosis by depleting PI (3)P from the early phagosome. PIs interconvert during phagocytosis and later stages of phagosomal maturation into the phagolysosome. SidP may contribute to phagocytosis maturation arrest by interfering with PIs interconversions.

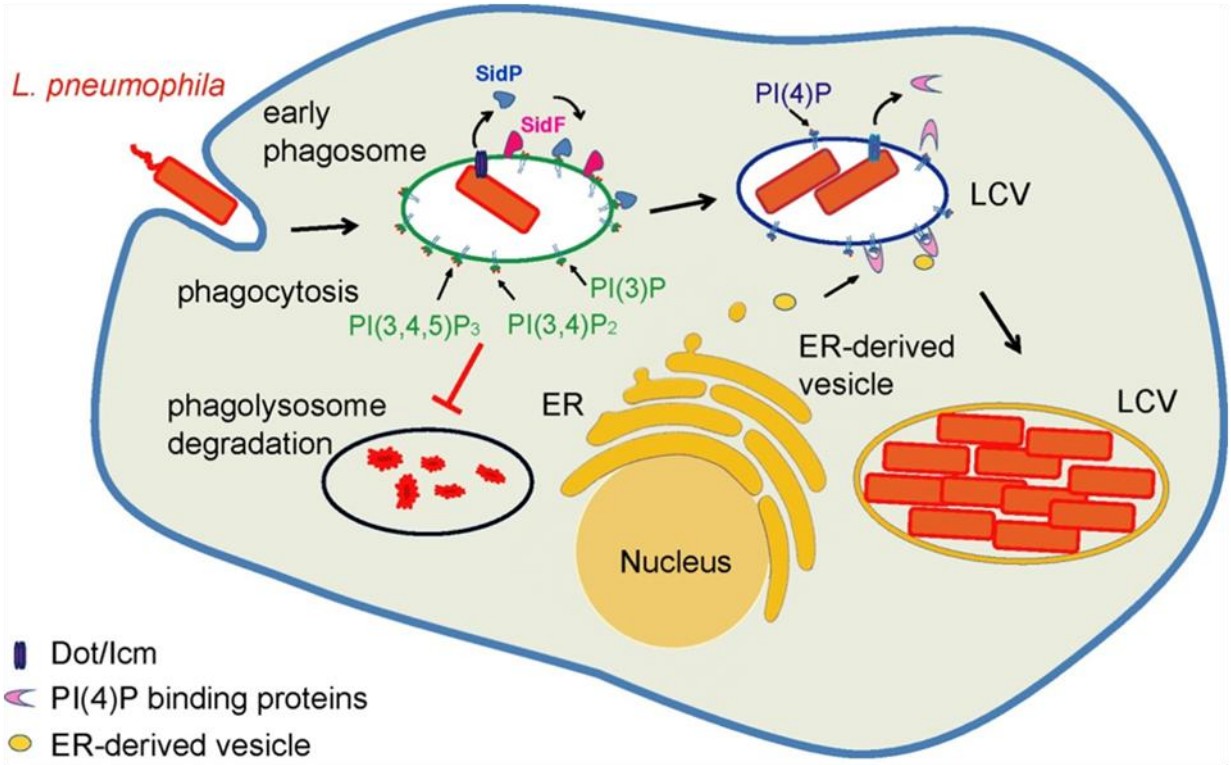

Figure 5.2 Functional model of modulating host PIs in *L. pneumophila infection*. *L. pneumophila* encodes two PI phosphatases, SidF and SidP. While SidF specifically hydrolyzes PI(3,4)P_2 and PI(3,4,5)P_3, SidP removes PI(3)P on the surface of early bacterial phagosomes. By the synergistic action of these two effectors, the LCV will be diverted from PI(3)P mediated phagolysomal pathway into a PI(4)P enriched compartment that is hospitable for the intracellular replication of the bacterium

model, SidF anchors on the LCV membrane and hydrolyzes PI(3,4,5)P_3 and PI(3,4)P_2 to PI(4,5)P_2 and PI(4)P. SidF can also indirectly prevent PI(3)P accumulation on the LCV by hydrolyzing PI(3,4,5)P_3, which is the substrate of host 5p- or 4p- phosphatases. PI(3,4,5)P_3 can be converted into PI(3)P by the catalytic function of 5p- or 4p-phosphatases during endocytic processes (Shin et al., 2005). This synergistic action of SidP and SidF in PI(3)P removal from the LCV may contribute in blocking the fusion of host endosomes or lysosomes with the LCV, which prevents bacterial degradation via the phagolysosomal pathway. The phosphatase activity of SidF may also contribute to the enrichment of PI(4)P on the LCV by hydrolyzing PI(3,4)P_2 Substrate. PI(4)P can then recruit several other bacterial effectors, such as SidC and SidM, which promote the recruitment and fusion of ER-derived vesicles with the LCV and its maturation. This model could be oversimplified, as the mechanism governing the regulation of the PI composition on LCV membranes is expected to be complex, and it likely involves many PI-metabolizing enzymes and several related Icm/Dot-secreted effector proteins.

Presently, we have very little knowledge and understanding of the interaction between *L. pneumophila* PI-binding effectors. SidP and SidF have only recently been discovered, and molecular details of their functions have yet to be identified. Furthermore, unlike the other pathogens discussed, the frequent occurrence of functional redundancy among *L. pneumophila* effector proteins makes it difficult to narrow down the role of each specific PI-phosphatase in pathogenicity. Studying and identifying these interactions will be invaluable when it comes to unraveling the molecular details of *L. pneumophila* infection. Deletion of SidF or simultaneous deletion of SidP and SidF did not cause any obvious defects in bacterial growth or infection.

Again, a possible explanation for the lack of phenotype is that other bacterial effector proteins or host proteins can compensate for the function of these two proteins. As previously described, our bioinformatics approach identified 29 open-reading frames containing the "CX_5R" motif, which are believed to be substrates of the Icm/Dot secretion system (Hsu et al., 2012; Zhu et al., 2011). Only two of these candidates, SidP and SidF have been identified and partially characterized, and so there may be several others that function as PI phosphatases and contribute to LCV lipid identity.

In addition, screening using "CX_5R" motif would not be able to identify all potential PI phosphatases in *L. pneumophila*, since the remaining major family of PI phosphatases, the "5-phosphatase family", does not contain the "Cx_5R" motif. Instead, the 5-phosphatase (5-Ptase) metal dependent family has two motifs: "WxGDxNxR" and "PxWCDRxL" (Jefferson and Majerus, 1996).Therefore, exploring other candidates and possible identification of other *L. pneumophila* PI phosphatases would definitely helpful to have a better picture of PI regulation on the LCV and the impact of this regulation on *L. pneumophila* pathogenicity.

5.2 Future directions

In terms of host cell biology, the most important challenge is to understand the role of SidP during the *L. pneumophila* infectious cycle, and the consequences of expressing SidP in host cells. Since *sidP* deletion mutants are still infectious, and given the high likelihood that there are other bacterial effectors that function redundantly with SidP, dissecting the function of SidP during *L. pneumophila* infection would be very difficult. Identification and elucidation of function of other *L. pneumophila* PI(3)P phosphatases would be helpful to understand the role of SidP in infection. *L.*

pneumophila strains from which the genes encoding PI(3)P phosphatases have been deleted singularly or/and simultaneously could be used to study the phenotype and pathogenicity of these strains.

Furthermore, generating and studying pathogenicity of *L. longbeachae* strain carrying LLO_3270 deletion mutants could be worth trying, since different species of *legionella* encode and translocate different sets of effector proteins. With the same logic, exogenous expression of LLO_3270 in mammalian cells and studying the possible effects on mammalian cellular pathways can be another alternative.

L. pneumophila has been shown to interact with host cells in a very specific manner. Host cells interact and cooperate in a host-specific-dependent manner with *L. pneumophila* effector protein during infection. For example, *L. pneumophila* Δ*sdhA* mutant *shows* only minor growth defect in *D*. *discoideum, meanwhile its intracellular growth is severely impaired in* macrophages. Most likely because *L. pneumophila* effector protein SdhA is involved in inhibition of death pathways in macrophages that *are absent in D*. *discoideum* (Laguna et al., 2006; O'Connor et al., 2012). Thus, investigation and careful quantification of the intracellular growth of *sidP* deletion mutant strain in different host cells, including amoebal, drosophila, and mammalian cells may reveal growth defect phenotypes in one or more of these host cells.

Although LCVs harboring *L. pneumophila* carrying a *sidP* deletion mutation were able to avoid lysosomal fusion and the *sidP deletion* mutant strain was able to form “replication permissive” LCVs (Figure 3.7), deletion of SidP may still affect the dynamics of the LCV maturation and change the acquisition of endosomal markers by the LCV during infection.

Investigating the possible effects of exogenous expression of SidP in the mammalian cell endocytic pathway may give us some indication about its role during infection. Both stable and transient expression of SidP in macrophages proved unsuccessful in our hands and we may need to deliver tagged-SidP into macrophages by microinjection. The effect of exogenous delivery of SidP on mammalian cell phagosome acidification or other aspect of endocytic pathway may be helpful to understand the role of SidP in pathogenicity.

During phagosome maturation, the phagosome membrane undergoes several changes. These include remodeling, changes in associated molecular markers, decrease in pH and increase in oxidative potential. These specific molecular and chemical markers can be used to study the possible role of SidP in arresting phagocytosis maturation. Using macrophages injected with the purified SidP protein, the role of SidP in phagocytosis maturation arrest can also be tested by tracking changes in phagosome acidity using Lyso Tracker Blue (Invitrogen), a fluorescent acidotropic reagent which serves as a marker of maturing phagosomes(Via LE, 1998),(Malik ZA, 2000). Phagocytosis can then be monitored using 3D live imaging, over a period of 15-60 minutes at 2 minutes time intervals. The number of acidic phagosomes positive can be quantified.

Studying and comparing the time required for digestion and clearance of digested fluorescent-*E. coli* in macrophages injected with the purified SidP protein can be used to test the effect of SidP on the dynamic of phagocytosis. Macrophages injected with the purified SidP can be tested for markers for the early phagosome (EEA1) or the phagolysosome (Cathepsin D and LAMP1) (Flannagan et al., 2009) at

several time points after adding the phagocytic stimuli. This experiment may reveal the possible delay in phagocytosis maturation in the presence of SidP, as indicated by delayed appearance of markers for late endosomes and phagolysosomes.

It is shown that eukaryotic PI phosphatase activities are regulated through interaction with their binding partners. Eukaryotic PI phosphatases like Fig4 can be recruited to the membrane, where their substrates are localized through their binding partners (Duex et al., 2006; Ikonomov et al., 2009). *L. pneumophila* genome has a large number of genes predicted to encode proteins or domains, which some are involved in host-pathogen interaction.(Newton H. J., 2010). CT-domain of SidP may be involved in protein-protein interactions that help SidP anchor onto the LCV membrane through binding to other proteins. Thus, I speculate that similar to eukaryotic phosphatases, some other yet unidentified host or *L. pneumophila* proteins may control regulation (especially temporal) of SidP activity and its localization. Yeast two- hybrid system (Bai and Elledge, 1996), or a Stable Isotope Labeling with Amino aCids (SILAC) experiment can be used for identifying putative candidates in the host cells as SidP binding partners (Ong et al., 2002). The physical interaction of SidP with its possible binding partner candidates can be tested by coimmunopercipitation. In fact, I have already started a SILAC experiment. N-terminally GFP-tagged SidP and GFP proteins have been exogenously expressed in human T98-G cells growing in SILAC media. I have already collected the cells and purified the GFP and GFP-tagged SidP, using GFP-binding beads. The purified protein samples are stored in -80 °C ready to be processed and analyzed using mass spectroscopy.

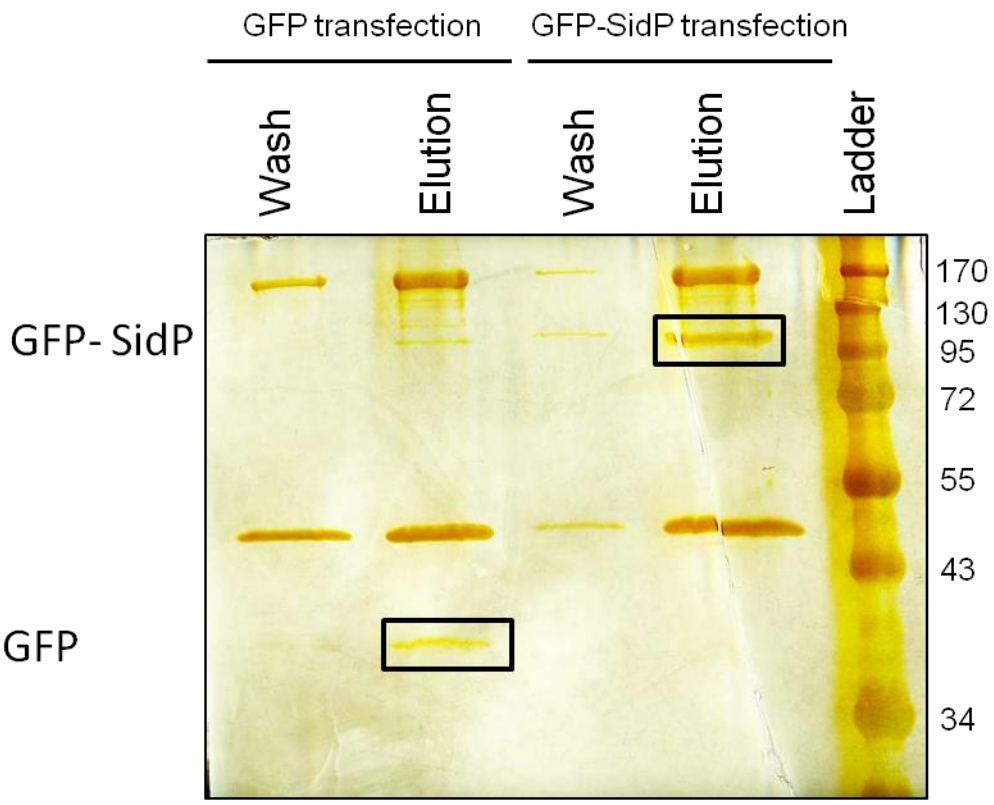

Figure 5.3 GFP and SidP-GFP protein purified from T98G cells grown in SILAC media. T98G cells growing in light SILAC media were transfected with plasmid expressing GFP, and the cells growing in heavy SILAC media were transfected with plasmid expressing GFP-SidP. Proteins were purified using GFP binding beads. To test the quality of the samples 1 µg of each were separated by SDS-PAGE followed by sliver staining

The CT-domain of SidP may be involved in *L. pneumophila* protein-protein interactions that help translocation of SidP by the Icm/Dot transporter system. *L. pneumophila* chaperones such as IcmS and IcmW have been shown to make stable IcmS/IcmW complexes, and interact with some of the substrates of Icm/Dot to make their interaction with the Icm/Dot system more efficient. I wanted to test the possible interaction of CT-domain of SidP with IcmS/IcmW complex *in vitro*. I already have expressed recombinant N-terminal His-SUMO tag-CT- SidP(residues 674-) in the Rosetta (DE3) E. coli strain, purified it to homogeneity using affinity chromatography followed by size exclusion chromatography (Figure 5.4). I have co-expressed recombinant N-terminal His-IcmS-IcmW-C-terminal Stag in the Rosetta cells. Currently I am working on optimization of IcmS-IcmW expression condition , since it seems that the IcmS-IcmW complex is not stable *in vitro*. When stable IcmS-IcmW proteins are available, their binding to CT-SidP can be tested in vitro.

The polyclonal antibodies that we have generated against SidP were not able to probe the *in vivo* localization of SidP during *L. pneumophila* infection because of non-specific signals. I have purified anti- SidP using affinity chromatography, however, the purified antibody also shows non-specific signal. Therefore, I am missing an essential tool to study the function of SidP during infection. Antibody production can be repeated using truncated SidP or by injecting the protein to a different choice of animal. This challenge could also be overcome by making *L. pneumophila* that expresses a tagged SidP that can be tracked using the epitope tag (Lp02Δ*sidP*/taggedSidP).

As mentioned in Chapter 3, we were not able to visualize the SidP PI(3)P phosphatase activity by tracking the intensity and dynamic of a PI(3)P probe, GFP-

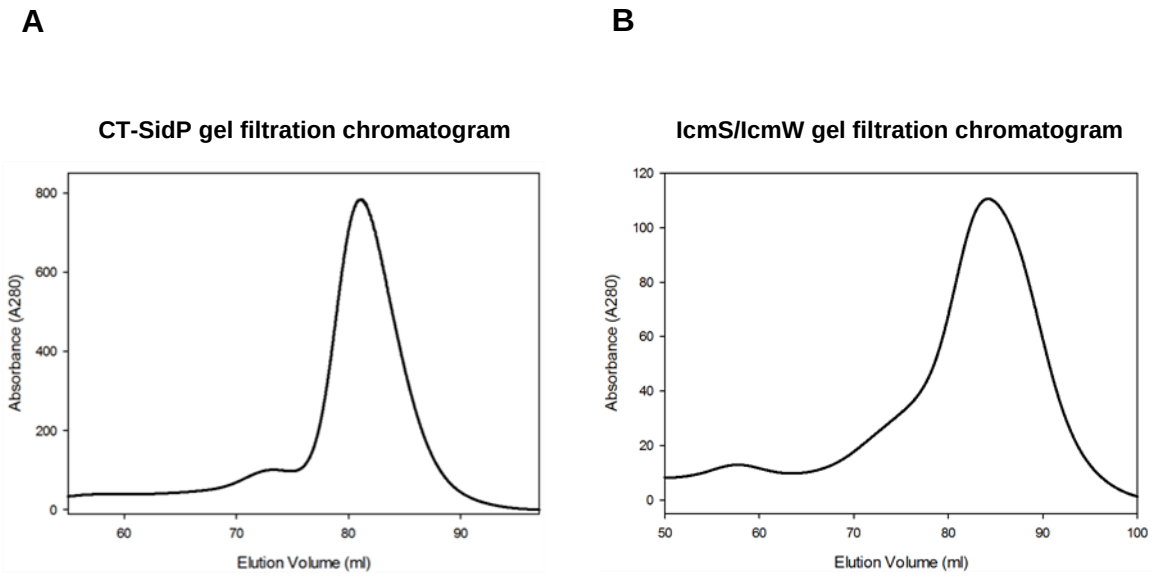

Figure 5.4 Gel filtration and SDS-PAGE of CT-SidP and IcmS/IcmW proteins. Tagged CT-SidP (A) and tagged IcmS/IcmW proteins (B) elute off the size-exclusion columns in the major peak after approximately 80 mL.

fusion-2X-FYVE domain, during *L. pneumophila* infection. This might reflect errors in timing in our capture of the dynamic changes of PI(3)P probe during infection. Therefore, live imaging of cells infected with a fluorescently labeled *L. pneumophila*, may help capture the possible transient changes of PI(3)P on the LCV in early stages of infection.

Besides vesicle trafficking, *L. pneumophila* phosphatases may interfere with other signaling cascades found in the host cell. Since SidP can hydrolyze PI(3,5) P_2 to generate PI(5)P (Figure 3.2), it would be interesting to see whether the production of PI(5)P can indirectly activate the Akt/survival pathway similar to the activation of the Akt/survival pathway of *S. flexneri*, *S. enterica* by PI(5)P (Knodler et al., 2005; Marcus et al., 2001; Pendaries et al., 2006; Steele-Mortimer et al., 2000).

Concluding remarks

The discovery of SidP as a *L. pneumophila* PI phosphatase underscores the significance of a common strategy employed by intracellular pathogens during infection, the exploitation of the host PI metabolism. Subversion of host PIs by bacterial virulence factors has been reported in other intracellular pathogens, such as *S. flexneri* (Niebuhr et al., 2002), *S. typhimurium* (Bakowski et al., 2008; Patel et al., 2009), and *M. tuberculosis* (Vergne et al., 2003a; Vergne et al., 2005). The presence of SidP homologs in other pathogenic bacteria, such as *Fluoribacter dumoffii* and *Rickettsiella grylli* (Figure 3.1) suggests that many intracellular pathogens use subversion of host PI metabolism as a powerful strategy to survive inside host cells.

The identification of a number of PI phosphatase proteins in *L. pneumophila and L. Longebeachae*, has given us an exciting opportunity to characterize these enzymes in more depth. My work and future work and also work of other members of our team will provide invaluable and novel information to start studying the role of PI signaling and metabolism in host-legionella interaction. My work will contribute to the understanding of host-pathogen interaction in general and may open a window for developing a new category of anti-microbial drugs by targeting pathogen effector proteins. Microbiology and the cell biology fields have contributed to development of many imaging and biochemical techniques. My findings may have a contribution for developing new tools for studying host-pathogen interactions in particular and cell biology and microbiology field in general.

APPENDIX I

I have identified three "CX_5R" containing PI phosphatases in *L. longbeachae*. All these effector proteins show detectable homology in their primary amino acid sequence to a *Caenorhabditis elegans* inositol polyphosphate-4-phosphatase. I have been interested in studying these phosphatases for the following reasons. First, their primary amino acid sequences show homology to a eukaryotic PI phosphatase. Second catalytic "CX_5R" motifs of all of these L. longbeachae PI phosphatases, and C. elegans inositol polyphosphate-4-phosphatase have identical amino acid residues (Figure I.1). Third, so far no structure of PI- 4-phosphatases family of mammalian PI phosphatases has been determined, meanwhile, the structure of at least one member of other PI phosphatases family has been determined.

I have started working on two of these effector proteins LLO_1412 and LLO_ 1652. Effector protein LLO_1652 is an 919 amino acid protein with the peptide sequence "CKSGKDR" located between residues 799 and 807 (Figure I.2A). effector protein LLO_1412 contains 1029 amino acids and its catalytic "CKSGKDR" motif is located between residues 879 and 887 (Figure I.2B).

I expressed recombinant LLO_1652 and LLO_1412 proteins in the Rosetta (DE3) E. coli strain, purified them to homogeneity using affinity chromatography followed by size exclusion chromatography (Figure I.2A, B, and I.3A, B). I then examined the purified proteins for *in vitro* PI phosphatase activity by a malachite green based assay (Figure I.4A). LLO_1652 and 1412 both are able to hydrolyze $PI(3,4)P_2$, $PI(4,5)P_2$ and $PI(3,4,5)P_3$. Consistent with what it was proposed in chapter 4 that the presence of a lysine residue after the conserved cysteine in the CX_5R motif is a likely determining

Figure I.1 Sequence alignment of the catalytic motif of *L. longbeachae* PI phosphatases and C. elegans inositol polyphosphate-4-phosphatase. Red box shows the catalytic motif of these proteins.

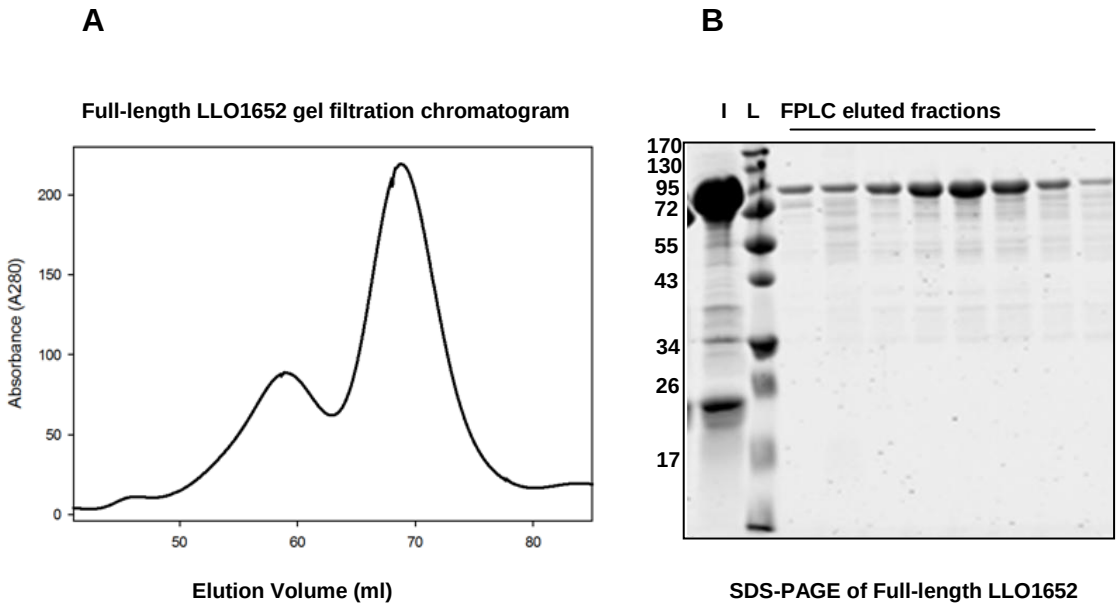

Figure I.2 Gel filtration and SDS-PAGE of LLO_1652. (A) Untagged-LLO_1652 elutes off the size-exclusion column as the major peak after approximately 70 mL. (B) The FPLC eluted fractions are collected and assayed by SDS. The injected protein is loaded in lane (I), the (L) lane is the molecular weight ladder (in kDa).

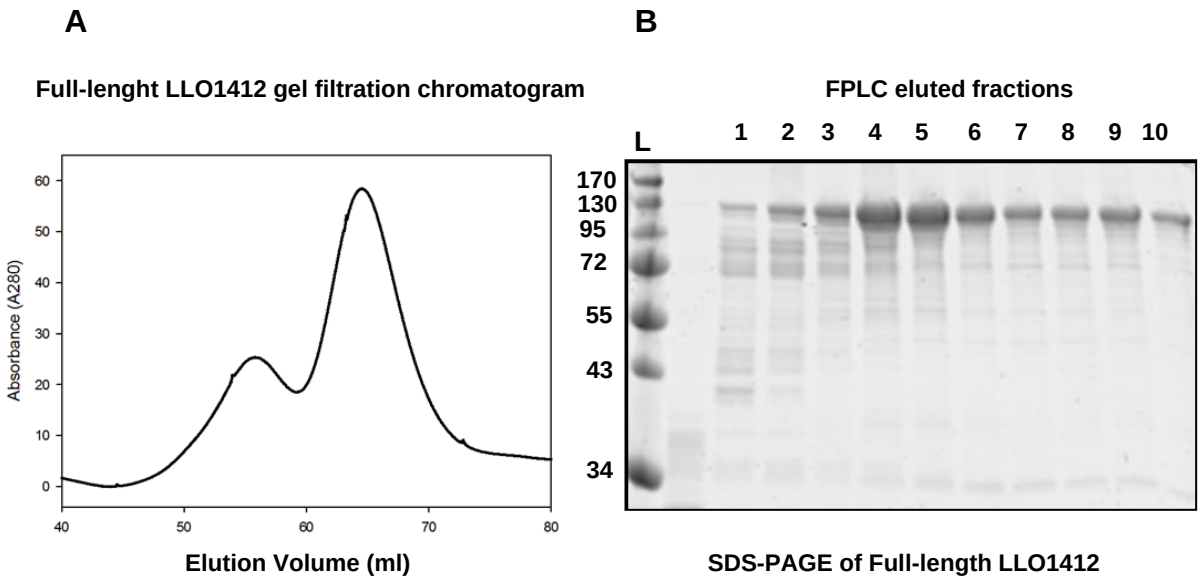

Figure I.3 Gel filtration and SDS-PAGE of LLO_1412. (A) Untagged-LLO_1412 elutes off the size-exclusion column in the major peak after approximately 60 mL. (B) The FPLC eluted fractions are collected and assayed by SDS. (L) Lane is the molecular weight ladder (in kDa).

A

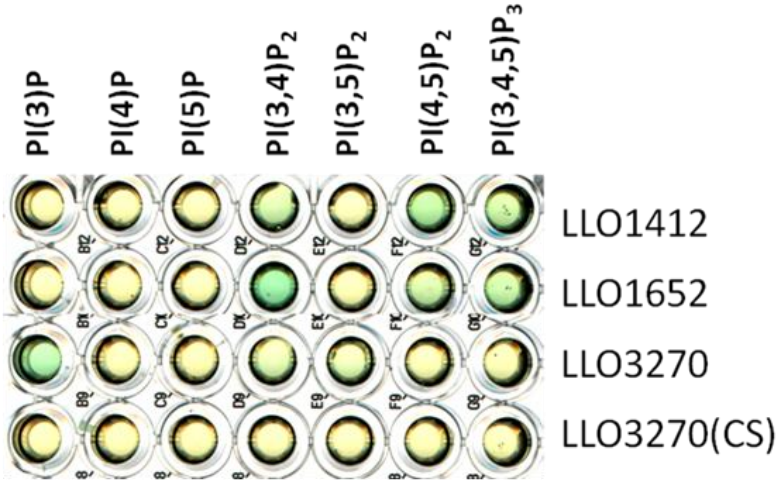
PI(3)P
PI(4)P
PI(5)P
PI(3,4)P2
PI(3,5)P2
PI(4,5)P2
PI(3,4,5)P3
LLO1412
LLO1652
LLO3270
LLO3270(CS)

B

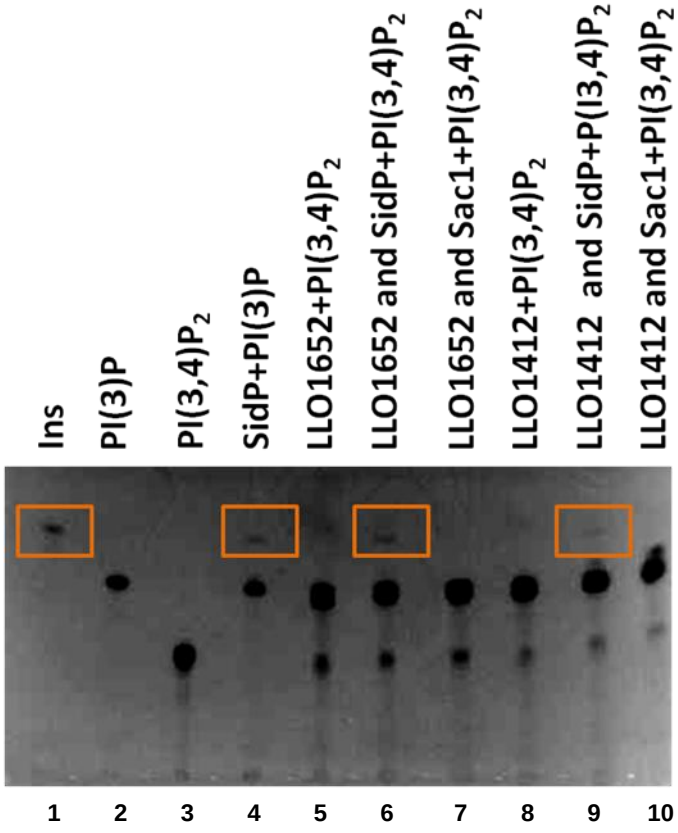
Ins
PI(3)P
PI(3,4)P2
SidP+PI(3)P
LLO1652+PI(3,4)P2
LLO1652 and SidP+PI(3,4)P2
LLO1652 and Sac1+PI(3,4)P2
LLO1412+PI(3,4)P2
LLO1412 and SidP+P(I3,4)P2
LLO1412 and Sac1+PI(3,4)P2
1
2
3
4
5
6
7
8
9
10

Figure I.4 *Legionella longbeachae* LLO_1652 and LLO_1412 are PI phosphatases. (A) PI substrate specificity of purified LLO_1652 and LLO_1412 as determined by the malachite green assay (green color indicates the release of free phosphate). PI(3,4)P_2, PI(4,5)P_2 and PI(3,4,5)P_3 are the preferred substrates. (B) Determination of LLO_1412 and LLO_1652 substrate specificity .Fluorescent lipids. were used as the substrates for the enzymatic reaction of PI phosphatases as labeled. In lane 5 and 8, the
the reactions were first carried out with di-C8- Bodipy-FL-PI(3,4)P_2, and LLO_1652 and LLO_1412, respectively The products of each reaction were further hydrolyzed by the addition of SidP, (lane 6, 9 for LLO_1652 and LLO_1412, respectively), or Sac1 (lane 7, 10 for LLO_1652 and LLO_1412, respectively).

factor for the recognition and hydrolyzing substrates with two adjacent phosphate groups, LLO_1652 and 1412 have a lysine after the conserved cysteine (orange box Figure I.1).

Since both LLO_1652 and 1412 do not hydrolyze any mono-phosphoinositide, malachite green assay cannot provide any information about which phosphate group is removed by these enzymes. In order to answer this question I used fluorescent phosphoinositide-based TLC method (Taylor and Dixon, 2001)(Figure I.4B). Both LLO_1652 and 1412 hydrolyzed PI(3,4)P_2 to a single phosphorylated PI product , and this product could not be further digested by the specific PI-4-phosphatase yeast Sac1 (Figure I.4B, lanes 7,10) (Guo et al., 1999). However, it could be hydrolyzed to phosphatidylinositol (Figure I.4B, lanes 6, 9; orange boxes) by SidP phosphatase that hydrolyzes PI(3)P. These results suggest that both LLO_1652 and LLO_1412 can specifically dephosphorylate PI(3,4)P_2 at the D4 position of the inositol ring.

Testing the *in vivo* phosphatase activity of LLO_1652 and LLO_1412 by exogenous expression of these proteins in mammalian cells and the measuring the cellular radiolabeled PIs, will be the next experiment to be done. Furthermore, looking at the impact of exogenous expression of these proteins on mammalian cellular pathways could be investigated, to study if these proteins can cause any phenotype in the cells that have been transfected by them. Along the same lines, making *L. longbeachae* strains from which the genes encoding these phosphatases have been deleted singularly or and/or simultaneously could be used to study the phenotype and pathogenicity of these strains.

On the structural studies side, crystallization trials of LLO_1652 and LLO_1412 failed to yield any crystals. However, I already have made some progress to make N-terminally truncated LLO_1652 proteins, which are expressed in high levels and can be purified to high homogeneity. Attempts to crystallize these LLO_1652 truncated proteins are in progress now (Figure I.5)and (Table I.1).

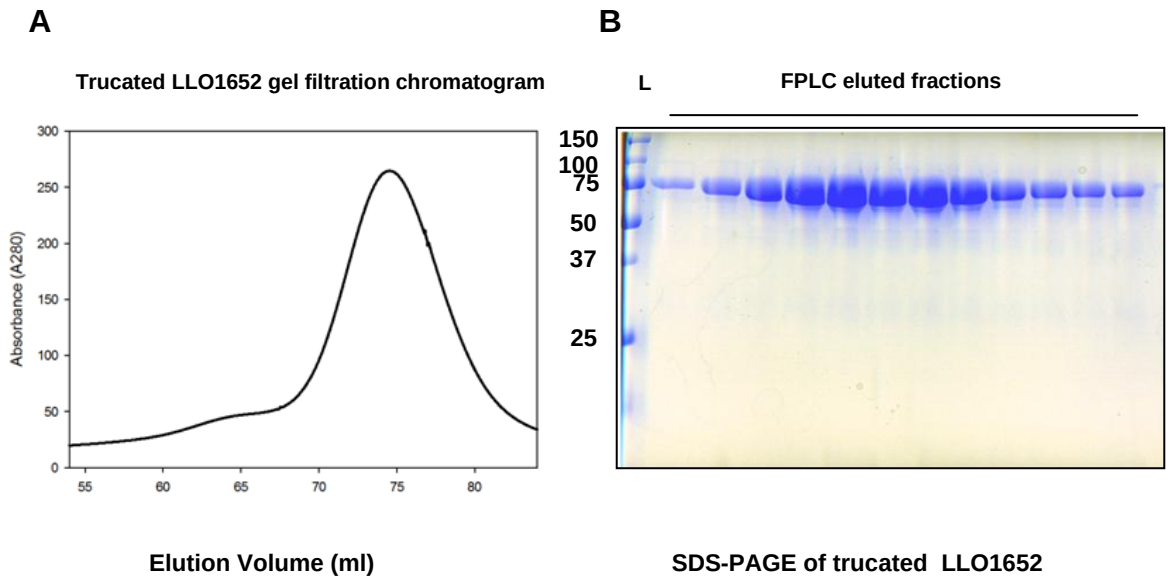

Figure I.5 Gel filtration and SDS-PAGE of truncated LLO_1652 (residues207-919). (A) Untagged-protein elutes off the size-exclusion column in the major peak after approximately 70 mL. (B) The FPLC eluted fractions are collected and assayed by SDS. (L) Lane is the molecular weight ladder (in kDa).

Truncated LLO_1652	**Quality**
LLO_1652 (residues 207-919)	Very good
LLO_1652 (residues 252-919)	Good
LLO_1652 (residues 302-919)	Not good
LLO_1652 (residues 340-919)	Bad
LLO_1652 (residues 392-919)	Very bad

Table: I.1: pET28a-His6-SUMO-LLO1652 truncated proteins list

REFERENCES

Abu Kwaik, Y. (1996). The phagosome containing Legionella pneumophila within the protozoan Hartmannella vermiformis is surrounded by the rough endoplasmic reticulum. Appl Environ Microbiol *62*, 2022-2028.

Al-Quadan, T., and Kwaik, Y.A. (2011). Molecular Characterization of Exploitation of the Polyubiquitination and Farnesylation Machineries of Dictyostelium Discoideum by the AnkB F-Box Effector of Legionella Pneumophila. Front Microbiol *2*, 23.

Al-Quadan, T., Price, C.T., and Abu Kwaik, Y. (2012). Exploitation of evolutionarily conserved amoeba and mammalian processes by Legionella. Trends Microbiol *20*, 299-306.

Alli, O.A., Gao, L.Y., Pedersen, L.L., Zink, S., Radulic, M., Doric, M., and Abu Kwaik, Y. (2000). Temporal pore formation-mediated egress from macrophages and alveolar epithelial cells by Legionella pneumophila. Infect Immun *68*, 6431-6440.

Almena, M., and Merida, I. (2011). Shaping up the membrane: diacylglycerol coordinates spatial orientation of signaling. Trends Biochem Sci *36*, 593-603.

Altman, E., and Segal, G. (2008). The response regulator CpxR directly regulates expression of several Legionella pneumophila icm/dot components as well as new translocated substrates. J Bacteriol *190*, 1985-1996.

Amer, A.O., and Swanson, M.S. (2002). A phagosome of one's own: a microbial guide to life in the macrophage. Curr Opin Microbiol *5*, 56-61.

Amor, J.C., Swails, J., Zhu, X., Roy, C.R., Nagai, H., Ingmundson, A., Cheng, X., and Kahn, R.A. (2005). The structure of RalF, an ADP-ribosylation factor guanine nucleotide exchange factor from Legionella pneumophila, reveals the presence of a cap over the active site. J Biol Chem *280*, 1392-1400.

Andersen, J.N., Mortensen, O.H., Peters, G.H., Drake, P.G., Iversen, L.F., Olsen, O.H., Jansen, P.G., Andersen, H.S., Tonks, N.K., and Moller, N.P. (2001). Structural and evolutionary relationships among protein tyrosine phosphatase domains. Mol Cell Biol *21*, 7117-7136.

Arasaki, K., and Roy, C.R. (2010). Legionella pneumophila promotes functional interactions between plasma membrane syntaxins and Sec22b. Traffic *11*, 587-600.

Arasaki, K., Toomre, D.K., and Roy, C.R. (2012). The Legionella pneumophila effector DrrA is sufficient to stimulate SNARE-dependent membrane fusion. Cell Host Microbe *11*, 46-57.

Backert, S., and Meyer, T.F. (2006). Type IV secretion systems and their effectors in bacterial pathogenesis. Curr Opin Microbiol *9*, 207-217.

Bai, C., and Elledge, S.J. (1996). Gene identification using the yeast two-hybrid system. Methods Enzymol *273*, 331-347.

Bakowski, M.A., Braun, V., and Brumell, J.H. (2008). Salmonella-containing vacuoles: directing traffic and nesting to grow. Traffic *9*, 2022-2031.

Bakowski, M.A., Braun, V., Lam, G.Y., Yeung, T., Heo, W.D., Meyer, T., Finlay, B.B., Grinstein, S., and Brumell, J.H. (2010). The phosphoinositide phosphatase SopB manipulates membrane surface charge and trafficking of the Salmonella-containing vacuole. Cell Host Microbe *7*, 453-462.

Balla, T. (2005). Inositol-lipid binding motifs: signal integrators through protein-lipid and protein-protein interactions. J Cell Sci *118*, 2093-2104.

Bardill, J.P., Miller, J.L., and Vogel, J.P. (2005). IcmS-dependent translocation of SdeA into macrophages by the Legionella pneumophila type IV secretion system. Mol Microbiol *56*, 90-103.

Barford, D., Das, A.K., and Egloff, M.P. (1998). The structure and mechanism of protein phosphatases: insights into catalysis and regulation. Annu Rev Biophys Biomol Struct *27*, 133-164.

Barford, D., Flint, A.J., and Tonks, N.K. (1994). Crystal structure of human protein tyrosine phosphatase 1B. Science *263*, 1397-1404.

Barton, G.J. (1993). ALSCRIPT: a tool to format multiple sequence alignments. Protein Eng *6*, 37-40.

Begley, M.J., Taylor, G.S., Brock, M.A., Ghosh, P., Woods, V.L., and Dixon, J.E. (2006). Molecular basis for substrate recognition by MTMR2, a myotubularin family phosphoinositide phosphatase. Proc Natl Acad Sci U S A *103*, 927-932.

Begley, M.J., Taylor, G.S., Kim, S.A., Veine, D.M., Dixon, J.E., and Stuckey, J.A. (2003). Crystal structure of a phosphoinositide phosphatase, MTMR2: insights into myotubular myopathy and Charcot-Marie-Tooth syndrome. Mol Cell *12*, 1391-1402.

Behnia, R., and Munro, S. (2005). Organelle identity and the signposts for membrane traffic. Nature *438*, 597-604.

Bellinger-Kawahara, C., and Horwitz, M.A. (1990). Complement component C3 fixes selectively to the major outer membrane protein (MOMP) of Legionella pneumophila and mediates phagocytosis of liposome-MOMP complexes by human monocytes. J Exp Med *172*, 1201-1210.

Beresford, N., Patel, S., Armstrong, J., Szoor, B., Fordham-Skelton, A.P., and Tabernero, L. (2007). MptpB, a virulence factor from Mycobacterium tuberculosis, exhibits triple-specificity phosphatase activity. Biochem J *406*, 13-18.

Berger, K.H., and Isberg, R.R. (1993). Two distinct defects in intracellular growth complemented by a single genetic locus in Legionella pneumophila. Mol Microbiol *7*, 7-19.

Berger, K.H., Merriam, J.J., and Isberg, R.R. (1994). Altered intracellular targeting properties associated with mutations in the Legionella pneumophila dotA gene. Mol Microbiol *14*, 809-822.

Birkeland, H.C., and Stenmark, H. (2004). Protein targeting to endosomes and phagosomes via FYVE and PX domains. Curr Top Microbiol Immunol *282*, 89-115.

Botelho, R.J., Efe, J.A., Teis, D., and Emr, S.D. (2008). Assembly of a Fab1 phosphoinositide kinase signaling complex requires the Fig4 phosphoinositide phosphatase. Mol Biol Cell *19*, 4273-4286.

Bozue, J.A., and Johnson, W. (1996). Interaction of Legionella pneumophila with Acanthamoeba castellanii: uptake by coiling phagocytosis and inhibition of phagosome-lysosome fusion. Infect Immun *64*, 668-673.

Brand, B.C., Sadosky, A.B., and Shuman, H.A. (1994). The Legionella pneumophila icm locus: a set of genes required for intracellular multiplication in human macrophages. Mol Microbiol *14*, 797-808.

Braun, V., Wong, A., Landekic, M., Hong, W.J., Grinstein, S., and Brumell, J.H. (2010). Sorting nexin 3 (SNX3) is a component of a tubular endosomal network induced by Salmonella and involved in maturation of the Salmonella-containing vacuole. Cell Microbiol *12*, 1352-1367.

Brombacher, E., Urwyler, S., Ragaz, C., Weber, S.S., Kami, K., Overduin, M., and Hilbi, H. (2009). Rab1 guanine nucleotide exchange factor SidM is a major phosphatidylinositol 4-phosphate-binding effector protein of Legionella pneumophila. J Biol Chem *284*, 4846-4856.

Bujny, M.V., Ewels, P.A., Humphrey, S., Attar, N., Jepson, M.A., and Cullen, P.J. (2008). Sorting nexin-1 defines an early phase of Salmonella-containing vacuole-remodeling during Salmonella infection. J Cell Sci *121*, 2027-2036.

Burstein, D., Zusman, T., Degtyar, E., Viner, R., Segal, G., and Pupko, T. (2009). Genome-scale identification of Legionella pneumophila effectors using a machine learning approach. PLoS Pathog *5*, e1000508.

Byrne, B., and Swanson, M.S. (1998). Expression of Legionella pneumophila virulence traits in response to growth conditions. Infect Immun *66*, 3029-3034.

Cambronne, E.D., and Roy, C.R. (2007). The Legionella pneumophila IcmSW complex interacts with multiple Dot/Icm effectors to facilitate type IV translocation. PLoS Pathog *3*, e188.

Campodonico, E.M., Chesnel, L., and Roy, C.R. (2005). A yeast genetic system for the identification and characterization of substrate proteins transferred into host cells by the Legionella pneumophila Dot/Icm system. Mol Microbiol *56*, 918-933.

Chang, B., Kura, F., Amemura-Maekawa, J., Koizumi, N., and Watanabe, H. (2005). Identification of a novel adhesion molecule involved in the virulence of Legionella pneumophila. Infect Immun *73*, 4272-4280.

Charpentier, X., Gabay, J.E., Reyes, M., Zhu, J.W., Weiss, A., and Shuman, H.A. (2009). Chemical genetics reveals bacterial and host cell functions critical for type IV effector translocation by Legionella pneumophila. PLoS Pathog *5*, e1000501.

Chen, J., de Felipe, K.S., Clarke, M., Lu, H., Anderson, O.R., Segal, G., and Shuman, H.A. (2004). Legionella effectors that promote nonlytic release from protozoa. Science *303*, 1358-1361.

Chong, A., Lima, C.A., Allan, D.S., Nasrallah, G.K., and Garduno, R.A. (2009). The purified and recombinant Legionella pneumophila chaperonin alters mitochondrial trafficking and microfilament organization. Infect Immun *77*, 4724-4739.

Choy, A., Dancourt, J., Mugo, B., O'Connor, T.J., Isberg, R.R., Melia, T.J., and Roy, C.R. (2012). The Legionella effector RavZ inhibits host autophagy through irreversible Atg8 deconjugation. Science *338*, 1072-1076.

Cianciotto, N.P., and Fields, B.S. (1992). Legionella pneumophila mip gene potentiates intracellular infection of protozoa and human macrophages. Proc Natl Acad Sci U S A *89*, 5188-5191.

Cirillo, S.L., Yan, L., Littman, M., Samrakandi, M.M., and Cirillo, J.D. (2002). Role of the Legionella pneumophila rtxA gene in amoebae. Microbiology *148*, 1667-1677.

Coburn, B., Sekirov, I., and Finlay, B.B. (2007). Type III secretion systems and disease. Clin Microbiol Rev *20*, 535-549.

Coers, J., Kagan, J.C., Matthews, M., Nagai, H., Zuckman, D.M., and Roy, C.R. (2000). Identification of Icm protein complexes that play distinct roles in the biogenesis of an organelle permissive for Legionella pneumophila intracellular growth. Mol Microbiol *38*, 719-736.

Collaborative Computational Project, N. (1994). The CCP4 suite: programs for protein crystallography. Acta Cryst *D*, 760-763.

Conover, G.M., Derre, I., Vogel, J.P., and Isberg, R.R. (2003). The Legionella pneumophila LidA protein: a translocated substrate of the Dot/Icm system associated with maintenance of bacterial integrity. Mol Microbiol *48*, 305-321.

Cosio, G., and Grinstein, S. (2008). Analysis of phosphoinositide dynamics during phagocytosis using genetically encoded fluorescent biosensors. Methods Mol Biol *445*, 287-300.

Cossart, P., and Sansonetti, P.J. (2004). Bacterial invasion: the paradigms of enteroinvasive pathogens. Science *304*, 242-248.

de Felipe, K.S., Glover, R.T., Charpentier, X., Anderson, O.R., Reyes, M., Pericone, C.D., and Shuman, H.A. (2008). Legionella eukaryotic-like type IV substrates interfere with organelle trafficking. PLoS Pathog *4*, e1000117.

Degtyar, E., Zusman, T., Ehrlich, M., and Segal, G. (2009). A Legionella effector acquired from protozoa is involved in sphingolipids metabolism and is targeted to the host cell mitochondria. Cell Microbiol *11*, 1219-1235.

Deleu, S., Choi, K., Pesesse, X., Cho, J., Sulis, M.L., Parsons, R., and Shears, S.B. (2006). Physiological levels of PTEN control the size of the cellular Ins(1,3,4,5,6)P(5) pool. Cell Signal *18*, 488-498.

Denu, J.M., and Dixon, J.E. (1995). A catalytic mechanism for the dual-specific phosphatases. Proc Natl Acad Sci U S A *92*, 5910-5914.

Denu, J.M., and Dixon, J.E. (1998). Protein tyrosine phosphatases: mechanisms of catalysis and regulation. Curr Opin Chem Biol *2*, 633-641.

Deretic V, S.S., Master S, Kyei G, Davis A, Naylor J, de Haro S, Harris J, Delgado M, Roberts E, Vergne I. (2007). Phosphoinositides in phagolysosome and autophagosome biogenesis. Biochem Soc Symp *74*, 141-148.

Derre, I., and Isberg, R.R. (2004). Legionella pneumophila replication vacuole formation involves rapid recruitment of proteins of the early secretory system. Infect Immun *72*, 3048-3053.

Derre, I., and Isberg, R.R. (2005). LidA, a translocated substrate of the Legionella pneumophila type IV secretion system, interferes with the early secretory pathway. Infect Immun *73*, 4370-4380.

Desjardins, M., Huber, L.A., Parton, R.G., and Griffiths, G. (1994). Biogenesis of phagolysosomes proceeds through a sequential series of interactions with the endocytic apparatus. J Cell Biol *124*, 677-688.

DeVinney R, S.-M.O., Finlay BB (2000). Phosphatases and kinases delivered to the host cell by bacterial pathogens. . Trends Microbiol *8* 29–33.

Dewitt, S., Tian, W., and Hallett, M.B. (2006). Localised PtdIns(3,4,5)P3 or PtdIns(3,4)P2 at the phagocytic cup is required for both phagosome closure and Ca2+ signalling in HL60 neutrophils. J Cell Sci *119*, 443-451.

Di Paolo, G., and De Camilli, P. (2006). Phosphoinositides in cell regulation and membrane dynamics. Nature *443*, 651-657.

Dolezal, P., Aili, M., Tong, J., Jiang, J.H., Marobbio, C.M., Lee, S.F., Schuelein, R., Belluzzo, S., Binova, E., Mousnier, A.*, et al.* (2012). Legionella pneumophila secretes a mitochondrial carrier protein during infection. PLoS Pathog *8*, e1002459.

Donaldson, J.G., and Jackson, C.L. (2000). Regulators and effectors of the ARF GTPases. Curr Opin Cell Biol *12*, 475-482.

Dorer, M.S., Kirton, D., Bader, J.S., and Isberg, R.R. (2006). RNA interference analysis of Legionella in Drosophila cells: exploitation of early secretory apparatus dynamics. PLoS Pathog *2*, e34.

Dubuisson, J.F., and Swanson, M.S. (2006). Mouse infection by Legionella, a model to analyze autophagy. Autophagy *2*, 179-182.

Duex, J.E., Tang, F., and Weisman, L.S. (2006). The Vac14p-Fig4p complex acts independently of Vac7p and couples PI3,5P2 synthesis and turnover. J Cell Biol *172*, 693-704.

Elliott, J.A., and Winn, W.C., Jr. (1986). Treatment of alveolar macrophages with cytochalasin D inhibits uptake and subsequent growth of Legionella pneumophila. Infect Immun *51*, 31-36.

Ellson, C.D., Anderson, K.E., Morgan, G., Chilvers, E.R., Lipp, P., Stephens, L.R., and Hawkins, P.T. (2001). Phosphatidylinositol 3-phosphate is generated in phagosomal membranes. Curr Biol *11*, 1631-1635.

Emsley, P., and Cowtan, K. (2004). Coot: model-building tools for molecular graphics. Acta Crystallogr D Biol Crystallogr *60*, 2126-2132.

Escoll, P., Rolando, M., Gomez-Valero, L., and Buchrieser, C. (2013). From Amoeba to Macrophages: Exploring the Molecular Mechanisms of Legionella pneumophila Infection in Both Hosts. Curr Top Microbiol Immunol.

Fauman, E.B., and Saper, M.A. (1996). Structure and function of the protein tyrosine phosphatases. Trends Biochem Sci *21*, 413-417.

Fauman, E.B., Yuvaniyama, C., Schubert, H.L., Stuckey, J.A., and Saper, M.A. (1996). The X-ray crystal structures of Yersinia tyrosine phosphatase with bound tungstate and nitrate. Mechanistic implications. J Biol Chem *271*, 18780-18788.

Feeley, J.C., Gibson, R.J., Gorman, G.W., Langford, N.C., Rasheed, J.K., Mackel, D.C., and Baine, W.B. (1979). Charcoal-yeast extract agar: primary isolation medium for Legionella pneumophila. J Clin Microbiol *10*, 437-441.

Fields, B.S. (1996). The molecular ecology of legionellae. Trends Microbiol *4*, 286-290.

Fields, B.S., Benson, R.F., and Besser, R.E. (2002). Legionella and Legionnaires' disease: 25 years of investigation. Clin Microbiol Rev *15*, 506-526.

Flannagan, R.S., Cosio, G., and Grinstein, S. (2009). Antimicrobial mechanisms of phagocytes and bacterial evasion strategies. Nat Rev Microbiol *7*, 355-366.

Forgac, M. (2007). Vacuolar ATPases: rotary proton pumps in physiology and pathophysiology. Nat Rev Mol Cell Biol *8*, 917-929.

Foti, M., Audhya, A., and Emr, S.D. (2001). Sac1 lipid phosphatase and Stt4 phosphatidylinositol 4-kinase regulate a pool of phosphatidylinositol 4-phosphate that functions in the control of the actin cytoskeleton and vacuole morphology. Mol Biol Cell *12*, 2396-2411.

Franco, I.S., Shuman, H.A., and Charpentier, X. (2009). The perplexing functions and surprising origins of Legionella pneumophila type IV secretion effectors. Cell Microbiol *11*, 1435-1443.

Franke, D., and Svergun, D.I. (2009). DAMMIF, a program for rapid ab-initio shape determination in small-angle scattering. J Appl Cryst *42*, 342-346.

Fraser, D.W., Tsai, T.R., Orenstein, W., Parkin, W.E., Beecham, H.J., Sharrar, R.G., Harris, J., Mallison, G.F., Martin, S.M., McDade, J.E.*, et al.* (1977). Legionnaires' disease: description of an epidemic of pneumonia. N Engl J Med *297*, 1189-1197.

Fratti, R.A., Backer, J.M., Gruenberg, J., Corvera, S., and Deretic, V. (2001). Role of phosphatidylinositol 3-kinase and Rab5 effectors in phagosomal biogenesis and mycobacterial phagosome maturation arrest. J Cell Biol *154*, 631-644.

Fu, Y., and Rubin, C.S. (2011). Protein kinase D: coupling extracellular stimuli to the regulation of cell physiology. EMBO Rep *12*, 785-796.

Gibson, F.C., 3rd, Tzianabos, A.O., and Rodgers, F.G. (1994). Adherence of Legionella pneumophila to U-937 cells, guinea-pig alveolar macrophages, and MRC-5 cells by a novel, complement-independent binding mechanism. Can J Microbiol *40*, 865-872.

Godi, A., Santone, I., Pertile, P., Marra, P., Di Tullio, G., Luini, A., Corda, D., and De Matteis, M.A. (1999). ADP-ribosylation factor regulates spectrin skeleton assembly on the Golgi complex by stimulating phosphatidylinositol 4,5-bisphosphate synthesis. Biochem Soc Trans *27*, 638-642.

Guan, K.L., and Dixon, J.E. (1991). Evidence for protein-tyrosine-phosphatase catalysis proceeding via a cysteine-phosphate intermediate. J Biol Chem *266*, 17026-17030.

Guo, S., Stolz, L.E., Lemrow, S.M., and York, J.D. (1999). SAC1-like domains of yeast SAC1, INP52, and INP53 and of human synaptojanin encode polyphosphoinositide phosphatases. J Biol Chem *274*, 12990-12995.

Haneburger, I., and Hilbi, H. (2013). Phosphoinositide lipids and the legionella pathogen vacuole. Curr Top Microbiol Immunol *376*, 155-173.

Hanisch, J., Kolm, R., Wozniczka, M., Bumann, D., Rottner, K., and Stradal, T.E. (2011). Activation of a RhoA/myosin II-dependent but Arp2/3 complex-independent pathway facilitates Salmonella invasion. Cell Host Microbe *9*, 273-285.

Harb, O.S., Venkataraman, C., Haack, B.J., Gao, L.Y., and Kwaik, Y.A. (1998). Heterogeneity in the attachment and uptake mechanisms of the Legionnaires' disease bacterium, Legionella pneumophila, by protozoan hosts. Appl Environ Microbiol *64*, 126-132.

Harding, C.R., Mattheis, C., Mousnier, A., Oates, C.V., Hartland, E.L., Frankel, G., and Schroeder, G.N. (2013). LtpD is a novel Legionella pneumophila effector that binds phosphatidylinositol-3-phosphate and inositol monophosphatase IMPA1. Infect Immun.

Hayashi, T., Miyake, M., Fukui, T., Sugaya, N., Daimon, T., Itoh, S., Oku, T., Tsuji, T., Toyoshima, S., and Imai, Y. (2008). Exclusion of actin-binding protein p57/coronin-1 from bacteria-containing phagosomes in macrophages infected with Legionella. Biol Pharm Bull *31*, 861-865.

Heidtman, M., Chen, E.J., Moy, M.Y., and Isberg, R.R. (2009). Large-scale identification of Legionella pneumophila Dot/Icm substrates that modulate host cell vesicle trafficking pathways. Cell Microbiol *11*, 230-248.

Hernandez, L.D., Hueffer, K., Wenk, M.R., and Galan, J.E. (2004). Salmonella modulates vesicular traffic by altering phosphoinositide metabolism. Science *304*, 1805-1807.

Hilbi, H. (2006a). Modulation of phosphoinositide metabolism by pathogenic bacteria. Cell Microbiol *8*, 1697-1706.

Hilbi, H. (2006b). Modulation of phosphoinositide metabolism by pathogenic bacteria.

. Cell Microbiol

***81*, 1697–1706.**

Holm, L., and Rosenstrom, P. (2010). Dali server: conservation mapping in 3D. Nucleic Acids Res *38*, W545-549.

Holm, L., and Sander, C. (1993). Protein structure comparison by alignment of distance matrices. J Mol Biol *233*, 123-138.

Horwitz, M.A. (1983a). Formation of a novel phagosome by the Legionnaires' disease bacterium (Legionella pneumophila) in human monocytes. J Exp Med *158*, 1319-1331.

Horwitz, M.A. (1983b). The Legionnaires' disease bacterium (Legionella pneumophila) inhibits phagosome-lysosome fusion in human monocytes. J Exp Med *158*, 2108-2126.

Horwitz, M.A. (1984). Phagocytosis of the Legionnaires' disease bacterium (Legionella pneumophila) occurs by a novel mechanism: engulfment within a pseudopod coil. Cell *36*, 27-33.

Horwitz, M.A. (1987). Characterization of avirulent mutant Legionella pneumophila that survive but do not multiply within human monocytes. J Exp Med *166*, 1310-1328.

Hsu, F., Zhu, W., Brennan, L., Tao, L., Luo, Z.Q., and Mao, Y. (2012). Structural basis for substrate recognition by a unique Legionella phosphoinositide phosphatase. Proc Natl Acad Sci U S A *109*, 13567-13572.

Huang, L., Boyd, D., Amyot, W.M., Hempstead, A.D., Luo, Z.Q., O'Connor, T.J., Chen, C., Machner, M., Montminy, T., and Isberg, R.R. (2011). The E Block motif is associated with Legionella pneumophila translocated substrates. Cell Microbiol *13*, 227-245.

Hubber, A., and Roy, C.R. (2010). Modulation of host cell function by Legionella pneumophila type IV effectors. Annu Rev Cell Dev Biol *26*, 261-283.

Hyvola, N., Diao, A., McKenzie, E., Skippen, A., Cockcroft, S., and Lowe, M. (2006). Membrane targeting and activation of the Lowe syndrome protein OCRL1 by rab GTPases. EMBO J *25*, 3750-3761.

Ikonomov, O.C., Sbrissa, D., Fenner, H., and Shisheva, A. (2009). PIKfyve-ArPIKfyve-Sac3 core complex: contact sites and their consequence for Sac3 phosphatase activity and endocytic membrane homeostasis. J Biol Chem *284*, 35794-35806.

Ingmundson, A., Delprato, A., Lambright, D.G., and Roy, C.R. (2007). Legionella pneumophila proteins that regulate Rab1 membrane cycling. Nature *450*, 365-369.

Isberg, R.R., O'Connor, T.J., and Heidtman, M. (2009). The Legionella pneumophila replication vacuole: making a cosy niche inside host cells. Nat Rev Microbiol *7*, 13-24.

Ivanov, S.S., Charron, G., Hang, H.C., and Roy, C.R. (2010). Lipidation by the host prenyltransferase machinery facilitates membrane localization of Legionella pneumophila effector proteins. J Biol Chem *285*, 34686-34698.

Jank, T., Bohmer, K.E., Tzivelekidis, T., Schwan, C., Belyi, Y., and Aktories, K. (2012). Domain organization of Legionella effector SetA. Cell Microbiol *14*, 852-868.

Jefferson, A.B., and Majerus, P.W. (1996). Mutation of the conserved domains of two inositol polyphosphate 5-phosphatases. Biochemistry *35*, 7890-7894.

Jia, Z., Barford, D., Flint, A.J., and Tonks, N.K. (1995). Structural basis for phosphotyrosine peptide recognition by protein tyrosine phosphatase 1B. Science *268*, 1754-1758.

Kagan, J.C., and Roy, C.R. (2002). Legionella phagosomes intercept vesicular traffic from endoplasmic reticulum exit sites. Nat Cell Biol *4*, 945-954.

Kagan, J.C., Stein, M.P., Pypaert, M., and Roy, C.R. (2004). Legionella subvert the functions of Rab1 and Sec22b to create a replicative organelle. J Exp Med *199*, 1201-1211.

King, C.H., Fields, B.S., Shotts, E.B., Jr., and White, E.H. (1991). Effects of cytochalasin D and methylamine on intracellular growth of Legionella pneumophila in amoebae and human monocyte-like cells. Infect Immun *59*, 758-763.

Knodler, L.A., Finlay, B.B., and Steele-Mortimer, O. (2005). The Salmonella effector protein SopB protects epithelial cells from apoptosis by sustained activation of Akt. J Biol Chem *280*, 9058-9064.

Knodler, L.A., and Steele-Mortimer, O. (2003). Taking possession: biogenesis of the Salmonella-containing vacuole. Traffic *4*, 587-599.

Koth, C.M., Orlicky, S.M., Larson, S.M., and Edwards, A.M. (2003). Use of limited proteolysis to identify protein domains suitable for structural analysis. Methods Enzymol *368*, 77-84.

Kozin, M.B., and Svergun, D.I. (2001). Automated matching of high- and low-resolution structural models. J Appl Cryst *34*, 33-41.

Krinos, C., High, A.S., and Rodgers, F.G. (1999). Role of the 25 kDa major outer membrane protein of Legionella pneumophila in attachment to U-937 cells and its potential as a virulence factor for chick embryos. J Appl Microbiol *86*, 237-244.

Laguna, R.K., Creasey, E.A., Li, Z., Valtz, N., and Isberg, R.R. (2006). A Legionella pneumophila-translocated substrate that is required for growth within macrophages and protection from host cell death. Proc Natl Acad Sci U S A *103*, 18745-18750.

Lau, H.Y., and Ashbolt, N.J. (2009). The role of biofilms and protozoa in Legionella pathogenesis: implications for drinking water. J Appl Microbiol *107*, 368-378.

Lee, J.O., Yang, H., Georgescu, M.M., Di Cristofano, A., Maehama, T., Shi, Y., Dixon, J.E., Pandolfi, P., and Pavletich, N.P. (1999). Crystal structure of the PTEN tumor suppressor: implications for its phosphoinositide phosphatase activity and membrane association. Cell *99*, 323-334.

Lemmon, M.A. (2008). Membrane recognition by phospholipid-binding domains. Nat Rev Mol Cell Biol *9*, 99-111.

Lichter-Konecki, U., Farber, L.W., Cronin, J.S., Suchy, S.F., and Nussbaum, R.L. (2006). The effect of missense mutations in the RhoGAP-homology domain on ocrl1 function. Mol Genet Metab *89*, 121-128.

Lifshitz, Z., Burstein, D., Peeri, M., Zusman, T., Schwartz, K., Shuman, H.A., Pupko, T., and Segal, G. (2013). Computational modeling and experimental validation of the Legionella and Coxiella virulence-related type-IVB secretion signal. Proc Natl Acad Sci U S A *110*, E707-715.

Liu, Y., and Bankaitis, V.A. (2010). Phosphoinositide phosphatases in cell biology and disease. Prog Lipid Res *49*, 201-217.

Lomma, M., Dervins-Ravault, D., Rolando, M., Nora, T., Newton, H.J., Sansom, F.M., Sahr, T., Gomez-Valero, L., Jules, M., Hartland, E.L.*, et al.* (2010). The Legionella pneumophila F-box protein Lpp2082 (AnkB) modulates ubiquitination of the host protein parvin B and promotes intracellular replication. Cell Microbiol *12*, 1272-1291.

Lowe, M. (2005). Structure and function of the Lowe syndrome protein OCRL1. Traffic *6*, 711-719.

Lu, H., and Clarke, M. (2005). Dynamic properties of Legionella-containing phagosomes in Dictyostelium amoebae. Cell Microbiol *7*, 995-1007.

Luo, Z.Q., and Isberg, R.R. (2004). Multiple substrates of the Legionella pneumophila Dot/Icm system identified by interbacterial protein transfer. Proc Natl Acad Sci U S A *101*, 841-846.

Machner, M.P., and Isberg, R.R. (2006). Targeting of host Rab GTPase function by the intravacuolar pathogen Legionella pneumophila. Dev Cell *11*, 47-56.

Machner, M.P., and Isberg, R.R. (2007). A bifunctional bacterial protein links GDI displacement to Rab1 activation. Science *318*, 974-977.

Maehama, T., and Dixon, J.E. (1998). The tumor suppressor, PTEN/MMAC1, dephosphorylates the lipid second messenger, phosphatidylinositol 3,4,5-trisphosphate. J Biol Chem *273*, 13375-13378.

Maehama, T., Taylor, G.S., Slama, J.T., and Dixon, J.E. (2000). A sensitive assay for phosphoinositide phosphatases. Anal Biochem *279*, 248-250.

Majerus, P.W., Kisseleva, M.V., and Norris, F.A. (1999). The role of phosphatases in inositol signaling reactions. J Biol Chem *274*, 10669-10672.

Malik ZA, D.G., Kusner DJ. (2000). Inhibition of Ca2+ Signaling by Mycobacterium tuberculosisIs Associated with Reduced Phagosome–Lysosome Fusion and Increased Survival within Human Macrophages. J of Experimental Medicine 2000 *191*, 287-302.

Mallo, G.V., Espina, M., Smith, A.C., Terebiznik, M.R., Aleman, A., Finlay, B.B., Rameh, L.E., Grinstein, S., and Brumell, J.H. (2008). SopB promotes phosphatidylinositol 3-phosphate formation on Salmonella vacuoles by recruiting Rab5 and Vps34. J Cell Biol *182*, 741-752.

Manford, A., Xia, T., Saxena, A.K., Stefan, C., Hu, F., Emr, S.D., and Mao, Y. (2010). Crystal structure of the yeast Sac1: implications for its phosphoinositide phosphatase function. Embo J *29*, 1489-1498.

Marcus, S.L., Wenk, M.R., Steele-Mortimer, O., and Finlay, B.B. (2001). A synaptojanin-homologous region of Salmonella typhimurium SigD is essential for inositol phosphatase activity and Akt activation. FEBS Lett *494*, 201-207.

Marra, A., Blander, S.J., Horwitz, M.A., and Shuman, H.A. (1992). Identification of a Legionella pneumophila locus required for intracellular multiplication in human macrophages. Proc Natl Acad Sci U S A *89*, 9607-9611.

Mason, D., Mallo, G.V., Terebiznik, M.R., Payrastre, B., Finlay, B.B., Brumell, J.H., Rameh, L., and Grinstein, S. (2007). Alteration of epithelial structure and function associated with PtdIns(4,5)P2 degradation by a bacterial phosphatase. J Gen Physiol *129*, 267-283.

Matthews, B.W. (1968). Solvent content of protein crystals. J Mol Biol *33*, 491-497.

Mauro, L.J., and Dixon, J.E. (1994). 'Zip codes' direct intracellular protein tyrosine phosphatases to the correct cellular 'address'. Trends Biochem Sci *19*, 151-155.

McAllister, G., Whiting, P., Hammond, E.A., Knowles, M.R., Atack, J.R., Bailey, F.J., Maigetter, R., and Ragan, C.I. (1992). cDNA cloning of human and rat brain myo-inositol monophosphatase. Expression and characterization of the human recombinant enzyme. Biochem J *284 (Pt 3)*, 749-754.

McDade, J.E., Shepard, C.C., Fraser, D.W., Tsai, T.R., Redus, M.A., and Dowdle, W.R. (1977). Legionnaires' disease: isolation of a bacterium and demonstration of its role in other respiratory disease. N Engl J Med *297*, 1197-1203.

McLean, I.W., and Nakane, P.K. (1974). Periodate-lysine-paraformaldehyde fixative. A new fixation for immunoelectron microscopy. J Histochem Cytochem *22*, 1077-1083.

Mitchell, C.A., Brown, S., Campbell, J.K., Munday, A.D., and Speed, C.J. (1996). Regulation of second messengers by the inositol polyphosphate 5-phosphatases. Biochem Soc Trans *24*, 994-1000.

Molmeret, M., and Abu Kwaik, Y. (2002). How does Legionella pneumophila exit the host cell? Trends Microbiol *10*, 258-260.

Molmeret, M., Bitar, D.M., Han, L., and Kwaik, Y.A. (2004). Disruption of the phagosomal membrane and egress of Legionella pneumophila into the cytoplasm during the last stages of intracellular infection of macrophages and Acanthamoeba polyphaga. Infect Immun *72*, 4040-4051.

Molmeret, M., Horn, M., Wagner, M., Santic, M., and Abu Kwaik, Y. (2005). Amoebae as training grounds for intracellular bacterial pathogens. Appl Environ Microbiol *71*, 20-28.

Moyer, B.D., Allan, B.B., and Balch, W.E. (2001). Rab1 interaction with a GM130 effector complex regulates COPII vesicle cis--Golgi tethering. Traffic *2*, 268-276.

Mukhopadhyay, R., and Rosen, B.P. (2002). Arsenate reductases in prokaryotes and eukaryotes. Environ Health Perspect *110 Suppl 5*, 745-748.

Muller, M.P., Peters, H., Blumer, J., Blankenfeldt, W., Goody, R.S., and Itzen, A. (2010). The Legionella effector protein DrrA AMPylates the membrane traffic regulator Rab1b. Science *329*, 946-949.

Murata, T., Delprato, A., Ingmundson, A., Toomre, D.K., Lambright, D.G., and Roy, C.R. (2006). The Legionella pneumophila effector protein DrrA is a Rab1 guanine nucleotide-exchange factor. Nat Cell Biol *8*, 971-977.

Murshudov, G.N., Vagin, A.A., and Dodson, E.J. (1997). Refinement of macromolecular structures by the maximum-likelihood method. Acta Crystallogr D Biol Crystallogr *53*, 240-255.

Nagai, H., Cambronne, E.D., Kagan, J.C., Amor, J.C., Kahn, R.A., and Roy, C.R. (2005). A C-terminal translocation signal required for Dot/Icm-dependent delivery of the Legionella RalF protein to host cells. Proc Natl Acad Sci U S A *102*, 826-831.

Nagai, H., Kagan, J.C., Zhu, X., Kahn, R.A., and Roy, C.R. (2002). A bacterial guanine nucleotide exchange factor activates ARF on Legionella phagosomes. Science *295*, 679-682.

Neunuebel, M.R., Mohammadi, S., Jarnik, M., and Machner, M.P. (2012). Legionella pneumophila LidA affects nucleotide binding and activity of the host GTPase Rab1. J Bacteriol *194*, 1389-1400.

Newsome, A.L., Baker, R.L., Miller, R.D., and Arnold, R.R. (1985). Interactions between Naegleria fowleri and Legionella pneumophila. Infect Immun *50*, 449-452.

Newton H. J., A.D.K., van Driel I. R., Hartland E. L. (2010). Molecular pathogenesis of infections caused by Legionella pneumophila. Clin Microbiol Rev *23*, 274–298.

Newton, H.J., Sansom, F.M., Bennett-Wood, V., and Hartland, E.L. (2006). Identification of Legionella pneumophila-specific genes by genomic subtractive hybridization with Legionella micdadei and identification of lpnE, a gene required for efficient host cell entry. Infect Immun *74*, 1683-1691.

Newton, H.J., Sansom, F.M., Dao, J., Cazalet, C., Bruggemann, H., Albert-Weissenberger, C., Buchrieser, C., Cianciotto, N.P., and Hartland, E.L. (2008). Significant role for ladC in initiation of Legionella pneumophila infection. Infect Immun *76*, 3075-3085.

Newton, H.J., Sansom, F.M., Dao, J., McAlister, A.D., Sloan, J., Cianciotto, N.P., and Hartland, E.L. (2007). Sel1 repeat protein LpnE is a Legionella pneumophila virulence determinant that influences vacuolar trafficking. Infect Immun *75*, 5575-5585.

Niebuhr, K., Giuriato, S., Pedron, T., Philpott, D.J., Gaits, F., Sable, J., Sheetz, M.P., Parsot, C., Sansonetti, P.J., and Payrastre, B. (2002). Conversion of PtdIns(4,5)P(2) into PtdIns(5)P by the S.flexneri effector IpgD reorganizes host cell morphology. EMBO J *21*, 5069-5078.

Ninio, S., and Roy, C.R. (2007). Effector proteins translocated by Legionella pneumophila: strength in numbers. Trends Microbiol *15*, 372-380.

Norris, F.A., Atkins, R.C., and Majerus, P.W. (1997). The cDNA cloning and characterization of inositol polyphosphate 4-phosphatase type II. Evidence for conserved alternative splicing in the 4-phosphatase family. J Biol Chem *272*, 23859-23864.

Norris, F.A., Wilson, M.P., Wallis, T.S., Galyov, E.E., and Majerus, P.W. (1998). SopB, a protein required for virulence of Salmonella dublin, is an inositol phosphate phosphatase. Proc Natl Acad Sci U S A *95*, 14057-14059.

Nystuen, A., Legare, M.E., Shultz, L.D., and Frankel, W.N. (2001). A null mutation in inositol polyphosphate 4-phosphatase type I causes selective neuronal loss in weeble mutant mice. Neuron *32*, 203-212.

O'Connor, T.J., Adepoju, Y., Boyd, D., and Isberg, R.R. (2011). Minimization of the Legionella pneumophila genome reveals chromosomal regions involved in host range expansion. Proc Natl Acad Sci U S A *108*, 14733-14740.

O'Connor, T.J., Boyd, D., Dorer, M.S., and Isberg, R.R. (2012). Aggravating genetic interactions allow a solution to redundancy in a bacterial pathogen. Science *338*, 1440-1444.

Ong, S.E., Blagoev, B., Kratchmarova, I., Kristensen, D.B., Steen, H., Pandey, A., and Mann, M. (2002). Stable isotope labeling by amino acids in cell culture, SILAC, as a simple and accurate approach to expression proteomics. Mol Cell Proteomics *1*, 376-386.

Otwinowski, Z., and Minor, W. (1997). Processing of X-ray diffraction data collected in oscillation mode. Methods Enzymol *276*, 307-326.

Pannifer, A.D., Flint, A.J., Tonks, N.K., and Barford, D. (1998). Visualization of the cysteinyl-phosphate intermediate of a protein-tyrosine phosphatase by x-ray crystallography. J Biol Chem *273*, 10454-10462.

Pape, T., and Schneider, T.R. (2004). HKL2MAP: a graphical user interface for macromolecular phasing with SHELX programs. J Appl Cryst *37*, 843-844.

Parrish, W.R., Stefan, C.J., and Emr, S.D. (2004). Essential role for the myotubularin-related phosphatase Ymr1p and the synaptojanin-like phosphatases Sjl2p and Sjl3p in regulation of phosphatidylinositol 3-phosphate in yeast. Mol Biol Cell *15*, 3567-3579.

Parrish, W.R., Stefan, C.J., and Emr, S.D. (2005). PtdIns(3)P accumulation in triple lipid-phosphatase-deletion mutants triggers lethal hyperactivation of the Rho1p/Pkc1p cell-integrity MAP kinase pathway. J Cell Sci *118*, 5589-5601.

Patel, J.C., and Galan, J.E. (2006). Differential activation and function of Rho GTPases during Salmonella-host cell interactions. J Cell Biol *175*, 453-463.

Patel, J.C., Hueffer, K., Lam, T.T., and Galan, J.E. (2009). Diversification of a Salmonella virulence protein function by ubiquitin-dependent differential localization. Cell *137*, 283-294.

Payne, N.R., and Horwitz, M.A. (1987). Phagocytosis of Legionella pneumophila is mediated by human monocyte complement receptors. J Exp Med *166*, 1377-1389.

Payrastre, B., Gaits-Iacovoni, F., Sansonetti, P., and Tronchere, H. (2012). Phosphoinositides and cellular pathogens. Subcell Biochem *59*, 363-388.

Pendaries, C., Tronchere, H., Arbibe, L., Mounier, J., Gozani, O., Cantley, L., Fry, M.J., Gaits-Iacovoni, F., Sansonetti, P.J., and Payrastre, B. (2006). PtdIns5P activates the host cell PI3-kinase/Akt pathway during Shigella flexneri infection. EMBO J *25*, 1024-1034.

Peracino, B., Wagner, C., Balest, A., Balbo, A., Pergolizzi, B., Noegel, A.A., Steinert, M., and Bozzaro, S. (2006). Function and mechanism of action of Dictyostelium Nramp1 (Slc11a1) in bacterial infection. Traffic *7*, 22-38.

Petoukhov, M.K., PV; Kikhney, AG; Svergun, D. (2007). ATSAS 2.1 - towards automated and web-supported small-angle scattering data analysis. Journal of Applied Crystallography *40*, s223-s228.

Pizarro-Cerda, J., and Cossart, P. (2004). Subversion of phosphoinositide metabolism by intracellular bacterial pathogens. Nat Cell Biol *6*, 1026-1033.

Pizarro-Cerdà J, C.P. (2004). (2004) Subvertion of phosphoinositide metabolism by intracellular

bacterial pathogens. Nat Cell Biol *6*, 1026–1033.

Price, C.T., Al-Khodor, S., Al-Quadan, T., and Abu Kwaik, Y. (2010a). Indispensable role for the eukaryotic-like ankyrin domains of the ankyrin B effector of Legionella pneumophila within macrophages and amoebae. Infect Immun *78*, 2079-2088.

Price, C.T., Al-Quadan, T., Santic, M., Jones, S.C., and Abu Kwaik, Y. (2010b). Exploitation of conserved eukaryotic host cell farnesylation machinery by an F-box effector of Legionella pneumophila. J Exp Med *207*, 1713-1726.

Price, C.T., Al-Quadan, T., Santic, M., Rosenshine, I., and Abu Kwaik, Y. (2011). Host proteasomal degradation generates amino acids essential for intracellular bacterial growth. Science *334*, 1553-1557.

Qiu, J., and Luo, Z.Q. (2013). Effector Translocation by the Legionella Dot/Icm Type IV Secretion System. Curr Top Microbiol Immunol *376*, 103-115.

Ragaz, C., Pietsch, H., Urwyler, S., Tiaden, A., Weber, S.S., and Hilbi, H. (2008). The Legionella pneumophila phosphatidylinositol-4 phosphate-binding type IV substrate SidC recruits endoplasmic reticulum vesicles to a replication-permissive vacuole. Cell Microbiol *10*, 2416-2433.

Ramel, D., Lagarrigue, F., Dupuis-Coronas, S., Chicanne, G., Leslie, N., Gaits-Iacovoni, F., Payrastre, B., and Tronchere, H. (2009). PtdIns5P protects Akt from dephosphorylation through PP2A inhibition. Biochem Biophys Res Commun *387*, 127-131.

Ramel, D., Lagarrigue, F., Pons, V., Mounier, J., Dupuis-Coronas, S., Chicanne, G., Sansonetti, P.J., Gaits-Iacovoni, F., Tronchere, H., and Payrastre, B. (2011). Shigella flexneri infection generates the lipid PI5P to alter endocytosis and prevent termination of EGFR signaling. Sci Signal *4*, ra61.

Rechnitzer, C., and Blom, J. (1989). Engulfment of the Philadelphia strain of Legionella pneumophila within pseudopod coils in human phagocytes. Comparison with other Legionella strains and species. APMIS *97*, 105-114.

Rittig, M.G., Burmester, G.R., and Krause, A. (1998). Coiling phagocytosis: when the zipper jams, the cup is deformed. Trends Microbiol *6*, 384-388.

Rodgers, F.G., and Gibson, F.C., 3rd (1993). Opsonin-independent adherence and intracellular development of Legionella pneumophila within U-937 cells. Can J Microbiol *39*, 718-722.

Rosenberger, C.M., and Finlay, B.B. (2003). Phagocyte sabotage: disruption of macrophage signalling by bacterial pathogens. Nat Rev Mol Cell Biol *4*, 385-396.

Rowbotham, T.J. (1980). Preliminary report on the pathogenicity of Legionella pneumophila for freshwater and soil amoebae. J Clin Pathol *33*, 1179-1183.

Rowbotham, T.J. (1986). Current views on the relationships between amoebae, legionellae and man. Isr J Med Sci *22*, 678-689.

Roy, C.R. (2002). Exploitation of the endoplasmic reticulum by bacterial pathogens. Trends Microbiol *10*, 418-424.

Roy, C.R., and Tilney, L.G. (2002). The road less traveled: transport of Legionella to the endoplasmic reticulum. J Cell Biol *158*, 415-419.

Russell, D.G., Mwandumba, H.C., and Rhoades, E.E. (2002). Mycobacterium and the coat of many lipids. J Cell Biol *158*, 421-426.

Sato, K., and Nakano, A. (2007). Mechanisms of COPII vesicle formation and protein sorting. FEBS Lett *581*, 2076-2082.

Schroeder, G.N., and Hilbi, H. (2008). Molecular pathogenesis of Shigella spp.: controlling host cell signaling, invasion, and death by type III secretion. Clin Microbiol Rev *21*, 134-156.

Scott, C.C., Dobson, W., Botelho, R.J., Coady-Osberg, N., Chavrier, P., Knecht, D.A., Heath, C., Stahl, P., and Grinstein, S. (2005). Phosphatidylinositol-4,5-bisphosphate hydrolysis directs actin remodeling during phagocytosis. J Cell Biol *169*, 139-149.

Segal, G., and Shuman, H.A. (1999). Legionella pneumophila utilizes the same genes to multiply within Acanthamoeba castellanii and human macrophages. Infect Immun *67*, 2117-2124.

Semenyuk, A.V., Svergun, D.I. (1991). GNOM - A Program Package For Small-Angle Scattering and Data-Processing. Journal of Applied Crystallography *24*, 537-548.

Shin, H.W., Hayashi, M., Christoforidis, S., Lacas-Gervais, S., Hoepfner, S., Wenk, M.R., Modregger, J., Uttenweiler-Joseph, S., Wilm, M., Nystuen, A*., et al.* (2005). An enzymatic cascade of Rab5 effectors regulates phosphoinositide turnover in the endocytic pathway. J Cell Biol *170*, 607-618.

Shin, S., and Roy, C.R. (2008). Host cell processes that influence the intracellular survival of Legionella pneumophila. Cell Microbiol *10*, 1209-1220.

Shohdy, N., Efe, J.A., Emr, S.D., and Shuman, H.A. (2005). Pathogen effector protein screening in yeast identifies Legionella factors that interfere with membrane trafficking. Proc Natl Acad Sci U S A *102*, 4866-4871.

Sievers, F., Wilm, A., Dineen, D., Gibson, T.J., Karplus, K., Li, W., Lopez, R., McWilliam, H., Remmert, M., Soding, J*., et al.* (2011). Fast, scalable generation of high-quality protein multiple sequence alignments using Clustal Omega. Mol Syst Biol *7*, 539.

Singh, R., Rao, V., Shakila, H., Gupta, R., Khera, A., Dhar, N., Singh, A., Koul, A., Singh, Y., Naseema, M*., et al.* (2003). Disruption of mptpB impairs the ability of Mycobacterium tuberculosis to survive in guinea pigs. Mol Microbiol *50*, 751-762.

Smialowski, P., and Frishman, D. (2010). Protein crystallizability. Methods Mol Biol *609*, 385-400.

Sollner, T., Bennett, M.K., Whiteheart, S.W., Scheller, R.H., and Rothman, J.E. (1993a). A protein assembly-disassembly pathway in vitro that may correspond to sequential steps of synaptic vesicle docking, activation, and fusion. Cell *75*, 409-418.

Sollner, T., Whiteheart, S.W., Brunner, M., Erdjument-Bromage, H., Geromanos, S., Tempst, P., and Rothman, J.E. (1993b). SNAP receptors implicated in vesicle targeting and fusion. Nature *362*, 318-324.

Steele-Mortimer, O. (2008). The Salmonella-containing vacuole: moving with the times. Curr Opin Microbiol *11*, 38-45.

Steele-Mortimer, O., Knodler, L.A., Marcus, S.L., Scheid, M.P., Goh, B., Pfeifer, C.G., Duronio, V., and Finlay, B.B. (2000). Activation of Akt/protein kinase B in epithelial cells by the Salmonella typhimurium effector sigD. J Biol Chem *275*, 37718-37724.

Stefan, C.J., Audhya, A., and Emr, S.D. (2002). The yeast synaptojanin-like proteins control the cellular distribution of phosphatidylinositol (4,5)-bisphosphate. Mol Biol Cell *13*, 542-557.

Stenmark, H. (2009). Rab GTPases as coordinators of vesicle traffic. Nat Rev Mol Cell Biol *10*, 513-525.

Stone, B.J., and Abu Kwaik, Y. (1998). Expression of multiple pili by Legionella pneumophila: identification and characterization of a type IV pilin gene and its role in adherence to mammalian and protozoan cells. Infect Immun *66*, 1768-1775.

Strahl, T., and Thorner, J. (2007). Synthesis and function of membrane phosphoinositides in budding yeast, Saccharomyces cerevisiae. Biochim Biophys Acta *1771*, 353-404.

Stuckey, J.A., Schubert, H.L., Fauman, E.B., Zhang, Z.Y., Dixon, J.E., and Saper, M.A. (1994). Crystal structure of Yersinia protein tyrosine phosphatase at 2.5 A and the complex with tungstate. Nature *370*, 571-575.

Sturgill-Koszycki, S., and Swanson, M.S. (2000). Legionella pneumophila replication vacuoles mature into acidic, endocytic organelles. J Exp Med *192*, 1261-1272.

Sun, E.W., Wagner, M.L., Maize, A., Kemler, D., Garland-Kuntz, E., Xu, L., Luo, Z.Q., and Hollenbeck, P.J. (2013). Legionella pneumophila infection of Drosophila S2 cells induces only minor changes in mitochondrial dynamics. PLoS One *8*, e62972.

Svergun, D. (1992). Determination of the regularization parameter in indirect-transform methods using perceptual criteria. Journal of Applied Crystallography *25*, 495-503

Svergun, D.I., Barberato, C., and Koch, M.H.J. (1995). CRYSOL - a Program to Evaluate X-ray Solution Scattering of Biological Macromolecules from Atomic Coordinates. J Appl Cryst *28*, 768-773

Svergun, D.I., Barberato, C., Koch, M.H. (1995). CRYSOL – a Program to Evaluate X-ray Solution Scattering of Biological Macromolecules from Atomic coordinates. Journal of Applied Crystallography *28*, 768–773.

Svergun, D.I., Petoukhov, M.V., and Koch, M.H. (2001). Determination of domain structure of proteins from X-ray solution scattering. Biophys J *80*, 2946-2953.

Swanson, M.S., and Hammer, B.K. (2000). Legionella pneumophila pathogenesis: a fateful journey from amoebae to macrophages. Annu Rev Microbiol *54*, 567-613.

Takenawa, T., and Itoh, T. (2006). Membrane targeting and remodeling through phosphoinositide-binding domains. IUBMB Life *58*, 296-303.

Taylor, G.S., and Dixon, J.E. (2001). An assay for phosphoinositide phosphatases utilizing fluorescent substrates. Anal Biochem *295*, 122-126.

Terebiznik, M.R., Vieira, O.V., Marcus, S.L., Slade, A., Yip, C.M., Trimble, W.S., Meyer, T., Finlay, B.B., and Grinstein, S. (2002). Elimination of host cell PtdIns(4,5)P(2) by bacterial SigD promotes membrane fission during invasion by Salmonella. Nat Cell Biol *4*, 766-773.

Tilney, L.G., Harb, O.S., Connelly, P.S., Robinson, C.G., and Roy, C.R. (2001). How the parasitic bacterium Legionella pneumophila modifies its phagosome and transforms it into rough ER: implications for conversion of plasma membrane to the ER membrane. J Cell Sci *114*, 4637-4650.

Tonks, N.K., and Neel, B.G. (2001). Combinatorial control of the specificity of protein tyrosine phosphatases. Curr Opin Cell Biol *13*, 182-195.

Urwyler, S., Brombacher, E., and Hilbi, H. (2009). Endosomal and secretory markers of the Legionella-containing vacuole. Commun Integr Biol *2*, 107-109.

Vancha, A.R., Govindaraju, S., Parsa, K.V., Jasti, M., Gonzalez-Garcia, M., and Ballestero, R.P. (2004). Use of polyethyleneimine polymer in cell culture as attachment factor and lipofection enhancer. BMC Biotechnol *4*, 23.

Vandersmissen, L., De Buck, E., Saels, V., Coil, D.A., and Anne, J. (2010). A Legionella pneumophila collagen-like protein encoded by a gene with a variable number of tandem repeats is involved in the adherence and invasion of host cells. FEMS Microbiol Lett *306*, 168-176.

Venkataraman, C., Haack, B.J., Bondada, S., and Abu Kwaik, Y. (1997). Identification of a Gal/GalNAc lectin in the protozoan Hartmannella vermiformis as a potential receptor for attachment and invasion by the Legionnaires' disease bacterium. J Exp Med *186*, 537-547.

Vergne, I., Chua, J., and Deretic, V. (2003a). Mycobacterium tuberculosis phagosome maturation arrest: selective targeting of PI3P-dependent membrane trafficking. Traffic *4*, 600-606.

Vergne, I., Chua, J., and Deretic, V. (2003b). Tuberculosis toxin blocking phagosome maturation inhibits a novel Ca2+/calmodulin-PI3K hVPS34 cascade. J Exp Med *198*, 653-659.

Vergne, I., Chua, J., Lee, H.H., Lucas, M., Belisle, J., and Deretic, V. (2005). Mechanism of phagolysosome biogenesis block by viable Mycobacterium tuberculosis. Proc Natl Acad Sci U S A *102*, 4033-4038.

Vergne, I., and Deretic, V. (2010). The role of PI3P phosphatases in the regulation of autophagy. FEBS Lett *584*, 1313-1318.

Vergne, I., Fratti, R.A., Hill, P.J., Chua, J., Belisle, J., and Deretic, V. (2004). Mycobacterium tuberculosis phagosome maturation arrest: mycobacterial phosphatidylinositol analog phosphatidylinositol mannoside stimulates early endosomal fusion. Mol Biol Cell *15*, 751-760.

Via LE, F.R., McFalone M, Pagan-Ramos E, Deretic D, et al. (1998). Effects of cytokines on mycobacterial phagosome maturation. J Cell Sci *111*, 897-905.

Vieira, O.V., Botelho, R.J., and Grinstein, S. (2002). Phagosome maturation: aging gracefully. Biochem J *366*, 689-704.

Vieira, O.V., Botelho, R.J., Rameh, L., Brachmann, S.M., Matsuo, T., Davidson, H.W., Schreiber, A., Backer, J.M., Cantley, L.C., and Grinstein, S. (2001). Distinct roles of class I and class III phosphatidylinositol 3-kinases in phagosome formation and maturation. J Cell Biol *155*, 19-25.

Vieira, O.V., Harrison, R.E., Scott, C.C., Stenmark, H., Alexander, D., Liu, J., Gruenberg, J., Schreiber, A.D., and Grinstein, S. (2004). Acquisition of Hrs, an essential component of phagosomal maturation, is impaired by mycobacteria. Mol Cell Biol *24*, 4593-4604.

Vincent, C.D., and Vogel, J.P. (2006). The Legionella pneumophila IcmS-LvgA protein complex is important for Dot/Icm-dependent intracellular growth. Mol Microbiol *61*, 596-613.

Viner, R., Chetrit, D., Ehrlich, M., and Segal, G. (2012). Identification of two Legionella pneumophila effectors that manipulate host phospholipids biosynthesis. PLoS Pathog *8*, e1002988.

Vogel, J.P., and Isberg, R.R. (1999). Cell biology of Legionella pneumophila. Curr Opin Microbiol *2*, 30-34.

Volkov, V.V., and Svergun, D.I. (2003). Uniqueness of ab initio shape determination in small-angle scattering. J Appl Cryst *36*, 860-864.

Voth, D.E., and Heinzen, R.A. (2007). Lounging in a lysosome: the intracellular lifestyle of Coxiella burnetii. Cell Microbiol *9*, 829-840.

Weber, S.S., Ragaz, C., and Hilbi, H. (2009). The inositol polyphosphate 5-phosphatase OCRL1 restricts intracellular growth of Legionella, localizes to the replicative vacuole and binds to the bacterial effector LpnE. Cell Microbiol *11*, 442-460.

Weber, S.S., Ragaz, C., Reus, K., Nyfeler, Y., and Hilbi, H. (2006). Legionella pneumophila exploits PI(4)P to anchor secreted effector proteins to the replicative vacuole. PLoS Pathog *2*, e46.

Weber, T., Zemelman, B.V., McNew, J.A., Westermann, B., Gmachl, M., Parlati, F., Sollner, T.H., and Rothman, J.E. (1998). SNAREpins: minimal machinery for membrane fusion. Cell *92*, 759-772.

Wilson, C.A., Kreychman, J., and Gerstein, M. (2000). Assessing annotation transfer for genomics: quantifying the relations between protein sequence, structure and function through traditional and probabilistic scores. J Mol Biol *297*, 233-249.

Xu, L., Shen, X., Bryan, A., Banga, S., Swanson, M.S., and Luo, Z.Q. (2010). Inhibition of host vacuolar H+-ATPase activity by a Legionella pneumophila effector. PLoS Pathog *6*, e1000822.

Zhang, Z.Y. (2002). Protein tyrosine phosphatases: structure and function, substrate specificity, and inhibitor development. Annu Rev Pharmacol Toxicol *42*, 209-234.

Zhang, Z.Y. (2003). Mechanistic studies on protein tyrosine phosphatases. Prog Nucleic Acid Res Mol Biol *73*, 171-220.

Zhang, Z.Y., Wang, Y., and Dixon, J.E. (1994a). Dissecting the catalytic mechanism of protein-tyrosine phosphatases. Proc Natl Acad Sci U S A *91*, 1624-1627.

Zhang, Z.Y., Wang, Y., Wu, L., Fauman, E.B., Stuckey, J.A., Schubert, H.L., Saper, M.A., and Dixon, J.E. (1994b). The Cys(X)5Arg catalytic motif in phosphoester hydrolysis. Biochemistry *33*, 15266-15270.

Zhong, S., Hsu, F., Stefan, C.J., Wu, X., Patel, A., Cosgrove, M.S., and Mao, Y. (2012). Allosteric activation of the phosphoinositide phosphatase Sac1 by anionic phospholipids. Biochemistry *51*, 3170-3177.

Zhu, W., Banga, S., Tan, Y., Zheng, C., Stephenson, R., Gately, J., and Luo, Z.Q. (2011). Comprehensive identification of protein substrates of the Dot/Icm type IV transporter of Legionella pneumophila. PLoS One *6*, e17638.

Zusman, T., Aloni, G., Halperin, E., Kotzer, H., Degtyar, E., Feldman, M., and Segal, G. (2007). The response regulator PmrA is a major regulator of the icm/dot type IV secretion system in Legionella pneumophila and Coxiella burnetii. Mol Microbiol *63*, 1508-1523.